GEOTECHNICAL CONTROLS ON ORGANO-SILANE MODIFICATION OF SOILS AND COAL COMBUSTION FLY ASH

by

Matthew Isaac Keatts

A thesis submitted to the faculty of
The University of North Carolina at Charlotte
in partial fulfillment of the requirements
for the degree of Master of Science in
Civil Engineering

Charlotte

2014

Approved by:

_____
Dr. John Daniels

_____
Dr. Miguel Pando

_____
Dr. Vincent Ogunro

_____
Dr. William Langley

ABSTRACT

MATTHEW ISAAC KEATTS. Geotechnical controls on organo-silane modification of soils and coal combustion fly ash. (Under the direction of DR. JOHN L. DANIELS)

Organo-silane (OS) surface modification works by chemically altering the surface of silica based materials and rendering them hydrophobic (waterproof). Limited research is present in the literature addressing the use of OS modified soils as an infiltration barrier. The goal of this research is to develop the relationships between varying degrees of hydrophobicity, varying levels of soil compaction, and water infiltration resistance for materials including Ottawa sand and coal fly ash (CFA). Initial testing was performed to determine key geotechnical engineering properties of the selected materials. Next, a range of treatment levels were established to achieve varying levels of hydrophobicity for two separate OS chemicals. OS modified material was then prepared to varying degrees of hydrophobicity and compacted to field relevant density levels. The hydraulic head required to overcome the infiltration resistance was determined, and therefore the hydraulic head below which no infiltration will occur. Additionally, saturated hydraulic conductivity and soil-water characteristic curve testing was performed. Water entry pressures of hydrophobic sand were found to range from 0 to 14 cm of H_2O, and water entry pressures of hydrophobic CFA were found to range from 0 to 542 cm of H_2O. Positive correlations were established between compaction, degree of hydrophobicity, and water entry pressure. Soil hydrophobicity was found to have little effect on the saturated hydraulic conductivity. Results indicate that hydrophobic soils are a viable option as an infiltration barrier, but additional research is recommended to address durability and field application.

ACKNOWLEDGEMENTS

I would like to thank Dr. Johan Enslin, director of the Energy Production and Infrastructure Center (EPIC) at UNC Charlotte, for providing the funding which supported this research. I would also like to thank Dr. John Daniels for advising me throughout the course of this research project. His positive support, guidance, and patience have been invaluable. I would also like to thank Dr. Miguel Pando, Dr. Vincent Ogunro, and Dr. William Langley for serving on my committee and invaluable support and guidance throughout my graduate school career. Finally, I would like to thank my family and friends for their support.

TABLE OF CONTENTS

LIST OF TABLES

LIST OF FIGURES

CHAPTER 1: INTRODUCTION

1.1 Statement of Problem

Infiltration of water into soil, coal ash impoundments, and solid waste landfills can be the root cause of many geotechnical and geoenvironmental engineering problems including loss of soil strength, leachate generation, groundwater contamination, and slope stability failure. Traditional means of controlling infiltration have included geosynthetic clay liners or other types of geomembranes. Organo-silane (OS) technology could serve as an alternative infiltration barrier method with potential advantages and cost savings. Although OS has proven useful in many industrial capacities, utilization in geotechnical engineering applications has been limited due to lack of engineering guidelines and supporting research. The purpose of this research is to begin to develop the engineering guidelines which will allow this technology to be implemented in large scale geotechnical field applications.

This research represents an important first step to developing guidelines for using OS technology in geotechnical engineering applications. OS treated soils could function as a stand-alone cover, liner, or capillary barrier. It could also be used as an additional factor of safety for designs that include these types of infiltration barrier systems. In addition to general geotechnical applications where preventing infiltration is a primary goal, specific applications to CFA impoundments are of important and immediate relevance to the coal energy industry and environmental regulations of CFA.

1.2 Scope of Research

The purpose of this research is to quantify the ability of OS treated soils to resist infiltration. This is done by determining the relationships between the hydrophobicity (contact angle) of the sample material, the level of compaction (density), and the water infiltration pressure (positive pore water pressure) that is required to force infiltration into the OS treated hydrophobic soil, and therefore determine the water pressure threshold below which no infiltration will occur. The water entry pressure may be used as a guideline for using OS treated hydrophobic soil as an infiltration barrier material.

Initial testing was performed to determine geotechnical engineering index properties of the selected materials. Next, OS chemical treatment levels were established to achieve varying degrees of hydrophobic silica sand and CFA. The contact angle measured by the sessile drop method was used to quantify the degree of hydrophobicity. Once the OS modified material was prepared to varying degrees of hydrophobicity it was compacted to field relevant density levels and the hydraulic head required to overcome the infiltration resistance was determined.

In addition to geotechnical index properties testing and water entry pressure testing, saturated hydraulic conductivity and soil water characteristic curve (SWCC) testing of the OS treated soils was performed to address the saturated and partially saturated hydraulic behavior of OS treated soils, respectively. Pore size distributions were estimated based on the SWCC, and experimental water entry pressures were compared to those predicted by the Washburn equation.

CHAPTER 2: REVIEW OF LITERATURE

2.1 Introduction

The phenomenon of soil-water repellency, or hydrophobicity, has been recognized in scientific literature for many years. The existence of naturally occurring hydrophobic soils was noted in the literature as early as 1910 (Schreiner and Shory 1910). Since that time researchers in many diverse scientific fields including hydrology, agriculture, soil science, soil physics, and chemistry have developed the theory, constitutive relations, and testing techniques that have advanced our knowledge of hydrophobic soils and their behaviors. Early work in the areas of capillarity, water movement through soils, and the interaction between the surface energies of solids and liquids laid the foundation upon which more recent research in the last half century has built the understanding of hydrophobic soils. Much of the existing literature addresses natural occurrences of hydrophobic soils and characterization techniques. Some work has been presented addressing artificially rendered hydrophobic soils, and wetting behaviors of hydrophobic soil. Limited research is present in the literature that addresses the engineering properties of aqueous phase OS modified soils, and the possibility of using artificially rendered hydrophobic soils as an infiltration barrier for geotechnical and geoenvironmental engineering applications. A survey of the most relevant literature on these subjects is presented in this chapter.

2.2 Background

The affinity or repellency of a solid surface such as soil for water is dependent upon the attractive forces between them (Das and Das 1976). If the attractive forces between the soil surface and the water molecules are greater than the surface tension of the water the water drop will wet the soil surface and the contact angle will be less than 90º. If the surface tension between the water molecules is greater than the attractive forces between the soil surface and the water molecules then the water drop will not wet the surface and the contact angle will be greater than 90º. Young's equation (1805) describes this relationship as follows:

$$\gamma_{sv} - \gamma_{sl} = \gamma_{lv} \cos\theta \quad (1)$$

where γ_{sv} is the tension at the solid-vapor interface, γ_{sl} is the tension at the solid-liquid interface, γ_{lv} is the tension at the liquid-vapor interface, and θ is the contact angle between the solid-liquid and liquid-vapor interface. The contact angle principle can be conceptualized by a single water drop resting on a surface. If the contact angle is less than 90º the water drop will spread out and wet the surface. If the contact angle is greater than 90º the water drop will "bead" and not wet the surface. This relationship holds for homogenous and planar surfaces. Figure 1 demonstrates this principle as follows:

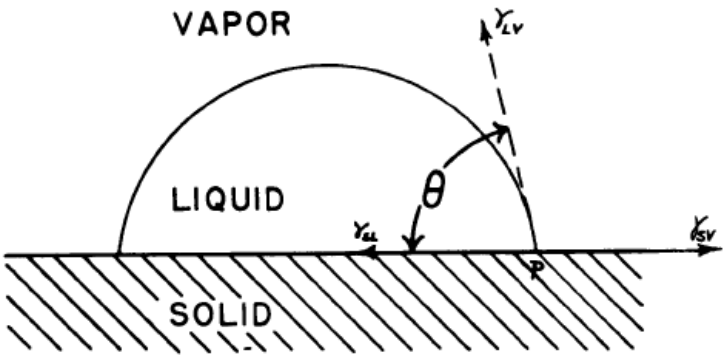

Figure 1: Contact angle of a sessile drop

To apply the concept of contact angles to soil surfaces two additional considerations need to be made as the observed contact angle (θ_{obs}) between the soil surface and a liquid will not be the same as the intrinsic contact angle between the soil material and the same liquid (i.e. silica sand and water vs. a silica sheet and water). The Wenzel equation introduces a correction factor (r) that adjusts the intrinsic contact angle for surface roughness. The Wenzel equation is as follows:

$$\cos(\theta_{obs}) = r \times \cos(\theta) \tag{2}$$

The observed contact angle (θ_{obs}) will be less than the intrinsic contact angle (θ) for contact angles less than 90º and larger if the intrinsic angle (θ) is above 90º (Bachmann et al. 2000a).

The second consideration that must be taken regarding contact angles of soils is the concept of chemically heterogeneous surfaces. The Cassie equation:

$$\cos(\theta_{obs}) = f_1 \cos(\theta_1) + f_2 \cos(\theta_2) \tag{3}$$

where f_1 is the fraction of the surface having intrinsic contact angle θ_1 and f_2 is the fraction of the surface having intrinsic contact angle θ_2. Bachmann et al (2000a) indicates that the observed contact angle will be a composite of the intrinsic contact angles of the materials present at the soil surface.

Next, the fact that soil exists as a three dimensional structure or "matrix" of particles with interconnecting void spaces must be addressed. Assuming the pore space in soils can be modeled as a collection of capillary tubes the Washburn equation (Washburn 1921) can be used to determine the capillary rise (h_c) in hydrophilic soils as well as the water entry pressure (h_p) of hydrophobic soils. The Washburn equation is as follows:

$$h_c\ (\theta < 90°)\ or\ h_p(\theta > 90°) = \frac{2\gamma \cos\theta}{r\rho g} \quad (4)$$

where θ is the liquid-solid contact angle, γ is the liquid-air surface tension (dyn/cm or N/m), r is the effective pore radius, ρ is the liquid density, g is the gravitational constant, and h_c is the height of capillary rise for θ < 90º or h_p is the water entry pressure for θ > 90º.

There are two additional important relationships that describe the wetting and movement of water through a porous medium. Darcy's law (1856) describes the flow of a liquid through a saturated porous medium such as soil. This law states that the volume flow rate per unit area is proportional to the pressure gradient if applied to the case of viscous flow through a porous medium treated as a bundle of capillaries,

$$Q = vA = kiA = k\frac{\Delta H}{L}A \quad (5)$$

where Q is the volume flow rate, *v* is the flow velocity, *k* is the permeability of the medium, i (or ΔH/L) is the hydraulic gradient, A is the total cross-sectional area of the porous medium, ΔH is the head loss over the length of the sample, and L is the sample length (Adamson and Gast 1997). This principle is most often used to determine the permeability or hydraulic conductivity (k_{hyd}) of a saturated soil in geotechnical engineering.

For unsaturated soils the Richards equation (Richards 1931) describes the wetting or drying behavior of the soil based on the following partial differential equation:

$$\frac{\partial\theta}{\partial t} = \frac{\partial}{\partial z}\left[K(\theta)\left(\frac{\partial\psi}{\partial z} + 1\right)\right] \quad (6)$$

where θ is the volumetric water content, t is time, z is the elevation above a vertical datum, K is the hydraulic conductivity, and ψ is the pressure head.

The preceding relationships describe how water and soil will behave on either the micro or macro scale, with the micro scale being at the molecular soil-water interface, and the macro being the movement of water through a matrix of soil particles. Building upon these principles, the following research has developed ways to quantify hydrophobicity and hydrophilicity of soils.

2.3 Characterization of Hydrophobic Soils

Many methods have been presented to quantify levels of hydrophobicity in soils. One of the first methods developed was the water drop penetration time (WDPT) test (Van't Woudt 1959). In this method a drop of water is placed on the soil surface and the time required for the drop to penetrate the surface is recorded. Letey (1969) demonstrated that soils for which the water drop does not penetrate within 5 seconds are considered hydrophobic, although the 5 second benchmark was arbitrarily selected. The WDPT method is best used to rapidly classify soils into the broad categories of hydrophilic or hydrophobic. Due to several limitations it may be a "better measure of repellency persistence than of initial resistance to wetting" (Wallis and Horne 1992).

The equilibrium capillary rise method has been used to determine the contact angle between a porous media and a wetting fluid. In this method the equilibrium height of capillary rise of a liquid in a soil column after 24 hours can be used to determine the contact angle between soil and liquid. The two unknown variables in the Washburn Equation (Eq.4) are the contact angle (θ) and the effective pore diameter (r). By using ethanol, for which $\theta = 0^{o}$, 'r' can be solved for a soil column of given compaction (density). The test is repeated with water as the wetting fluid and the contact angle of the soil can be determined. Letey (1962) demonstrated that this testing method is valid for

various soils and sands that were both untreated and treated to alter the contact angle. Drawbacks of this method are that it is best suited for hydrophilic soils for which water will naturally infiltrate the soil columns and the 24 hour time period required for equilibrium capillary rise to be reached. Due to the duration of the test the contact angle calculated by this method is probably not the initial value.

Emerson and Bond (1963) developed a dynamic capillary rise method which measures the rate of water infiltration into a column of soil to determine the contact angle. This test method must also be run twice to back out the contact angle. Emerson and Bond recommend testing soils for which $\theta>0°$ then igniting the soils in a muffle furnace to remove any hydrophobic coatings to effectively create equivalent soils for which $\theta = 0°$. Positive hydrostatic pressure head is then applied to the equally compacted columns of ignited and unignited soils and Darcy's equation (Eq. 5) for saturated flow is used to calculate the maximum height of capillary rise for the respective soils. Cosine of the contact angle is equal to the ratio of the heights of capillary rise for the unignited and ignited soils. Due to the use of positive water pressure application, both hydrophilic and hydrophobic soils can be tested. Also, the test duration of approximately 15 minutes per test is much quicker than the equilibrium method (24 hours) and gives a better approximation of the instantaneous or advancing contact angle.

As Young's equation (Eq. 1) indicates, the contact angle between a liquid and solid is a function of the surface tension of the wetting liquid. The critical surface tension is defined as the highest surface tension of a liquid which will wet the particular solid at a zero contact angle. Zisman (1964) studied the wetting and adhesion properties of solids by liquids of varying surface tensions. He found a soil which is extremely water repellent

($\theta >> 90°$) will have a low critical surface tension, therefore a solution with lower surface tension will be required to wet it (Das and Das 1976). Building off the critical surface tension work of Zisman (1964), the ninety degree surface tension (NDST) method (Watson and Letey 1970), and the molarity of ethanol drop (MED) method (King 1981) are both modifications of the WDPT test that relate the surface tension of a liquid drop to $\cos \theta$. Both methods use solutions with a range of surface tensions for the drop of wetting fluid in the WDPT method to shorten the testing time and improve the approximation of the soil contact angle.

Water entry pressure (h_p) has also been proposed as a method of characterizing hydrophobic soils (Carrillo et al. 1999; Wang et al. 2000). The water entry pressure (or "breakthrough pressure") is the positive pressure head required to initiate infiltration in hydrophobic soils. Carrillo measured the water entry pressure of hydrophobic sand by using a water ponding (WP) technique. Carrillo demonstrated that there is a positive correlation between the contact angle and water entry pressure, as well as the WDPT and the NDST methods for hydrophobic sand. Wang also reported that the water entry pressure increases for more hydrophobic coarse sand, fine sand, and loamy sand using the WP technique as well as a tension-pressure infiltrometer method. The water entry pressure methods of characterizing hydrophobic soils do a better than the previously mentioned methods of indirectly measuring the initial contact angle. See Section 2.7 for additional discussion and research involving the water entry pressure.

Finally, the sessile drop method (SDM) is a method that directly measures the contact angle between a surface and a wetting fluid. In this method a goniometer apparatus is used to view and measure the actual initial contact angle between a drop of

water placed on a planar soil surface. Soil surfaces are prepared by affixing a monolayer of soil particles to a glass slide using two sided tape. Bachmann (Bachmann et al. 2000a, 2000b and 2003) demonstrated that this method accurately and quickly obtains the soil water contact angle for a range of soil particle sizes. This method inherently accounts for chemical heterogeneity and surface roughness. The contact angle measurements by the sessile drop method were found to be in agreement with hydrophobic and hydrophilic characterizations by the WDPT method, the Wilhelmy Plate Method, the capillary rise method, and a modified capillary rise method. The adhesive tape used in preparing the samples was shown to have "insignificant" impact on the soil-water contact angle. This method is best used to characterize hydrophobic soils.

2.4 Soil Water Characteristic Curves

The soil water characteristic curve (SWCC) describes the relationship between the soil volumetric water content (%) and soil suction (kPa or cm of H_2O). Some early literature also reports soil suction in units of pF which is the logarithm of head measured in centimeters of water. Soil suction is typically reported in the SWCC as either total suction or matric suction. Total suction is a composite of matric suction and osmotic suction. Osmotic suction results from dissolved solutes, and matric suction results from the combined effects of pore geometry and adsorption forces (most prevalent in fine grain soils). The volumetric moisture content is typically reported for presentation of the SWCC. The soil water characteristic curve can describe either an adsorption (wetting) process or a desorption (drying) process. More water is generally retained by soil during the drying process than is adsorbed by the soil for the same value of suction during the wetting process (Lu and Likos 2004).

Many mathematical representations have been developed to model the wetting and drying behavior of unsaturated soils. "Fitting parameters" are used to optimize the models representation of the SWCC data. These parameters are unique to each model and describe different aspects of the wetting and drying process of unsaturated soil.

Brooks and Corey (1964) proposed one of the earliest SWCC models. Their two part model for the SWCC is as follows:

$$\theta = \begin{cases} \theta_s & \psi < \psi_b \\ \theta_r + (\theta_s - \theta_r)\left(\frac{\psi_b}{\psi}\right)^{\lambda} & \psi \geq \psi_b \end{cases} \quad (7)$$

where θ is the volumetric moisture content, θ_s is the saturated volumetric moisture content, θ_r is the residual moisture content, ψ is the total soil suction, ψ_b is the air-entry pressure, and λ is the fitting parameter "pore size distribution index."

For modeling purposes the normalized volumetric moisture content (Θ) may be reported which is defined as follows:

$$\Theta = \frac{\theta - \theta_r}{\theta_s - \theta_r} \quad (8)$$

Taking this into consideration, the Brooks and Corey (BC) model may also be written as follows:

$$\Theta = \begin{cases} 1 & \psi < \psi_b \\ \left(\frac{\psi_b}{\psi}\right)^{\lambda} & \psi \geq \psi_b \end{cases} \quad (9)$$

The van Genuchten model (1980) was developed as a smooth, closed form, three parameter model. The van Genuchten (VG) model is as follows:

$$\Theta = \left[\frac{1}{1 + (a\psi)^n}\right]^m \quad (10)$$

where *a*, *n*, and *m* are fitting parameters. The suction term (ψ) appearing on the right-hand side of the equation may be expressed in either units of pressure (i.e., ψ = kPa, as shown) or head (i.e., h = m). In the former case, the '*a*' parameter is designated more specifically as α, where α has inverse units of pressure (kPa^{-1}). In the latter case, the *a* parameter is designated β, where β has inverse units of head (m^{-1}). Both α and β are related to the air-entry condition, where α approximates the inverse of the air-entry pressure, and β approximates the inverse of the air-entry head or the height of the capillary fringe. The *n* parameter is related to the pore size distribution of the soil and the *m* parameter is related to the overall symmetry of the characteristic curve. The *m* parameter is frequently constrained by direct relation to the *n* parameter as

$$m = 1 - \frac{1}{n} \quad or \quad m = 1 - \frac{1}{2n} \tag{11}$$

The VG model allows for an inflection point in the model, and is generally considered more flexible than the BC model (Lu and Likos 2004).

Fredlund and Xing (1994) developed a model based on consideration of pore size distribution in a form similar to the VG model as follows:

$$\Theta = \mathrm{C}\,(\psi)\left[\frac{1}{\ln[e + (\psi/a)^n]}\right]^m \tag{12}$$

where ψ is suction (kPa), a, n, and m are fitting parameters, e is the natural logarithmic constant, and C(ψ) is a correction factor that forces the model through a prescribed suction value of 10^6 kPa at zero water content.

$$\mathrm{C}\,(\psi) = \left[1 - \frac{\ln(1 + \psi/\psi_r)}{\ln(1 + 10^6/\psi_r)}\right] \tag{13}$$

where ψ_r is the suction (kPa) estimated at the residual condition (Lu and Likos 2004).

There are many different testing methods for measuring the SWCC. The chilled mirror hygrometer (or dewpoint potentiometer), the filter paper test, thermal conductivity sensors, capacitance sensors, the osmotic suction technique, and the vapor equilibrium technique are all indirect methods that do not measure suction directly, but some other dependent variable. Tensiometers and axis translation techniques (Tempe cell and pressure plate methods) directly measure soil suction. Nam et al. (2009) demonstrated that the various testing techniques all provide results that generally agree for natural soils, and furthermore that the VG model and the FX model similarly model the soil water characteristic curves. Nam (2009) also states that, although there are drawbacks, the chilled mirror hygrometer method is preferable because of its simplicity and relative short testing time.

Miller (2002) studied the effect of plasticity and compaction effort on the SWCC. For the soils tested in the study it was found that increasing plasticity increased the rate of change in suction for given change in moisture content. In general, the lower plasticity soils (sands) had a flatter SWCC than higher plasticity soils (clays). The study also found that increasing compaction efforts would increase the suction measurements for a soil at a given moisture content, and that this effect was more pronounced for high plasticity soils. The SWCC was determined over a suction range from 100 kPa to 1000 kPa for this study.

Wang (2000) discusses the SWCC and specifically the water entry pressure in relation to hydrophobic soils. Hydrophilic soils, with contact angles (θ) less than 90°, have a negative water entry pressure value or a positive suction. Hydrophobic soils, with contact angles (θ) greater than 90°, have a positive water entry pressure value or a

negative suction. The following figure demonstrates this principle with regards to the SWCC.

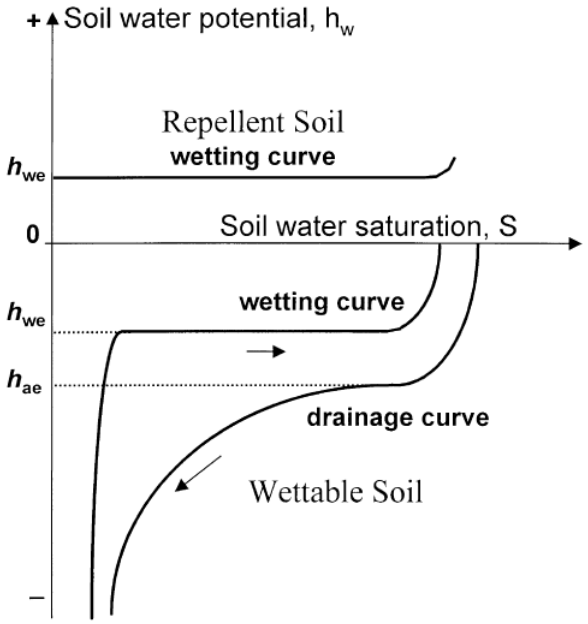

Figure 2: Typical SWCC's for a wettable and a repelent soil (Wang et al. 2000)
The h_{we} and h_{ae} denote water-entry and air-entry values

2.5 Natural Occurrence of Hydrophobic Soil

Naturally occurring hydrophobic soils have been an area of interest around the world for many decades due in part to their impact on runoff and erosion, the movement of water through soil, and agriculture (Debano 1981). Research in this area has addressed soils rendered hydrophobic by many naturally occurring phenomena including organic matter (i.e. peat, plant litter), humic acid, fungi, and heat (i.e. fire). Amelioration strategies for overcoming "undesirable" hydrophobic soils (Fink and Myers 1969) and methods of characterizing hydrophobicity in soils were some of the early goals of research which addressed naturally occurring hydrophobic soils. More recent research

has advanced to attempt to address the causes, soil physics, and hydrological behavior (including preferential flow paths) of hydrophobic soils (Debano 2000 and Doerr 2000).

Buczko et al. (2006) and Greiffenhagen et al. (2006) investigated the characteristics of hydrophobic sandy soils of German pine forests (Pinus sylvestris). Both found that the hydrophobicity of the forest soils demonstrated seasonal variation with soils being more hydrophobic in warmer and dryer months, and lower in colder and wetter months. Both used the WDPT test to characterize the hydrophobic soil.

Bryant et al. (2007) studied the effect of compaction on naturally hydrophobic soils of eucalyptus forests (Eucalyptus globulus) in Portugal. He found that increasing compaction decreased the soil surface water repellency and could potentially increase surface wetting and infiltration despite the fact that increasing compaction decreases the hydraulic conductivity of soils. The WDPT test was used to characterize the soil hydrophobicity.

Anurudda et al. (2010) and Moody et al. (2009) both studied the effects of heat on hydrophobic soils. Anurudda showed that heat treating naturally occurring hydrophobic soils increased water repellency when the soil was dried between 60 and 175°C. However, the soil became hydrophilic when heated beyond 175°C. Anurudda demonstrated that the mini tensiometer-TDR coil probe apparatus were capable of measuring rapid changes in volumetric moisture content and soil-water potential for determining the SWCC of water repellent soils under positive water pressure head. Moody found that both hydraulic conductivity (K_f) and sorptivity (S) are inversely related to water repellency.

The following table (Table 1) presents a summary of some research into naturally occurring hydrophobic soils, soil types studied, origin of the soil, and potential causes of the naturally occurring hydrophobic soils:

Table 1: Research involving naturally occuring hydrophobic soils

Researcher	Soil Types	Hydrophopic Cause	Origin
Van't Woudt (1959)	Sand, Volcanic Ash	Organic Coatings (Pine Forest, Native Heath)	New Zealand
Emerson and Bond (1963)	Tintinara Sand	"Naturally Occuring"	South Australia
King (1981)	Sand	Organic materials (fungal hyphae, humic acid, plant compost)	South Australia
Nguyen et al. (1999)	Ouddorp Sand	Organic and humic materal	Netherlands
Dekker and Ritsema (2000)	Ouddorp Sand, Loam, Clay, Peat	Organic Coatings (Pine-Beech Forest)	Netherlands
Wang et al. (2000)	Ouddorp Sand	Organic and humic material	Netherlands
Buczko et al. (2006)	Sand, Loam, Clay, Peat	Humic Substances (Pine Forest)	Germany
Greiffenhagen et al. (2006)	Glacial Till, Sand	Pine Forest	Germany
Bryant et al. (2007)	Sand, Silt, Clay	Eucalyptus Forest	Portugal
Moody et al. (2009)	Fine Sand, Silt, Clay, Ash	Fire (heat, combustion byproducts, ash)	Colorado, United States
Anurudda et al. (2010)	Volcanic Ash Soil	Heat, Pine Forest	Japan

2.6 Artificial Hydrophobic Modification of Soils

In addition to naturally occurring hydrophobic soils, artificially rendered hydrophobic soils have been an area of interest for many years. Artificially rendered hydrophobic soils have primarily been studied in laboratory settings for the purposes of modeling naturally occurring hydrophobic soils. Artificially rendered hydrophobic soils allow for the creation of soils with stable hydrophobicity and contact angles up to 160°

(Fink 1970). Both are desirable traits for hydrophobic soils for the purposes of establishing constitutive relationships, characterization techniques, and general testing of hydrophobic soils. Hydrophobic soils have often been created in the lab using methods which require organic solvents to apply the hydrophobic compound. This does not lend itself to large scale field applications due to obvious negative environmental impacts. Field application of artificial hydrophobic soils have been limited, and even more so with regards to CFA.

Fink et al. (1970) utilized thirteen organic water repellent chemicals in five organic coating classes to render a variety of sands hydrophobic. The goal of this research was to compare the effectiveness of the families of hydrophobic organic coatings for the purposes of water harvesting in the desert. In this research the silicone resins outperformed the amino acetates, the quaternary ammonium salts, the substituted phenols, and the flouro-carbon organic coating chemicals in both breakthrough pressures, and contact angles.

Bauters et al. (1998, 2000) utilized blasting silica sand treated with octadecyltrichloro-silane (OTS) in ethanol solution for the purpose of studying preferential flow paths (unstable wetting front with fingers) during infiltration. Soil samples were prepared to 0, 3.1, 5, 5.7, and 9% hydrophobic soil particles by mixing treated soil with untreated. Bauters reported that due to the particle size, gradation, and pore geometry the 3.1% OTS sand would have 37% of the pore spaces affected by water repellent material and the 9% OTS sand would have all of the pore spaces containing at least one soil particle that was water repellent. Tests were performed to determine the SWCC, WDPT, hydraulic conductivity, and wetting front geometry. It was noted in the

research that the wetting behavior of the soil particle matrix was such that for hydrophobic soils the large pore spaces fill with water first during infiltration, and for hydrophilic soils the small pore spaces fill first. The research demonstrated that during infiltration the wetting front becomes unstable and formed fingers as water repellency increased. Bauters also concluded that soil physics theory developed for hydrophilic soils is valid for hydrophobic soils provided that the contact angle effect is accounted for.

Daniels et al. (2009) studied the influence of organo-silane treatment on the compaction and leachabiltiy of CFA, as well as the potential use of OS for soil stabilization. The CFA was treated with water-OS solutions at varying concentrations as the molding moisture content in the compaction characteristic and leachate studies. Similar OS treatment solutions were used to surface treat a roadway near Puerta Cortez, Honduras for the stabilization study. It was found that the optimum moisture content (OMC) decreased and the maximum dry density (MDD) increased for OS treated CFA using standard compaction effort (12400 ft-lbf/ft^3 (600kN-m/m^3)). For the soil stabilization application the natural soils treated with OS demonstrated a decreased OMC, increased MDD, an increased California Bearing Ration (CBR), and a reduction of the hydraulic conductivity by three orders of magnitude as shown in the following table adapted from Daniels (2009):

Table 2: Comparison between unmodified and OS-modified soils

Soil	Standard Compaction Effort		Expansion Index (%)	CBR (%)	Hydraulic conductivity (cm/s)
	Optimum Moisture Content, %	Maximum Dry Density, kN/m^3			
Unmodified	25.2	13.7	2.0	3.2	9.2 x 10^{-5}
OS-Modified	18.7	15.3	0.25	6.3	1 x 10^{-7}

The preceding research demonstrates some of the applications of artificially rendered hydrophobic soils. The following table (Table 3) presents a summary of some research into artificial hydrophobic soils, soil types studied, hydrophobic chemicals used, and the solvent used for chemical application:

Table 3: Research involving artificially rendered hydrophobic soils

Researcher	Soil Type	Hydrophopic Compounds	Solvent
Fink and Myers (1969)	Silica Sand	Sodium methyl silanolate (Union Carbide R-20)	Water
Fink (1970)	Natural Sands	Silicone Resins	Multiple Application Methods
		Amine Acetates	
		Quaternary ammonium salts	
		Substituted phenols	
		Fluorochemicals	
Emmerich et al. (1987)	Sand Silt Clay (Natural Soils)	Multiple waxes	N/A
		Sodium methyl siliconate (Dow Corning 772)	Water
		Sodium methyl siliconate + Latex	Water
Bauters et al. (1998)	Silica Sand	Octadecyltrichlorosilane (OTS)	Ethanol
Carrillo et al. (1999)	Silica Sand	Octadecylamine	Water
		Peat extract	Ethanol or Benzyl Alcohol
Bachmann et al. (2000)	Sand, Silt	Dimethyldichlorosilane	Not Reported
Bauters et al. (2000)	Silica Sand	Octadecyltrichlorosilane (OTS)	Ethanol
Nieber et al. (2000)	Silica Sand	Octadecyltrichlorosilane (OTS)	Ethanol
Daniels et al. (2009)	Silica Sand and Coal Fly Ash	Organo-Silane (Zydex Zycosoil)	Water
Ramirez-Flores et al. (2010)	Silt, Sand	Dichlorodimethylsilane (DCDMS)	Hexane

2.7 Water Entry Pressure of Hydrophobic Soils

As previously mentioned the water entry pressure of a hydrophobic soil is a direct measurement of soil water repellency. It is also a direct measurement of infiltration resistance which is a primary goal of this line of research. Water entry pressure

measurements are advantageous in that they account for the soil matrix and pore geometry where other methods primarily test surface energies at the surface of a soil sample. The following are some examples of research that studied the water entry pressure of hydrophobic soils and some if their results.

Carrillo et al. (1999) studied the relationship between the contact angle determined by the water entry pressure value (θ_w) and the ninety degree surface tension value (γ_{nd}) for hydrophobic soils. A positive linear correlation was found to exist between the two variables. Two sands of different gradation treated with Octadecylamine or solvent extracts of peat moss were tested in these studies. Hydrophobic soils with stable "ranges" of contact angles were achieved with the amine treatment, but the sands treated with solvent extracts of peat moss were found to be unstable. Contact angels ranging from 96° to 110° were reported in the research and water entry pressures (h_p) ranging from 2.4 to 13.4 cm of H_2O were achieved. The following figures demonstrate some of the results.

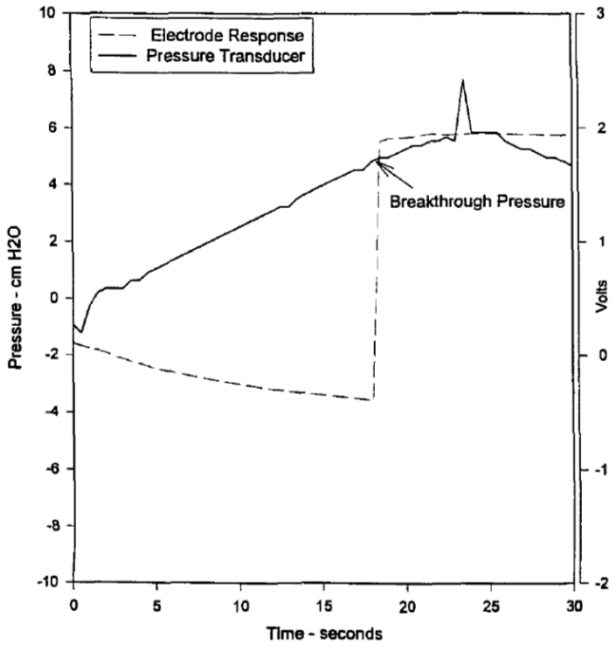

Figure 3: Typical pressure transducer and electode response during the measurement of water entry pressure head, h_p (Carrillo et al. 1999)

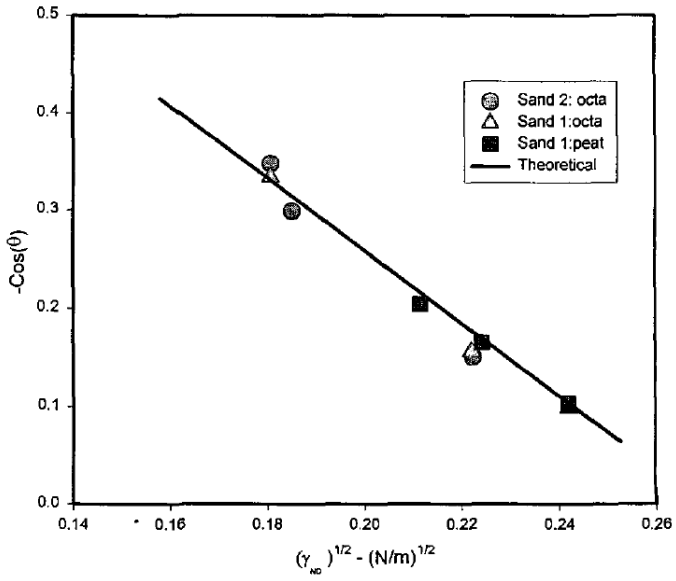

Figure 4: The relationship between liquid-solid contact angle, cos θ, and the 90° surface tension, γND, for the various treated sands. (Carrillo et al. 1999)

Wang et al. (2000) studied the water entry pressure of naturally hydrophobic sands (Ouddorp sand) utilizing a ponding method and a tension-pressure infiltrometer method. Water entry pressures ranging from 2 to 12 cm of H_2O were achieved. Wang states that the magnitude of water-entry value reflects the combined effects of various soil properties and state variables on water mobility in the soil. It is a hydraulic indicator of soil water repellency or wettability.

Fink et al. (1969, 1970, 1976) has performed some of the most extensive and relevant research on the water entry pressure of hydrophobic soils for the purpose of water harvesting applications. This research studied the water entry pressure of natural sandy soils and sands treated with sodium methyl silonolate in aqueous solution. Soil water repellency was established by contact angle measurements utilizing the sessile water drop technique. Contact angles up to 158° were reported. Water entry pressures between 10 and 160 cm of H2O were reported as related to the surface treatment ratio (g solution per m^2 soil). The following are some results.

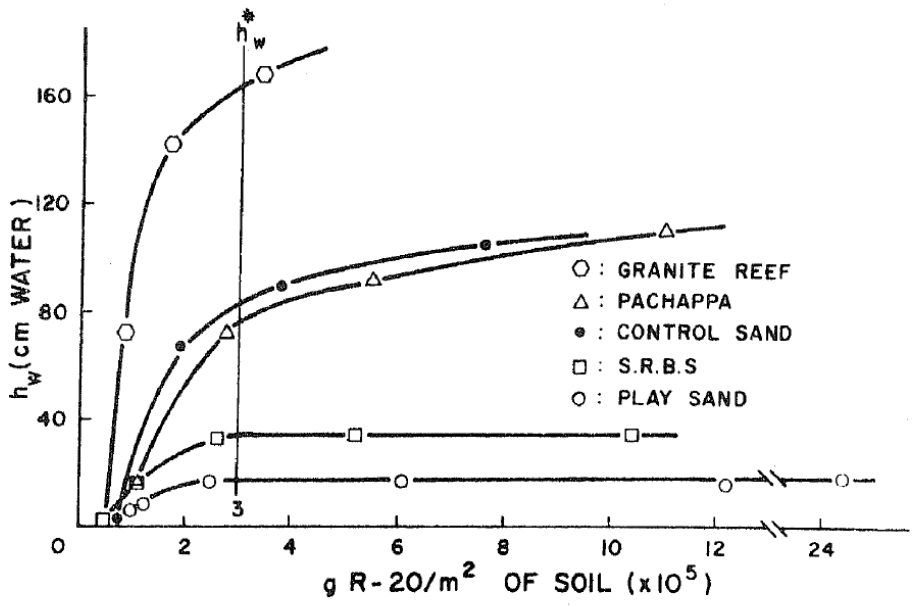

Figure 5: Water entry pressure of silicone-treated soils versus application rate of silicone per unit area of soil. (Fink et al. 1969)

Fink also demonstrated that increasing the bulk density of a soil by packing (increased compaction effort) should decrease the effective pore radius and, consequently, increase the water entry pressure (Figure 6). This is in agreement with the inverse relationship between effective pore radius and water entry pressure in the Washburn equation (Eq. 4). Fink's research expanded to include many additional hydrophobic organic coatings (Fink 1970) and durability studies (Fink 1976).

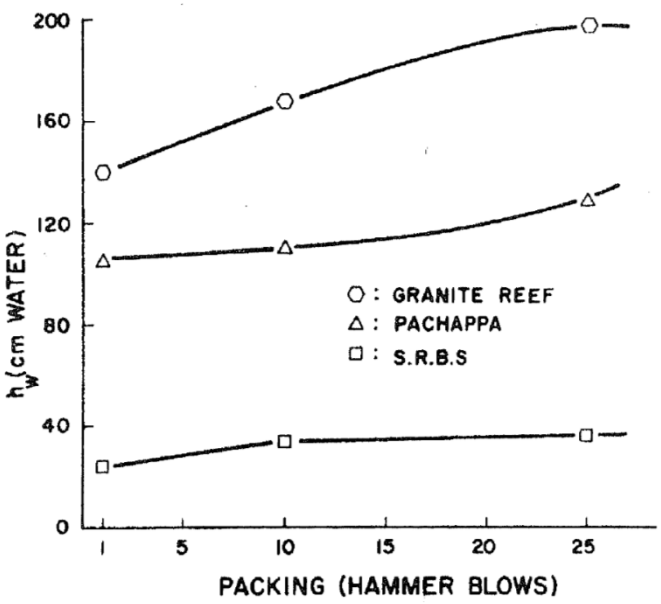

Figure 6: Water entry pressure of water repellent soils versus degree of soil packing (Fink and Myers 1969)

CHAPTER 3: MATERIALS AND METHODS

3.1 Materials

The materials utilized for laboratory testing were coal fly ash (CFA), Ottawa sand, two organo-silane chemicals, and de-ionized water. All testing was performed in the geotechnical and geoenvironmental labs at the University of North Carolina at Charlotte unless otherwise noted.

3.1.1 Coal Fly Ash

Coal fly ash was collected from an undisclosed southeastern utility company's CFA impoundment at a coal fired power plant. The CFA had been previously moisture conditioned and transported by truck to the impoundment location ("dry method" of transport). The CFA was set aside for collection. It was not previously placed or compacted in the CFA impoundment before collection. Approximately thirty 5-gallon buckets of CFA were collected for testing.

3.1.2 Ottawa Sand

Ottawa sand was purchased from Gilson Company, Inc. (product # HM-106). The source of the sand was U.S. Silica Company's Ottawa, Illinois plant (U.S. Silica, P.O. Box 187, Berkeley Springs, WV 25411). The sand was selected for its relatively uniform gradation, purity, particle size, and rounded shape. Typical properties of the selected sand are presented in the following table:

Table 4: Typical properties of Ottowa Silurian sand (US Silica Co.)

Color	White	Effective Size (mm)	0.45
Mineral	Quartz	pH	7
Grain Shape	Round	Specific Gravity	2.65
Bulk Density-Compacted (lbs/ft^3)	109	Uniformity Coefficient	1.18
Bulk Density-Uncompacted (lbs/ft^3)	102	Percent Silicone Dioxide, SiO_2 (%)	99.8

3.1.3 Organo-Silane Chemicals

Two separate aqueous phase organo-silane chemicals were used to render the materials hydrophobic. The first was Zydex Zicosoil (Zydex Industries, Gorwa, India). Zicosoil is a pale-yellow viscous liquid that dissolves in water. It has a density of 1.05 g/cm^3 at 25°C, and a pH of 7. The Zycosoil solution contains ethylene glycol as a solvent. The second chemical selected was Wacker 501 Drysoil (WackerChemie AG, Munich, Germany). It is a clear and colorless liquid that readily dissolves in water. It has a density of 1.24 g/cm^3 and a pH of 13. Both chemicals list potassium methyl siliconate as the active ingredient, but the exact chemical compositions are proprietary information. Henceforth, Zydex Zycosoil and Wacker 501 Drysoil will be referred to as OS_1 and OS_2 respectively.

3.1.4 De-Ionized Water

De-ionized water or distilled water was used for all testing. Tap water was also tested as a reference. Electrical conductivity, resistivity, pH, and oxidation reduction potential (ORP) of all water sources available in the UNCC lab were determined. The results are in the following table:

Table 5: Properties of water used for testing

Water Type	Conductivity			Resistivity	pH	ORP
	μS/cm	S/m	S/m	MΩ-cm		abs mV
DI	3.07	0.000307	3.07E-04	0.325733	5.62	-6.9
Distilled	0.57	0.000057	5.70E-05	1.754386	5.95	-9.1
Tap Water	50.2	0.00502	5.02E-03	0.01992	6.18	-12.3

3.2 Geotechnical Engineering Properties

An initial investigation of the geotechnical engineering properties of the sand and CFA materials was performed to characterize the materials.

3.2.1 Moisture Content

The as received moisture content of the two soil materials was determined in accordance with ASTM D2216. Soil specimen of both CFA and Sand were sampled from their "as-delivered" packages and transferred to sample cups of known mass. The samples were then oven dried at 110°C for 24 hours. Moisture content of the CFA and Ottawa sand were determined.

3.2.2 Specific Gravity

The specific gravities of sand and CFA were determined by the water pycnometer (volumetric flask) method in general accordance with ASTM D854. First, the clean and dry pycnometers were calibrated by filling to above the calibration line with DI water and de-airing the water. Once the pycnometers were de-aired the water level was reduced to the calibration line and the mass and temperature of the pycnometer was recorded. The calibrated volume of the pycnometer was determined using the density of water at the calibration temperature.

The calibrated pycnometer was then filled with oven dry soil and de-aired water until a slurry was formed. The slurry was then agitated continuously while being de-

aired by a combination of heat and vacuum. Once de-aired, the pycnometer and slurry were allowed to return to room temperature, and additional de-aired water in temperature equilibrium with the pycnometer was added to reach the calibration line. The mass and temperature of the pycnometer were recorded. The soil slurry was then placed in a drying dish and the oven dry mass of the soil was determined. Upon completion of the test the specific gravity of the soil samples were determined.

3.2.3 Particle Size Analysis

The particle size distribution of the Ottawa sand and CFA were determined in accordance with ASTM D422-63. Air dry samples of sand and CFA were used for this test. Since 100% of the sand sample was retained on sieves larger than the No. 200 sieve, the particle size distribution of the sand sample was determined using only the sieve analysis. Since a majority of the CFA material passed through the No. 200 sieve, the particle size distribution of the CFA sample was determined using only the hydrometer analysis. Although sieves smaller than the No. 200 size are available, dry CFA does not lend itself to sieve analysis due to excessive dusting and loss of mass.

To determine the particle size distribution of the sand, a range of sieves were selected between size No. 10 (2.00 mm) and No.200 (75 μm). The sieves were stacked in decreasing size and a known mass of sand was applied to the top sieve. The sieves and sand were then vibrated for approximately two minutes. The mass of soil retained on each sieve was recorded. A particle size distribution was developed for the sand.

To determine the particle size distribution of the CFA a hydrometer analysis was performed. First the hygroscopic moisture content of the air dry CFA was determined. Next a 50g sample of CFA was mixed thoroughly with a dispersion agent (120ml of

sodium hexametaphosphate solution) then transferred to a 1000ml sedimentation cylinder. DI water was added to bring the slurry of soil, sodium hexametaphosphate, and water to the 1000ml calibration line, and then the cylinder was agitated for 1 minute by repeated inversion to mix the solution. After agitation was complete a hydrometer (Type 151H) was inserted into the solution. Hydrometer and temperature readings were taken at the appropriate time intervals. After hydrometer readings were complete, the slurry was transferred to a No. 200 sieve, washed and dried. The remaining fraction of material was then sieved. Hydrometer readings were used to determine particle diameters, combined with the sieve results and a particle size distribution for the CFA was developed.

3.2.4 Compaction Characteristics

The maximum and minimum index density of the Ottawa sand and the compaction characteristics of CFA were determined by different methods. The index density of the sand was determined in accordance with ASTM D4254 "Standard Test Methods for Minimum Index Density and Unit Weight of Soils and Calculation of Relative Density" and ASTM D4253 "Standard Test Methods for Maximum Index Density and Unit Weight of Soils Using a Vibratory Table." The compaction characteristics of the CFA were determined in accordance with ASTM D698 "Standard Test Methods for Laboratory Compaction Characteristics of Soil Using Standard Effort," ASTM D1557 "Standard Test Methods for Laboratory Compaction Characteristics of Soil Using Modified Effort," and a procedure presented by Daniel and Benson (1990) was used for "reduced effort" compaction characteristic determination.

The maximum index density (ρ_{dmax}) of the sand was determined in accordance with ASTM D4253 Method 1A for oven dry soil and an electromagnetic vibratory table. In this test the oven dry sand was placed in a 2830 cm^3 (0.100 ft^3) mold of known mass, which was securely mounted to the vibratory table. The mold was filled with sand and the surface was leveled using a straight edge. Next a guide sleeve, surcharge plate and surcharge equivalent to 13.8±0.1 kPa (2.00±0.02 lb/in^2) was placed on the mold. The entire assembly was then vibrated at 60 Hz for 8 minutes. After vibration the vertical displacement of the surcharge plate was recorded and the maximum index density (ρ_{dmax}) and minimum void ratio (e_{min}) were calculated.

The minimum index density (ρ_{dmin}) was determined in accordance with ASTM D4254 Method C for oven dried sand placed in the mold by inverting a graduated cylinder. In this method the sand is placed in the 2830 cm^3 (0.100 ft^3) mold in the loosest state possible. Once the mold is full the top surface is leveled using a straight edge with minimal disturbance to the soil sample. The mass of sand is determined and the minimum index density (ρ_{dmin}) and maximum void ratio (e_{max}) were calculated.

The compaction characteristics of CFA using modified effort were determined in accordance with ASTM D1557 Method A. For this test a cylindrical mold was used for which the diameter was 4 in., the height was 4.5 in. and the volume was 943.0cm^3 (0.333 ft^3). (The same mold was used in all compaction tests.) The CFA was placed in the mold in 5 layers with 25 blows per layer. Each blow was performed using a rammer (drop hammer). For this test the rammer has a travel of 45.72 cm (18.00 in.) and a mass of 4.5364 kg (10.00 lb). Once the CFA was compacted in the mold the collar was removed and the top surface of the sample was leveled using a straight edge. The mold and soil

sample were then removed and weighed. The compacted soil sample was then extruded from the mold, and the moisture content of the sample was determined. This procedure was repeated on samples from a dry condition to almost fully saturated at 2% molding moisture increments. In this manner the relationship between density and moisture content for modified compaction effort was determined. From the graphical plot of these variables the optimum moisture content (OMC) and maximum dry density (ρ_{dmax}) of CFA were determined.

The compaction characteristics of CFA using standard effort were determined in accordance with ASTM D698 Method A. This procedure is the same as the one previously outlined for the Modified Effort test with the following exceptions:

1. The soil was placed in the mold using 3 layers with 25 blows per layer.
2. The rammer had a travel of 30.48 cm (12.00 in.) and a mass of 2.495 kg (5.5lb)

The moisture-density relationship, OMC, and ρ_{dmax} for CFA using standard effort were determined.

The compaction characteristics of CFA using reduced effort were determined in accordance with procedure presented by Daniel and Benson (1990). This procedure is the same as the one previously outlined for the Standard Proctor test with the only exception being that the soil was placed in the mold using 3 layers with 15 blows per layer. The moisture-density relationship, OMC, and ρ_{dmax} for CFA using reduced effort were determined.

3.2.5 X-Ray Fluorescence (XRF) Analysis

XRF analysis was performed by the independent GeoAnalytical Laboratory at Washington State University. The molecular constituents of CFA were determined using the XRF testing procedure. Clean dry Ottawa sand was assumed to be 99.8% silica and 0.2% other oxides based on the typical chemical analysis provided by the manufacturer (U.S. Silica Co.).

3.2.6 Particle Morphology

Particle morphology of the Ottawa sand was determined by image analysis using a digital microscope with 200x magnification capabilities. Particle morphology of the CFA was determined at UNC Charlotte using a tunneling electron microscope (TEM).

3.3 Sample Preparation

The goals of this section of the research were to first establish a method of quantifying the degree of hydrophobicity for OS modified soils, then determine the range of treatment ratios over which the soil samples would display varying degrees of hydrophobicity, and finally create samples that were prepared to the varying degrees of hydrophobicity.

3.3.1 Measuring the Contact Angle (θ)

The contact angle was measured using the sessile drop technique (Bachmann et al. 2000). This technique was performed by applying a drop of water to the soil surface and measuring the angle formed at the intersection of the soil and water surfaces. The first step was to prepare planar monolayer soil surfaces for testing. OS modified soils were passed through a No. 20 sieve to remove any agglomerations. Processed material was sprinkled onto double sided tape (3M Part # 112L) affixed to a glass slide (GSC

International Part # 4-13051). The area of the tape was approximately two inches by one inch. Soil was pressed into the tape by applying a clean slide to the surface and weighing the slide with 200g for 10 seconds. The slide was then tapped repeatedly to remove any loose particles. This process of applying soil particles and compressing was repeated two additional times to insure full coverage of the tape and to form a consistent "mono-layer" of soil particles.

Once the slide was prepared it was transferred to a goniometer apparatus which provided a sample holding table capable of being leveled, a backlighting source, and a supporting arm which held a 1.3M USB digital microscope (AVEN model #26700-200) capable of 10X to 200X magnification.

3.3.2 Contact Angle vs. Treatment Ratio

To develop the relationship between the treatment ratio and the contact angle multiple small samples (40-60g) were prepared using a range of treatment ratios. The contact angle was measured using the sessile drop method that was described in the previous section (Sec. 3.3.1). To treat the sand and CFA, carefully prepared solutions of OS and DI water were prepared to 1.0, 0.1, and 0.001 g OS/mL DI water. Using these solutions the soil samples could be dosed with carefully controlled masses of the OS chemical.

Once the 60g samples of sand and 40g samples of CFA were dosed with the appropriate volume of chemical solutions to introduce the desired mass of OS chemical, DI water was added to bring the mixing moisture content of the samples to 40% by mass for the CFA and 25% by mass for the sand. This was done to ensure full saturation of the sample and promote contact between every available OS molecule with every available

bonding site on the soil particle surfaces. Samples were mixed continuously for at least 60 seconds. Samples were allowed to cure for 24-48 hours at 70°C (158°F). The sample drying oven was vented to the exterior of the building in case of any potential hazardous fumes from the curing reaction process.

Once the samples were cured they were processed to remove any agglomerations and transferred to non-reactive, clean, dry, high density polyethylene (HDPE) storage containers. At this time the samples were ready for contact angle measurement. Multiple iterations of this procedure were required to determine the range of treatment ratios that would produce samples of varying degrees of hydrophobicity between θ=90° and the maximum achievable contact angle of approximately θ=125° for the sand and θ=145° for the CFA.

3.3.3 Large Sample Preparation

Large samples were prepared for additional testing once treatment ratios were established. Sand and CFA were oven dried for 24 hr. at 70°C. Next, 2000g to 3000g of material were weighed and placed in a stainless steel mixing pan. The appropriate amount of OS for a given target treatment ratio (and contact angle) was added to a clean dry polyethylene 150ml sample cup with a screw on cap. Water was added to the concentrated OS in the sample cup, the mixture was shaken for 30 seconds, and the solution was added to the soils. Additional water was added to the samples by first placing water in the sample cup used for the OS solution so that all of the chemical could be transferred to the sample. This process was continued until the moisture content of the samples reached 25% and 40% for the sand and CFA respectively.

Once the OS solution was transferred to the soil, the samples were mixed either by hand or using mechanical cake mixer for 5 minutes. Samples were then transferred to drying oven set at 70°C for 24 to 48 hours, or until the mass of the sample stabilized. Cured samples were removed from the oven and covered to allow time for cooling.

Once cooled the samples were processed by breaking up any aggregations by hand or using a pestle and passing through a #10 sieve. Any material that did not initially pass through the sieve was further processed until all material passed through the sieve. Processing of the CFA samples was performed in a fume hood to mitigate excessive dust propagation. After processing, the samples were sealed and stored in clean and dry plastic bags.

3.4 Water Entry Pressure (WEP)

Water entry pressures (WEP's) were measured using apparatus and procedures adapted from previous examples in the literature (Fink and Myers 1969; Fink 1970; Carrillo et al. 1999; Wang et al. 2000).

3.4.1 WEP of Hydrophobic Sand

A permeameter (Humboldt model HM-3892) was used as a confining cell to hold the compacted sand samples for WEP testing. The sample was prepared using dry cured material. Before each test the permeameter was cleaned and dried, and the bottom porous stone (Humboldt model # HM-4184.247) and filter paper (Humboldt model #HM-4189.25) were installed. Sand was placed in the cell using three methods depending on the target compaction level.

For the lowest density samples ($\rho = 1.56$ g/cm^3) soil was placed in a graduated cylinder, placed in the permeameter, inverted, and slowly withdrawn from the cylinder to prepare the sample to the loosest possible state.

For the medium density level ($\rho = 1.66$ g/cm^3) the soil was placed in the sample similar to the loose preparation, but then it was compacted by tapping the cell with a rubber mallet. The tapping of the cell was continued until the desired sample height, and therefore volume and density were achieved.

For the highest density level ($\rho = 1.76$ g/cm^3) the soil was placed in the cell in 1" compaction lifts, and each lift was compacted by vibration and tamping. Once the desired mass of sand was inserted into the cell a top cap and surcharge of 2 psf was applied while vibrating the cell on a vibratory table for 8 minutes or until the desired sample height was achieved.

After the sample was prepared to the desired density the top filter paper, porous stone, and cap were installed. Care was taken to avoid jarring the prepared samples to prevent any density changes. It was also important to make sure the top porous stone was completely dry and the top cap was vented to prevent any backpressure. Next, cell was connected to a standpipe capable of applying positive water pressure to the bottom surface of the sand. The height of water in the standpipe was slowly increased to reach the height of the bottom sand sample in the cell. Care was taken to ensure the water lines, permeameter base, bottom porous stone and bottom filter paper were fully saturated before beginning the test.

The WEP test proceeded by increasing the pressure head until infiltration was initiated. The pressure head was increased in increments of 1cm of H_20 approximately

every 10 seconds by adding a set volume of water to the standpipe. This rate of pressure increase was continued until the WEP was reached. The critical WEP value was identified by a drop in the height of water in the standpipe, visual confirmation of infiltration into the sample, or both. See figures 63 through 65 in Appendix B for images of the testing procedure.

3.4.2 WEP of Hydrophobic CFA

A different setup was required to measure the WEP of the CFA and address challenges associated with using an extremely hydrophobic fine grain material. This included difficulties de-airing the cell, sidewall leakage, substantially higher WEP's resulting in sample displacement, and volume change of the sample. A constant head sand/gravel permeameter (ELE International model ELE25-0562) with monometer ports was modified to function as the confining cell for the WEP testing of hydrophobic CFA. Rigid spacers were inserted into the cell to bring the height of the sample down to approximately 2" high. This served three functions:

1. Reducing the volume of the sample to limit volume change during application of water pressure
2. Aligning the bottom porous stone with a manometer port to allow for de-airing of the cell
3. Locking the sample in place within the cell to prevent any displacement of the sample due to high water entry pressures

The permeameter cell was cleaned and dried before each test, and the inside of the cell wall was coated with a Teflon dry film lubricant. The bottom rigid spacer was then inserted into the cell followed by a porous stone and filter paper. The porous stone was

prepared by wrapping an oversized filter paper around the porous stone and affixing with tape. The wrapped porous stone was then sealed to the cell sidewall using a bentonite seal. The Teflon dry film lubricant and the bentonite seal both contributed to mitigating sidewall leakage. CFA was then added to the cell and prepared to low, medium and high density levels (1.02, 1.12, and 1.22 g/cm^{3}respectively) using compaction techniques similar to those for the sand material. After the sample was prepared the top filter paper, porous stone, rigid spacer and top cap were applied.

WEP testing of the CFA proceeded in a similar fashion to that of the sand with the following two exceptions. First, the rate of pressure increase was approximately 5cm of H_20 per 10s. Secondly, once the WEP reached a value of approximately 300cm of H_20, compressed air was applied to the standpipe and the additional pressure was measured with a pressure gauge. In this way pressures up to 1000cm of H_20 could be applied. See figures 66-78 in Appendix B for images of the testing procedure.

3.5 Hydraulic Conductivity

The hydraulic conductivity of the sand was determined in accordance with ASTM D2434 "Standard Test Method for Permeability of Granular Soils (Constant Head)." The hydraulic conductivity of the CFA was determined in accordance with "Suggested Method of Test for Permeability of Porous Granular Materials by the Falling-Head Permeameter" which was proposed by Gray (1970). Prepared samples from the WEP testing were used for the hydraulic conductivity testing immediately following the WEP testing since they were already prepared to the target hydrophobicity levels, density levels, and saturated during the course of WEP testing.

3.6 Soil Water Characteristic Curve

The soil water characteristic curve was determined utilizing a dewpoint potentiometer (or chilled mirror hygrometer) in accordance with methods presented by Decagon Devices (2010) and ASTM D6836 (2008). A Decagon Devices model WP4c dewpoint potentiometer was used to determine the soil suction (kPa) for samples prepared to a range of moisture contents at a given density. With this method, to determine the wetting isotherm (or wetting/sorption curve), a sample was prepared to a desired density in the dry condition. Water was then added to the sample to increase the volumetric moisture content by approximately 2% or less. The sample was then covered and allowed to come to equilibrium for 24 hours. The sample was then placed in the WP4c dewpoint potentiometer and the soil suction determined based on the relative humidity of the air above the sample once the sample had come to temperature equilibrium within the sealed testing chamber. This process of increasing the moisture content, allowing for equilibration time, and testing the sample was repeated until the saturation point was reached and the suction readings decreased to zero.

The procedure was altered to prepare the drying isotherm (or drying/desorption curve). Starting with a saturated sample, the sample was heated to remove a predetermined mass of water which decreased the volumetric moisture content by approximately 2%. Once the desired mass of water was removed from the sample, the sample was covered and allowed to come to temperature and moisture equilibrium for 24 hours. The sample was then placed in the WP4c dewpoint potentiometer and the soil suction was recorded. The process of drying the sample, allowing for equilibration, and testing the sample was repeated until the sample was completely dry. The soil water

characteristic curve was developed showing the relationship between volumetric moisture content and matric suction.

It is important to note that the relative humidity method measures the total suction value. Total suction (ψ_T) is the sum of osmotic suction (ψ_O) and matric suction (ψ_M). To be able to present the SWCC in terms of matric suction the osmotic suction component of the total suction was removed. This was done by measuring the electrical conductivity (EC) of a solution of CFA and DI water and using the following relationship to determine osmotic suction:

$$\psi_O = -EC \times 0.036 \quad \text{(kPa)} \tag{14}$$

The sand was assumed to have an osmotic suction equal to zero as de-ionized water and pure silica sand (99.8% Silicon Dioxide) were used in the testing procedure.

SWCC testing was also performed by Dr. Ning Lu and Dr. Alexandra Wayllace at the Colorado School of Mines (CSM)/United States Geological Survey (USGS) Geotechnical Testing Laboratory using the recently developed Transient Water Release and Imbibition Method (TRIM) (Wayllace and Lu 2012).

3.7 Pore Size Distribution

Pore size distributions were developed from the SWCC results using a technique presented by Lu and Likos (2004). In general, for an increment or decrement of soil suction, the thickness of the adsorbed water film on the soil particle surfaces was calculated from the relative humidity and moisture content data from the SWCC. This thickness was added to the air filled pore radius (or Kelvin radius) to obtain the pore radius. This method of preparing the pore size distribution is analogous to determining the specific surface of soil particles by nitrogen adsorption.

3.8 Experimental vs. Predicted WEP

As previously mentioned the Washburn equation (Eq. 4) for capillary rise can be used to predict the WEP based on the contact angle and pore diameter of the samples. The contact angle (θ) was determined by the sessile drop technique (Bachmann 2000). Pore diameters as determined by a numerical integration technique utilizing the SWCC (Lu and Likos 2004) as well as empirical relationships to simple cubic packing and tetrahedral packing of spheres were used to predict the pressure head required to initiate infiltration into the hydrophobic sand and CFA. These results were compared to the experimental WEP values.

CHAPTER 4: RESULTS

4.1 Moisture Content

Moisture content of the soil is reported for the "as-delivered" state. The CFA was collected from moisture conditioned CFA material at a southeastern coal combustion power plant location. Material was stored and transported in sealed 5 gallon buckets. The moisture content should be representative of moisture conditioned CFA before placement and compaction at the coal ash landfill from which it was sampled. The moisture content of the CFA in "as-delivered" state was 29.7%. The moisture content of the sand in the "as-delivered" state was 1.9%.

4.2 Specific Gravity

The specific gravity of the Ottawa sand as determined by the water pycnometer method was 2.65. The specific gravity of the CFA was determined to be 2.22.

4.3 Particle Size Analysis

The particle size distribution was determined for both untreated sand and untreated CFA. The results are displayed in Figure 7 and Table 6**Error! Reference source not found.** respectively. Select particle diameters and the uniformity coefficient (C_u) are displayed in the following table:

Table 6: Particle diameters and coefficient of uniformity from particle size analysis

Material	D_{10}	D_{15}	D_{60}	C_u
	(mm)	(mm)	(mm)	(-)
Sand	0.440	0.455	0.630	1.43
CFA	0.014	0.017	0.034	2.43

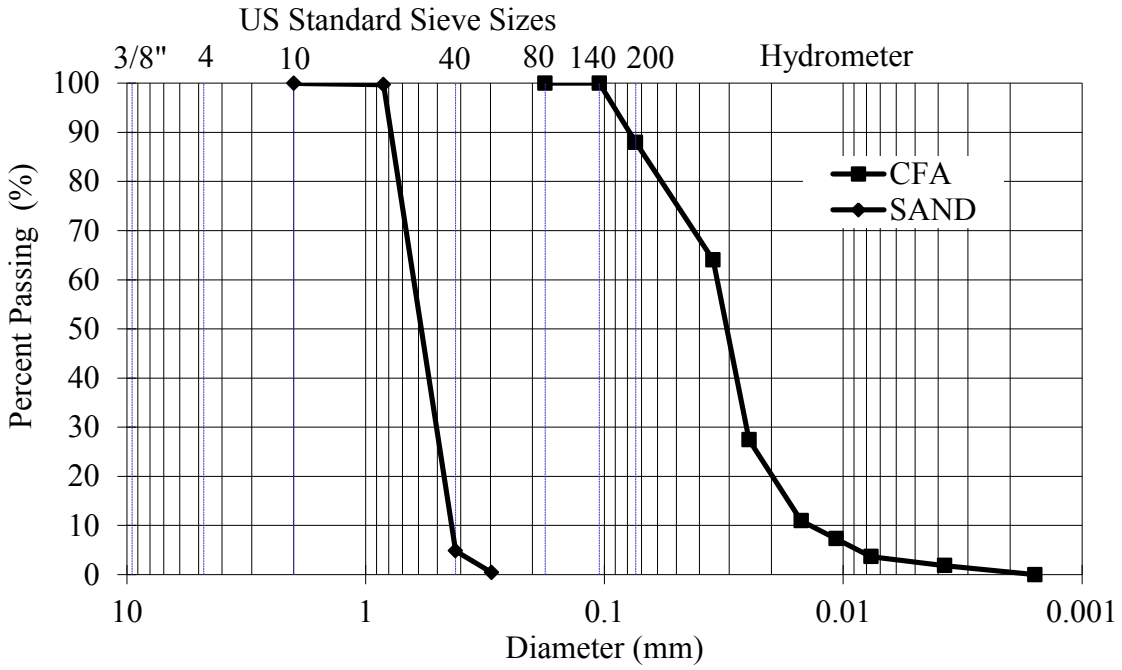

Figure 7: Particle size distribution of sand and CFA

4.4 Compaction Characteristics

The compaction characteristics of the sand and CFA are presented in Table 7 and Figure 8. The maximum dry unit weight, maximum dry density, and optimum moisture content are reported for untreated coal fly ash.

Table 7: Compaction characteristics of CFA

Compaction Energy	(-)	Reduced Effort	Standard Effort	Modified Effort
Optimum Moisture Content, OMC	(%)	26	33	36
Maximum Dry Unit Weight, $\gamma_{d,max}$	(kN/m^3)	10.79	11.03	11.95
	(pcf)	68.7	70.2	76.07
Maximum Dry Density, $\rho_{d,max}$	(g/cm^3)	1.08	1.12	1.22

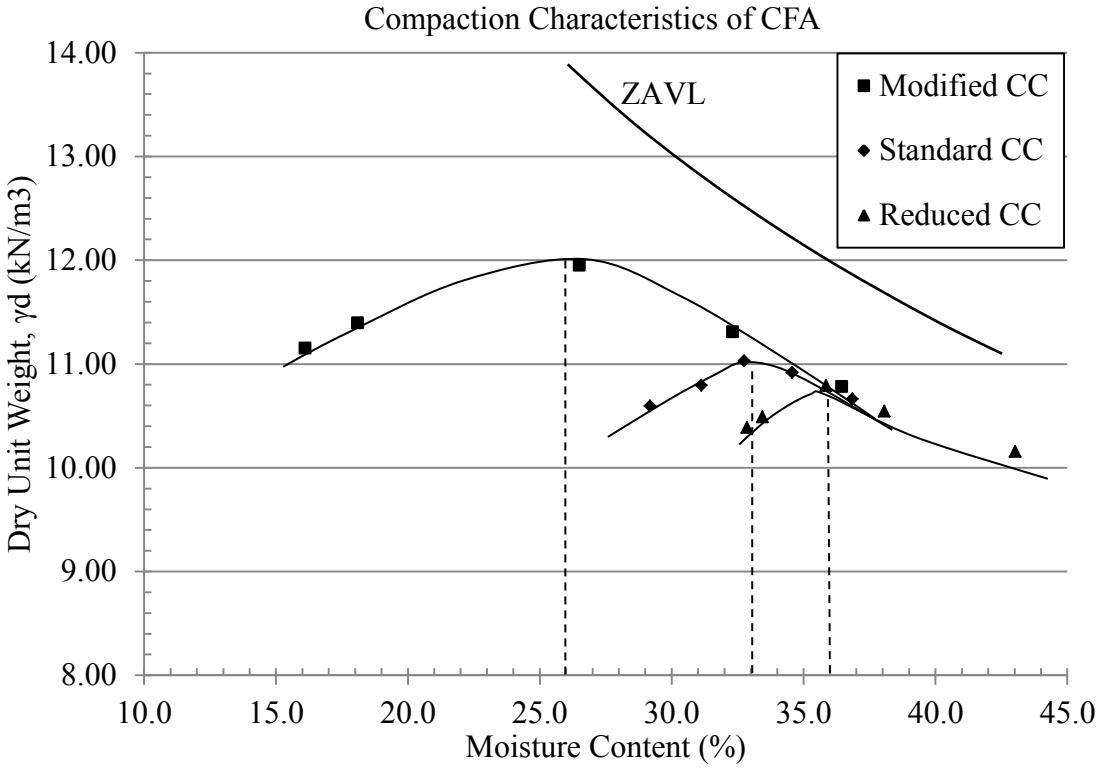

Figure 8: Moisture-density relationship for CFA

4.5 XRF Analysis (Particle Mineralogy)

The chemical composition of CFA as determined by XRF analysis is displayed in Table 8 below. It shows that the two major constituents in CFA are silica (SiO_2) and alumina (Al_2O_3) which represent 51.5% and 26.9% of the CFA mass respectively. Trace

elements account for 0.35% of the mass of CFA. The Ottawa sand was not analyzed for chemical composition, although the manufacturer reports it as being 99.8% silica (SiO_2) with trace amounts of other oxides.

Table 8: Chemical composition of CFA

Non-Normalized Major Elements (Weight %)		Non-Normalized Trace Elements (ppm)			
SiO_2	51.53	Ni	111	Ga	65
TiO_2	1.44	Cr	168	Cu	186
Al_2O_3	26.85	Sc	40	Zn	120
FeO*	5.14	V	293	Pb	75
MnO	0.01	Ba	786	La	89
MgO	0.76	Rb	124	Ce	181
CaO	0.99	Sr	653	Th	32
Na_2O	0.26	Zr	261	Nd	82
K_2O	2.37	Y	117	U	17
P_2O_5	0.19	Nb	30.2	Cs	10
				As >/=	15
Sum	89.55				
LOI (%)	9.63				
Sum of Trace Elements (ppm)					3465
Trace Elements Percent Weight (%)					0.35
Sum of Percent Weight (Major + Trace)					89.89
Sum of Percent Weight (Major + Trace + Toxides)					89.98
With LOI					99.61
* if $Fe3^+$ Present					100.18

4.6 Image Analysis (Particle Morphology)

Microscopic image analysis of the Ottawa sand, shown in Figure 9 and Figure 10, reveals a predominantly rounded shape. SEM image analysis for the CFA, shown in Figure 11 and Figure 12, shows a spherical and amorphous shape for the CFA.

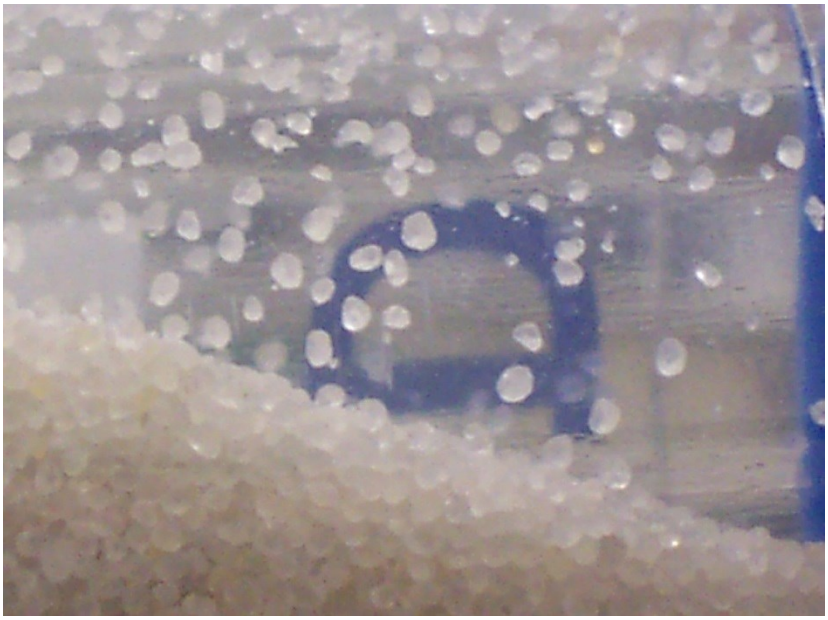

Figure 9: Microscopic image of Ottawa sand

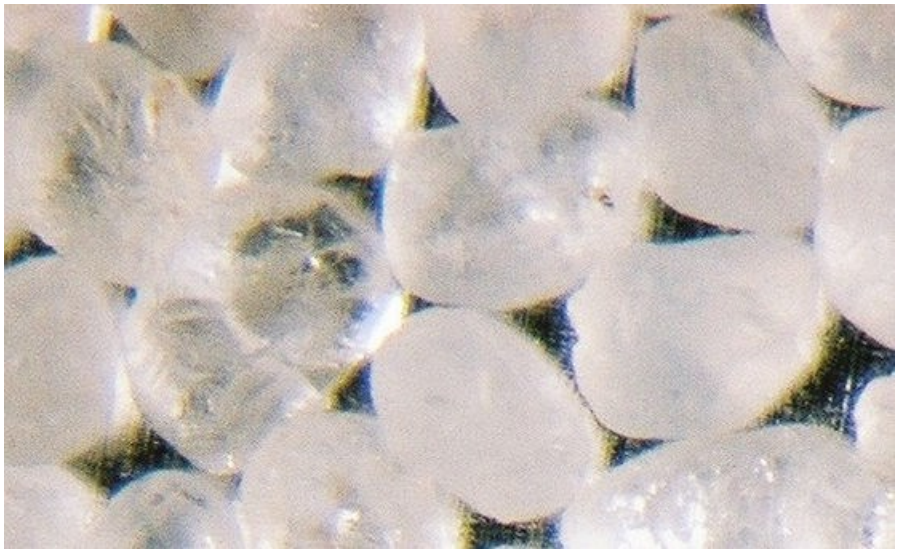

Figure 10: U.S. Silica Ottowa sand under 45X magnification

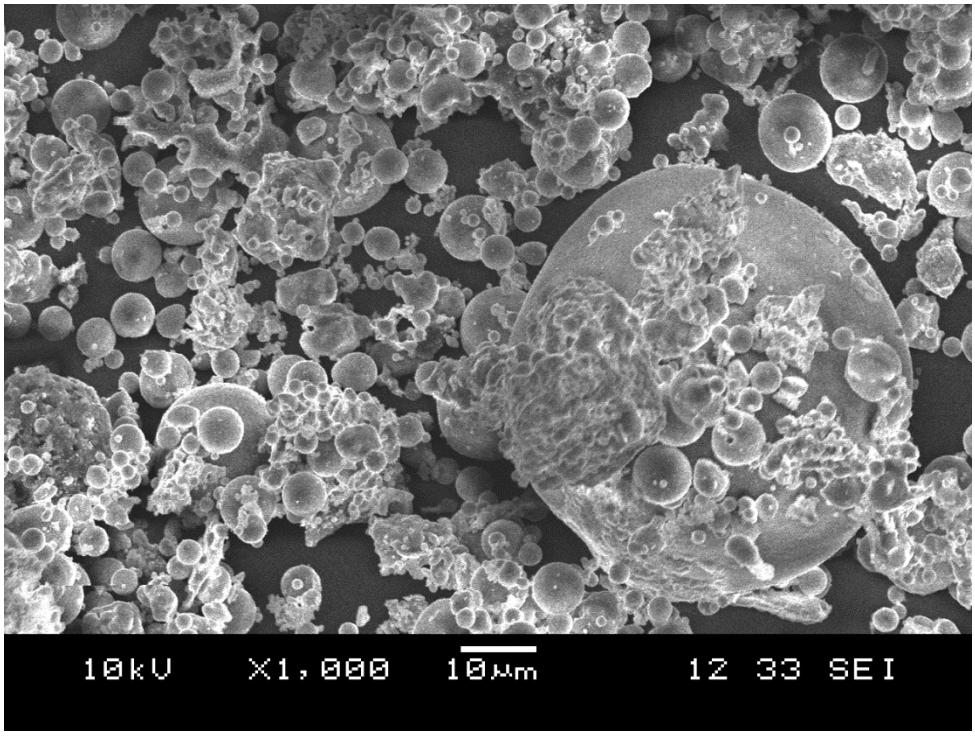

Figure 11: SEM image of CFA (magnification x1000)

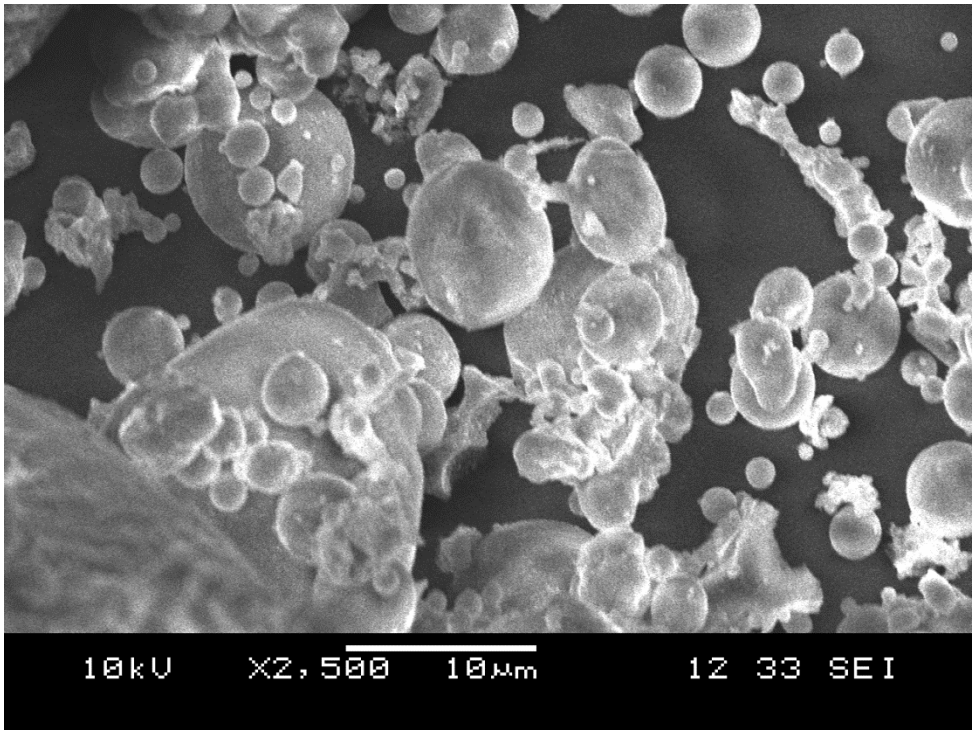

Figure 12: SEM image of CFA (magnification x2500)

4.7 Treatment Ratio vs. Contact Angle

The relationship between treatment ratio and contact angle was determined for both sand and CFA using two OS chemical on each material. The results of this testing are displayed below in Figure 13, Figure 14, Figure 15, and Figure 16.

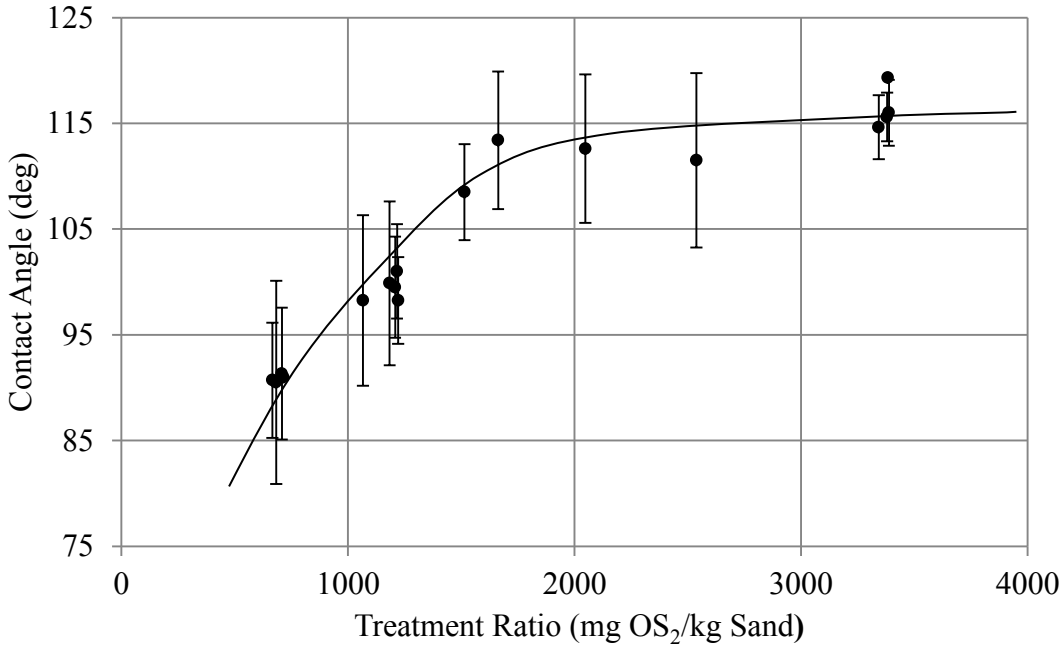

Figure 13: Contact angle vs. treatment ratio for sand and OS_2

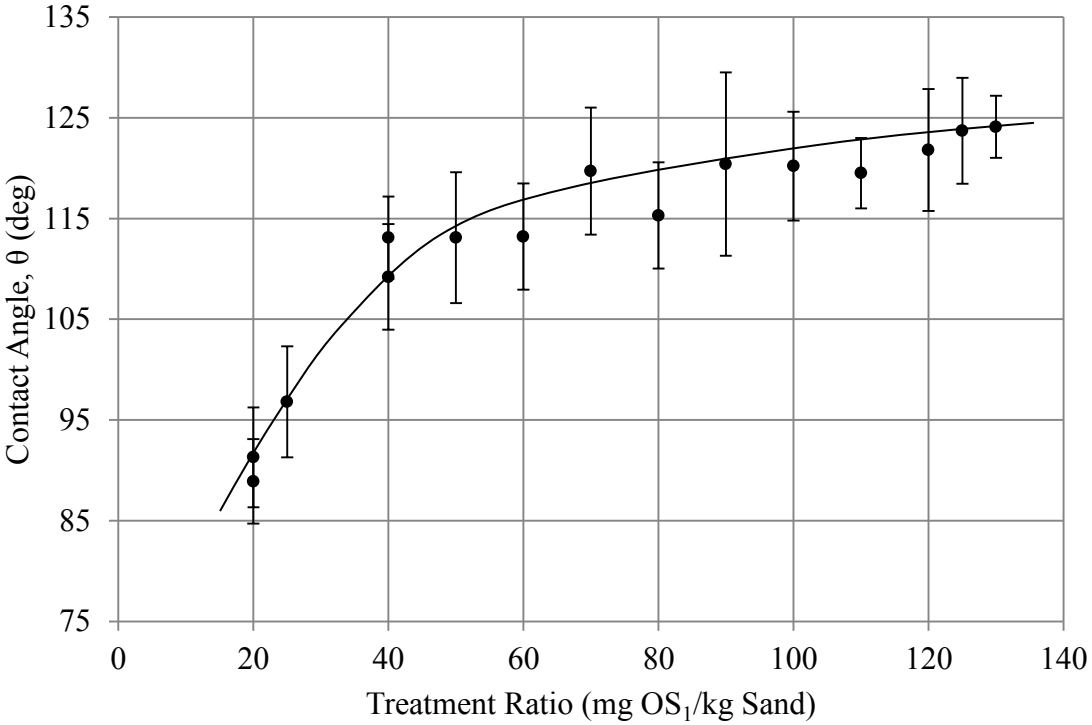

Figure 14: Contact angle vs. treatment ratio for sand and OS_1

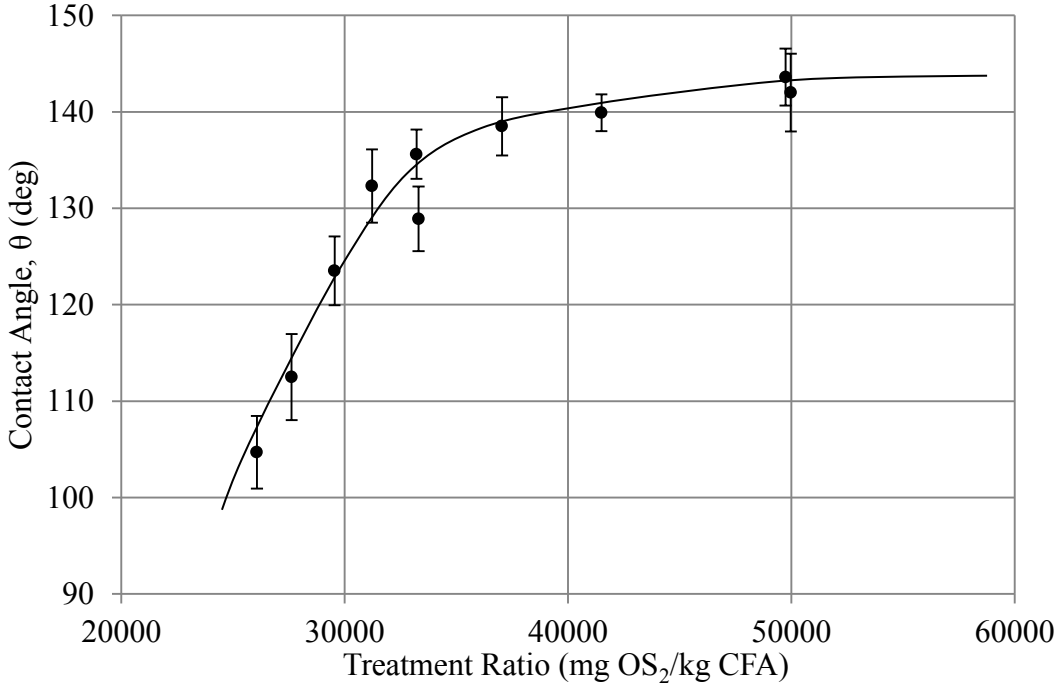

Figure 15: Contact angle vs. treatment ratio for CFA and OS_2

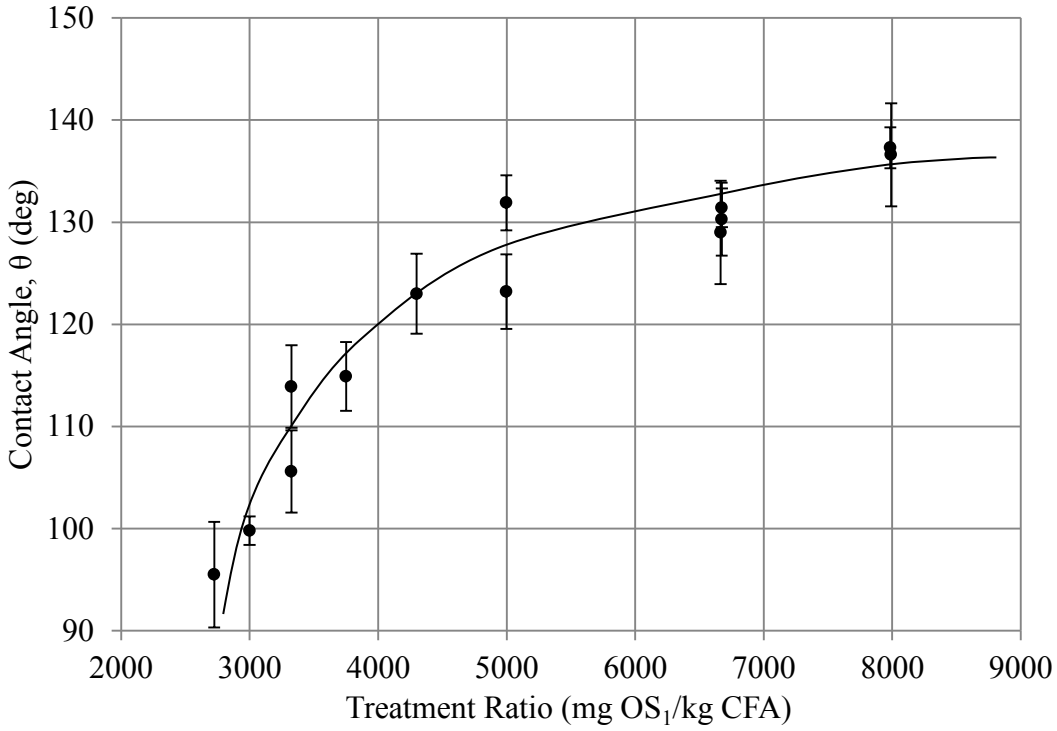

Figure 16: Contact angle vs. treatment ratio for CFA and OS_1

4.8 Water Entry Pressure

The water entry pressure of the hydrophobic sand and CFA was determined over a range of hydrophobicity and compaction levels. The sand was able to resist infiltration of pressures between 10 and 14 cm of H20 at the highest treatment levels and compaction levels for the two OS treatment chemicals used. The CFA was able to resist infiltration up to pressures in excess of 500cm of H_2O at the highest treatment and compaction levels for the material treated with OS_2. The CFA treated with OS_1 was found to be hydrophilic at all treatment levels and compaction levels. Multiple sample preparations were attempted for CFA treated with OS_1. Figures 18, 19 and 20 present the results of water entry pressure testing on the hydrophobic sand treated with OS_1, hydrophobic sand treated with OS_2, and hydrophobic CFA treated with OS_2 respectively.

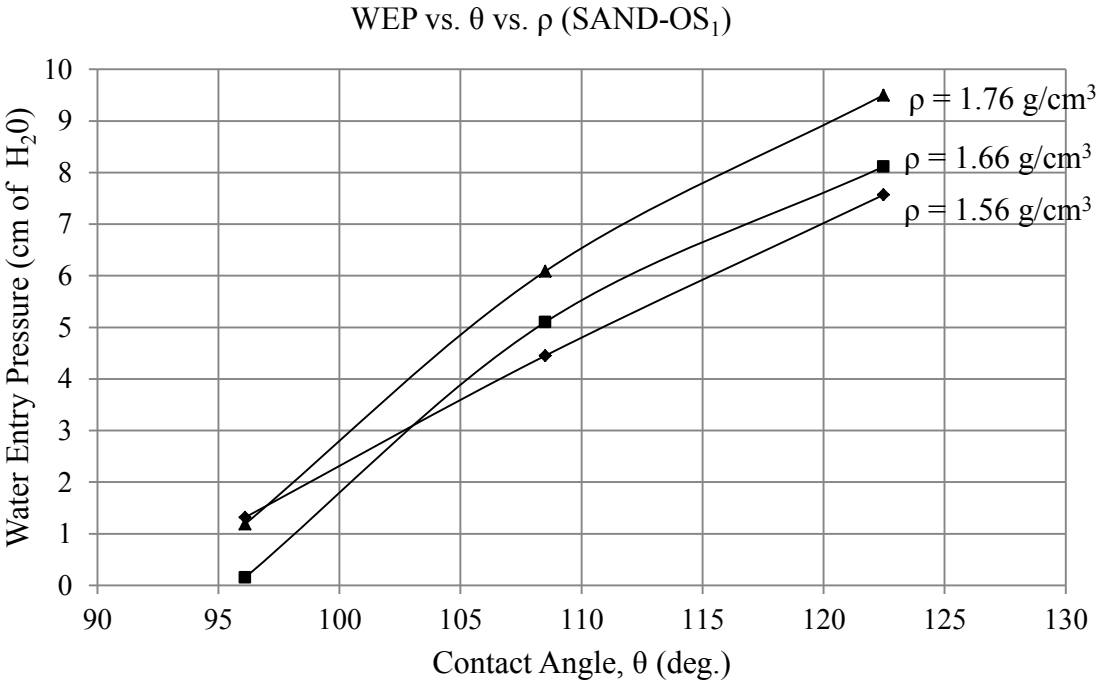

Figure 17: Water entry pressure of sand treated with OS_1

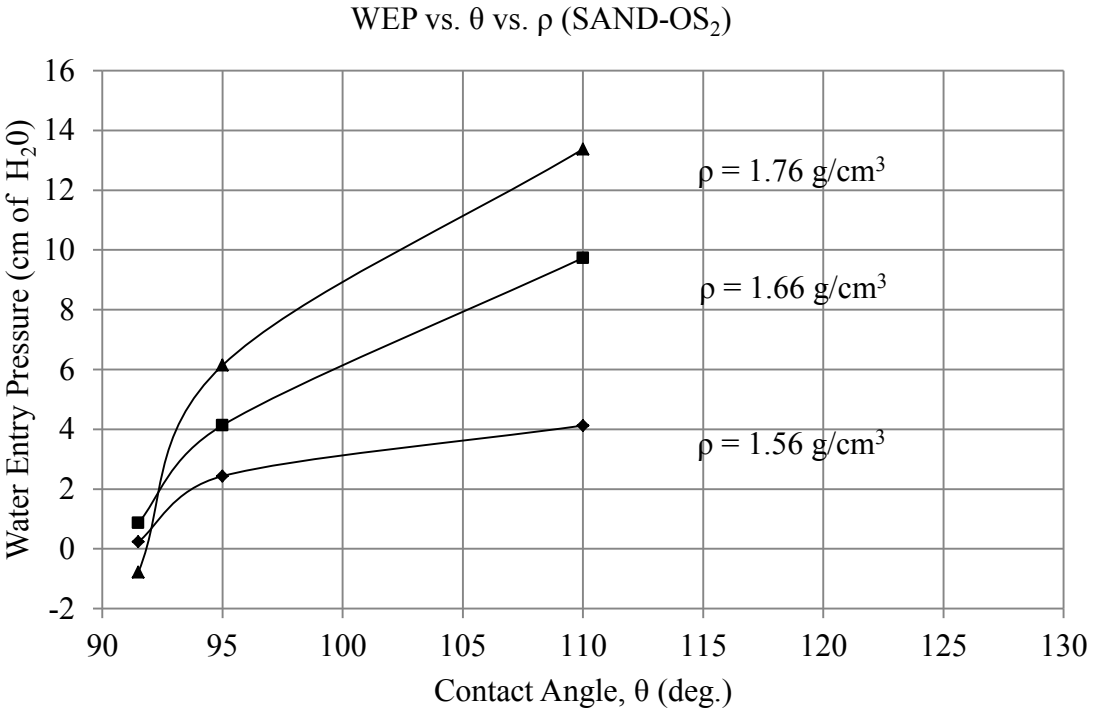

Figure 18: Water entry pressure of sand treated with OS_2

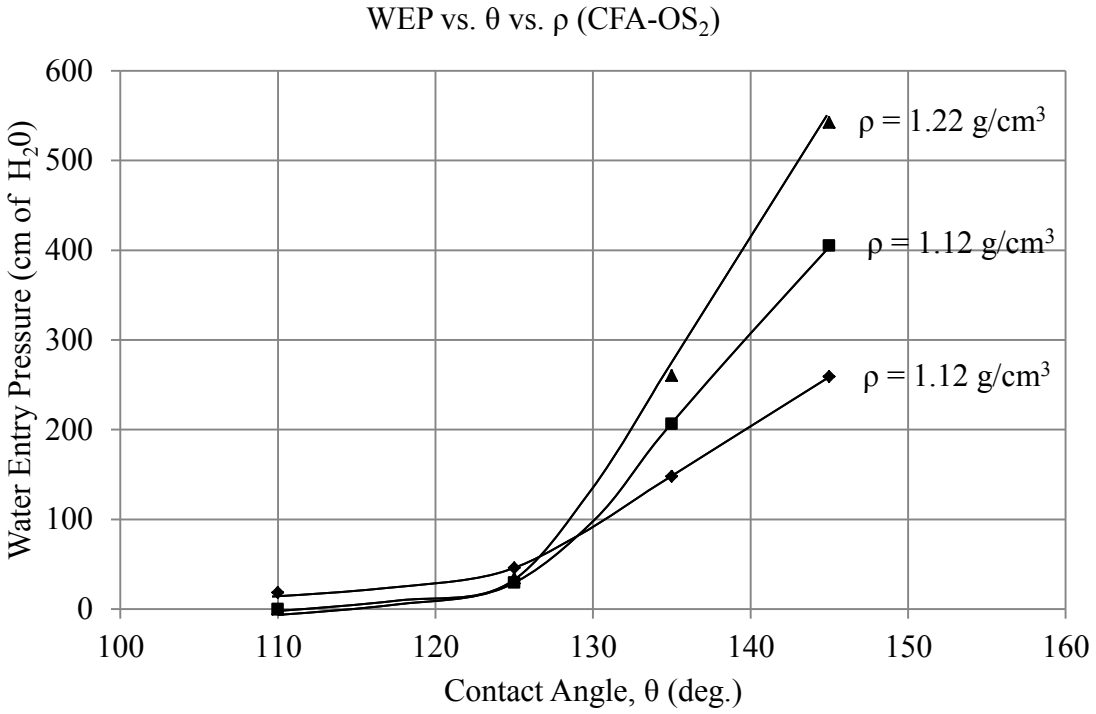

Figure 19: Water entry pressure of CFA treated with OS_2

4.9 Hydraulic Conductivity

Saturated hydraulic conductivity was determined for the untreated and treated sand. Generally, the saturated hydraulic conductivity (k_{sat}) of the sand ranged from 0.022 to 0.033 cm/s at 20°C. Untreated sand was 100% saturated during testing. Saturation of the treated sand ranged from 87% to 94% during testing. Results of the hydraulic conductivity testing are presented in Table 9 and Figure 20.

Table 9: Hydraulic conductivity of untreated and treated sand

Hydraulic Conductivity @ 20°C			
Contact Angle, θ (degree)	Target Density (g/cm^3)		
	1.56	1.65	1.76
Untreated	0.0290	0.0316	0.0297
92	0.0324	0.0281	0.0219
96	0.0335	0.0221	0.0225
112	0.0336	0.0226	0.0318
118	0.0285	0.0291	0.0245
Average	0.0314	0.0267	0.0261
Std. Dev.	0.0025	0.0042	0.0044

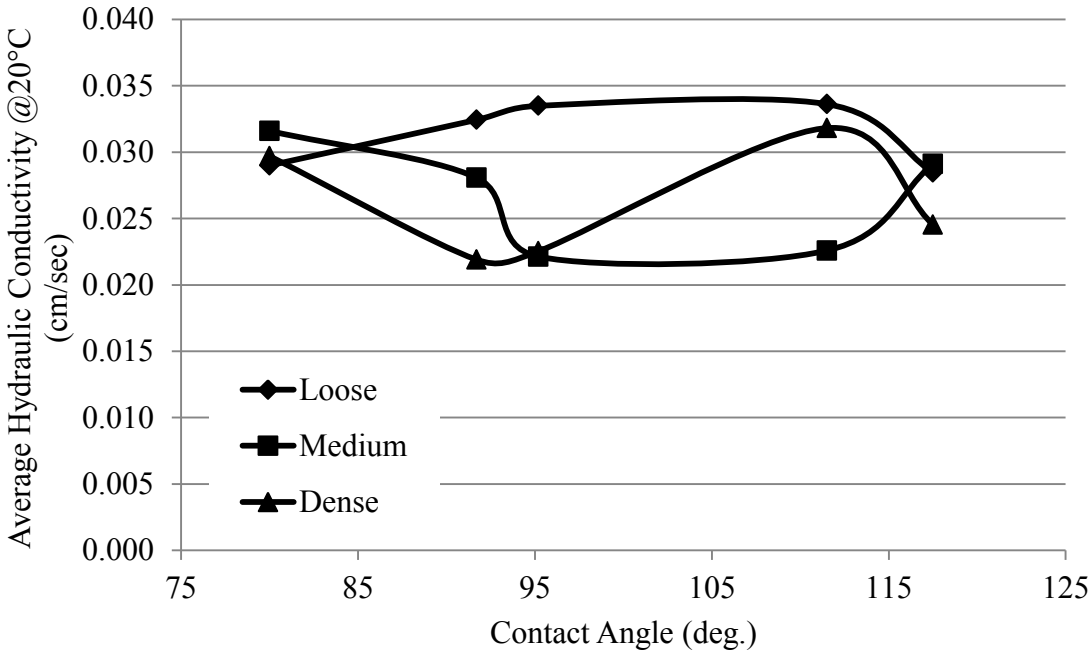

Figure 20: Hydraulic conductivity of sand vs. varying degrees of hydrophobicity and compaction levels

The hydraulic conductivity of treated and untreated CFA was attempted. Untreated CFA was found to have a hydraulic conductivity of $4x10^{-5}$ cm/s. Hydraulic conductivity of the treated material was not possible using standardized testing procedures.

4.10 Soil Water Characteristic Curves

Soil water character curve testing was performed at the CSM/USGS laboratory by Dr. Alexandra Wayllace and Dr. Ning Lu using the TRIM Method (Wayllace and Lu 2012). The SWCC and hydraulic conductivity function (HFC) were determined for the untreated sand, treated sand, and untreated CFA. The testing of the treated CFA was not possible due to inability of saturating the sample during the TRIM testing procedure. Samples were prepared and tested to the parameters shown in Table 10. Van Genuchten curve fitting parameters are presented in Table 11. Results of the SWCC testing are shown in Figure 21, Figure 22, and Figure 23.

Table 10: TRIM method sample preparation parameters

Samples	Dry density (g/cm^3)	Gs	Porosity
Sand untreated	1.66	2.65	0.3736
Sand treated	1.66	2.65	0.3736
CFA untreated	1.12	2.22	0.4955
CFA treated	1.12	2.22	0.4955

Table 11: SWCC and HCF modeling parameters (TRIM method)

Samples	SWRC and HCF wetting					SWRC and HCF drying				
	a (kPa^{-1})	n	θ_r	θ_S	k_{sat} (cm/s)	a (kPa^{-1})	n	θ_r	θ_S	k_{sat} (cm/s)
Sand untreated	1.77	2.14	0.05	0.32	5.00E-02	0.6	2.04	0.05	0.37	1.35E-02
Sand treated	2.04	3.53	0.03	0.29	1.00E-02	1.22	1.89	0.03	0.35	2.90E-02
CFA untreated	0.05	1.75	0.04	0.45	1.30E-05	0.02	1.94	0.04	0.5	1.50E-05
CFA treated	-	-	-	-	-	-	-	-	-	-

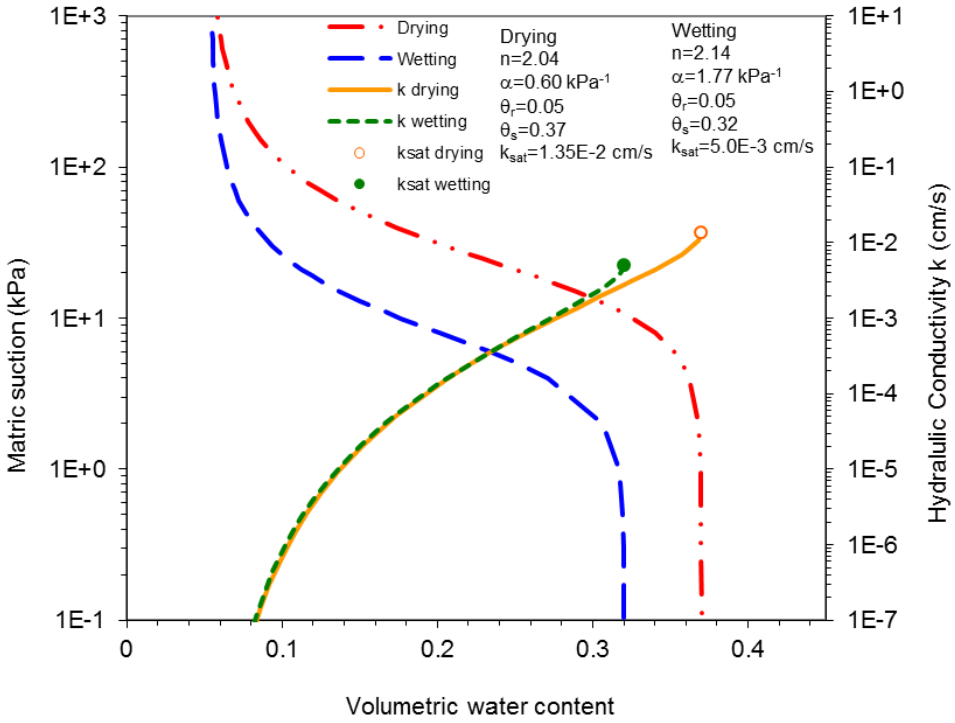

Figure 21: SWCC and HCF for untreated sand (TRIM method)

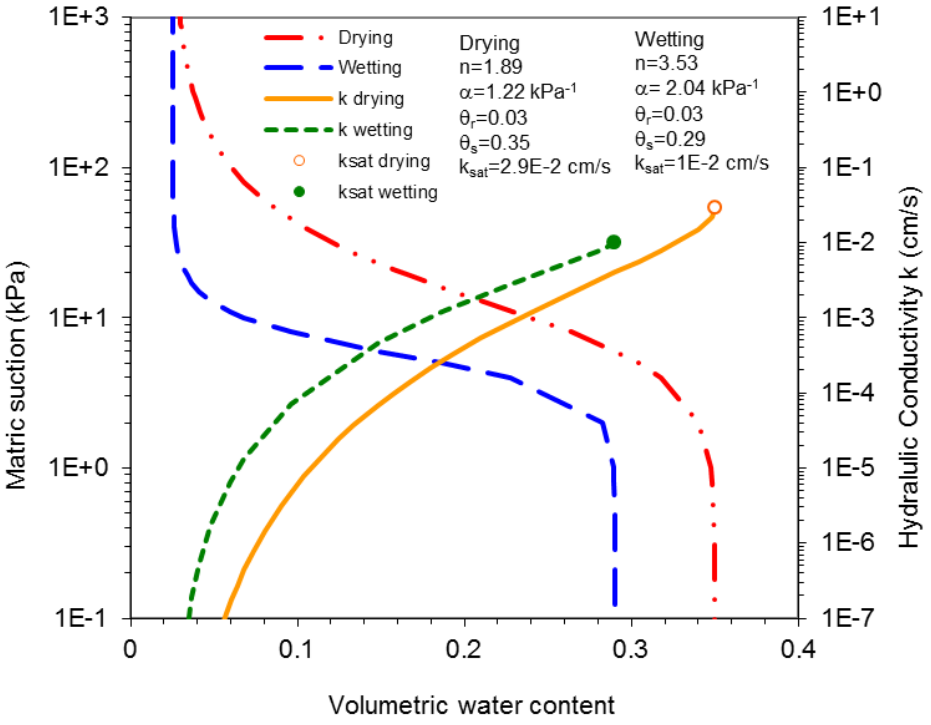

Figure 22: SWCC and HCF for treated sand (TRIM method)

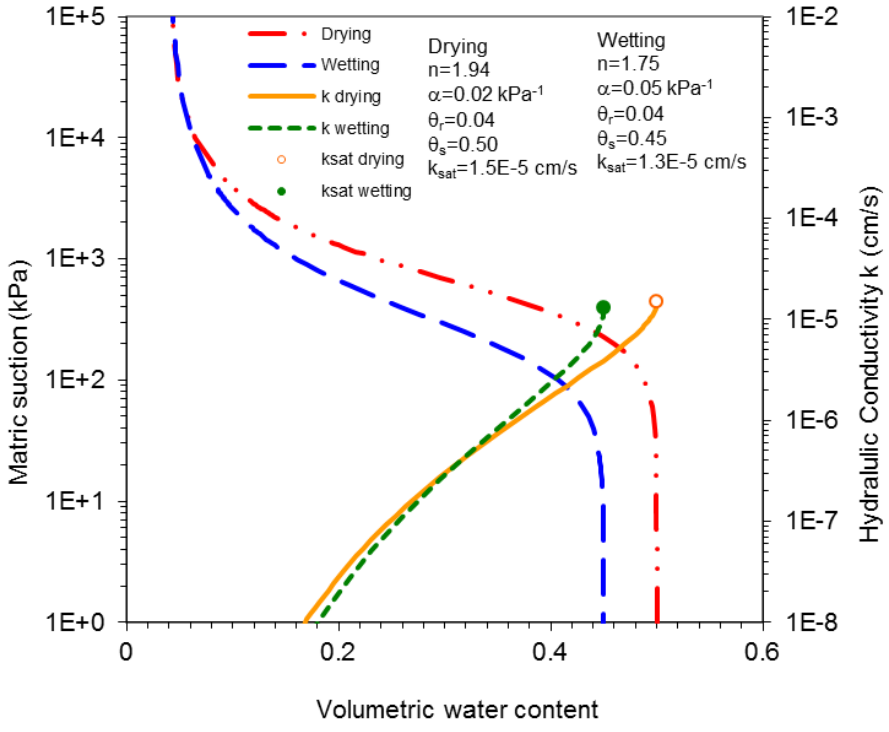

Figure 23: SWCC and HCF for untreated CFA (TRIM method)

SWCC testing of the untreated CFA was also performed at UNC-C using a dewpoint potentiometer (Decagon WP4c). The SWCC data was modeled using the Brooks and Corey (BC), van Genuchten (VG), and Fredlund and Xing (FX) fitting parameters. Fitting parameters for the aforementioned models are presented in Table 12. The drying and wetting curves for untreated CFA as determined by the decagon WP4c are presented in Figure 24, and a comparison of the three models is presented in Figure 25.

Table 12: SWCC modeling parameters for untreated CFA (Dewpoint Potentiometer)

Model	Parameter		Value
BC	ψ_a	Air Entry Suction Head (kPa)	33.763
	λ_r	Pore-Size Dist. Index	0.36391
	Θ_r	Residual MC	0
VG	α	Pivot Point (~ψa)	0.008623
	n	Slope About Pivot	1.622
	m	Rotation of Sloping Portion	0.383477
	Θ_s	Saturated MC	0.39282
	Θ_r	Residual MC	0
FX	a	~α	150
	b	~n	1.4
	c	~m	1.5
	Θ_s	Saturated MC	0.40933
	Θ_r	Residual MC	0.0

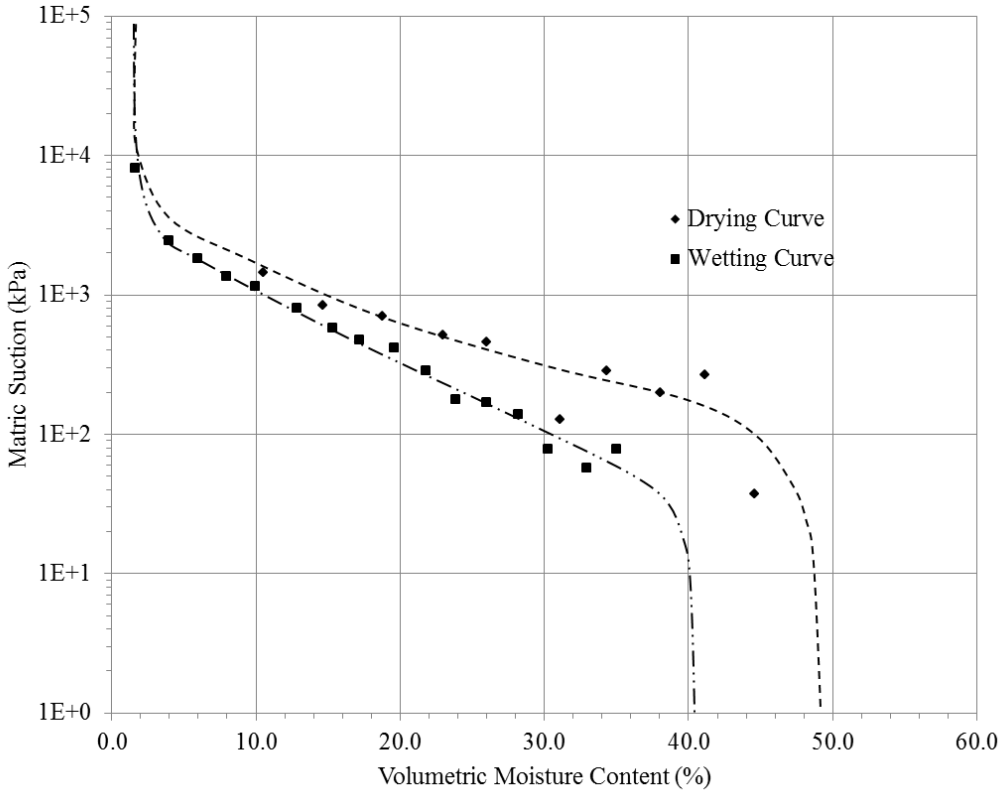

Figure 24: SWCC for untreated CFA (Dewpoint Potentiometer)

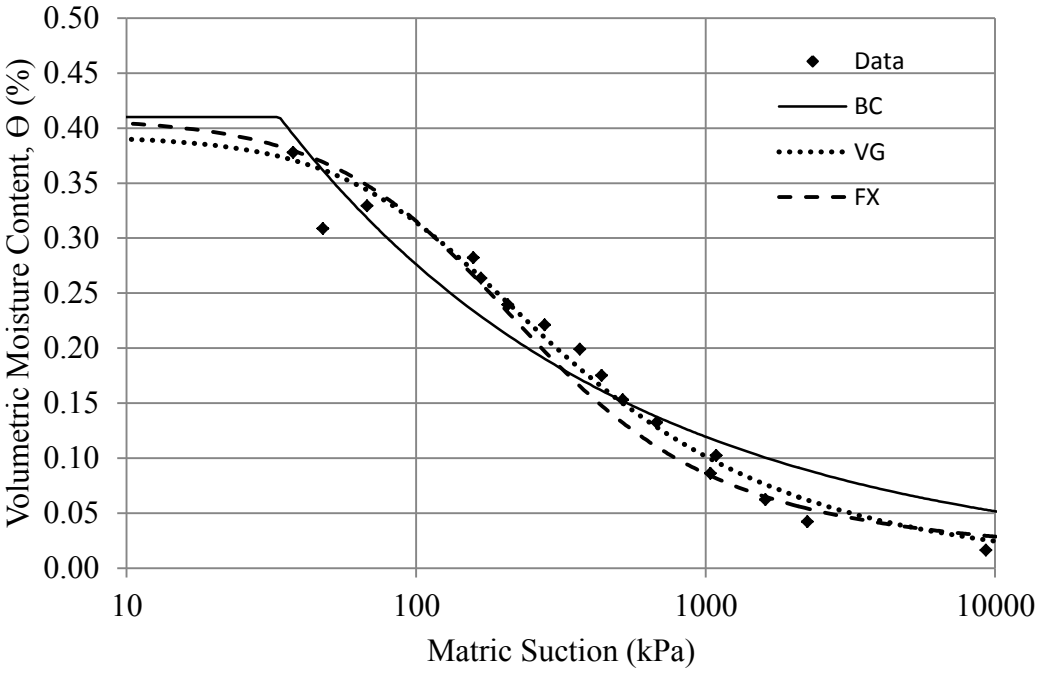

Figure 25: Comparison of three models for SWCC (Dewpoint Potentiometer)

4.11 Pore Size Distribution

The pore size distribution for the untreated sand compacted to 1.66 g/cm^3 was determined using the wetting curve of the SWCC based on a numerical integration procedure presented by Lu and Likos (2004). The majority of pore diameters for the untreated sand sample were between 0.048 and 0.380mm, and the average pore diameter was determined to be 0.214mm. The wetting curve of the SWCC in terms of matric suction and gravimetric moisture content for the untreated sand sample is displayed in Figure 26. Figure 27 illustrates the pore volume per unit mass versus average pore radius, and Figure 28 shows the cumulative pore volume per unit mass versus average pore radius.

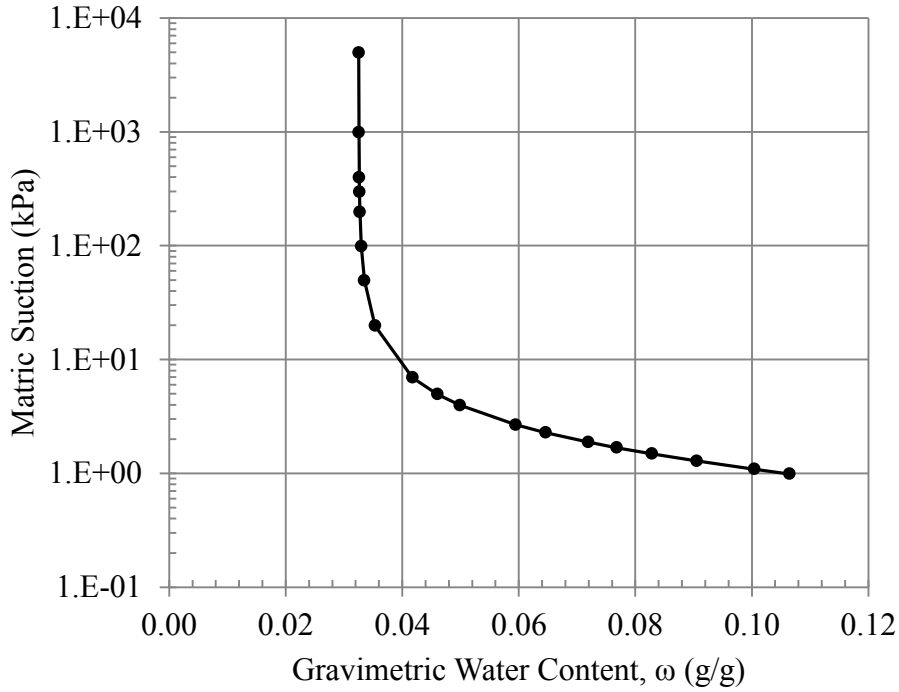

Figure 26: SWCC used for pore size distribution (sand)

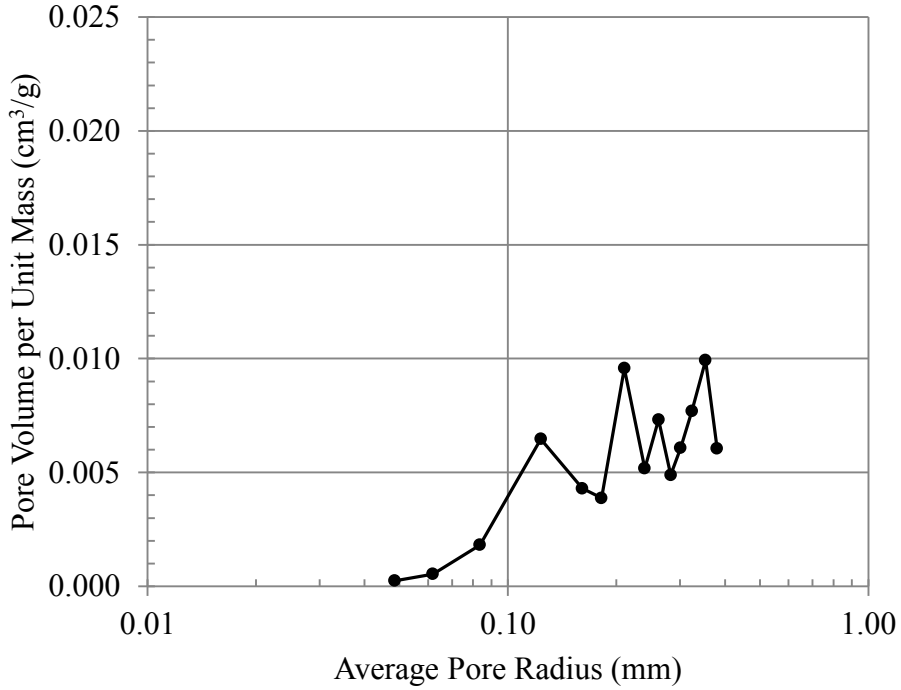

Figure 27: Pore volume per unit mass vs. average pore radius (sand)

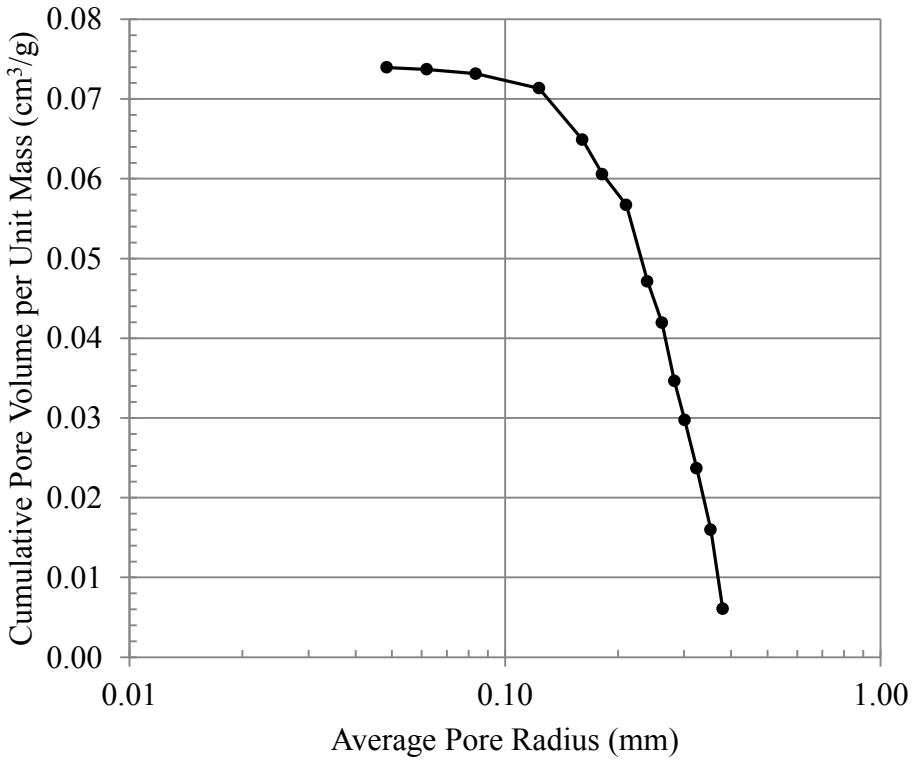

Figure 28: Cummulative pore volume per unit mass vs. average pore radius (sand)

The pore size distribution for the untreated CFA compacted to 1.12 g/cm^3 was also determined using the wetting curve of the SWCC. The majority of pore diameters for the untreated CFA sample were between 0.005 and 0.235mm, and the average pore diameter was determined to be 0.120mm. The wetting curve of the SWCC in terms of matric suction and gravimetric moisture content for the untreated sand sample is displayed in Figure 29. Figure 30 illustrates the pore volume per unit mass versus average pore radius, and Figure 31 shows the cumulative pore volume per unit mass versus average pore radius.

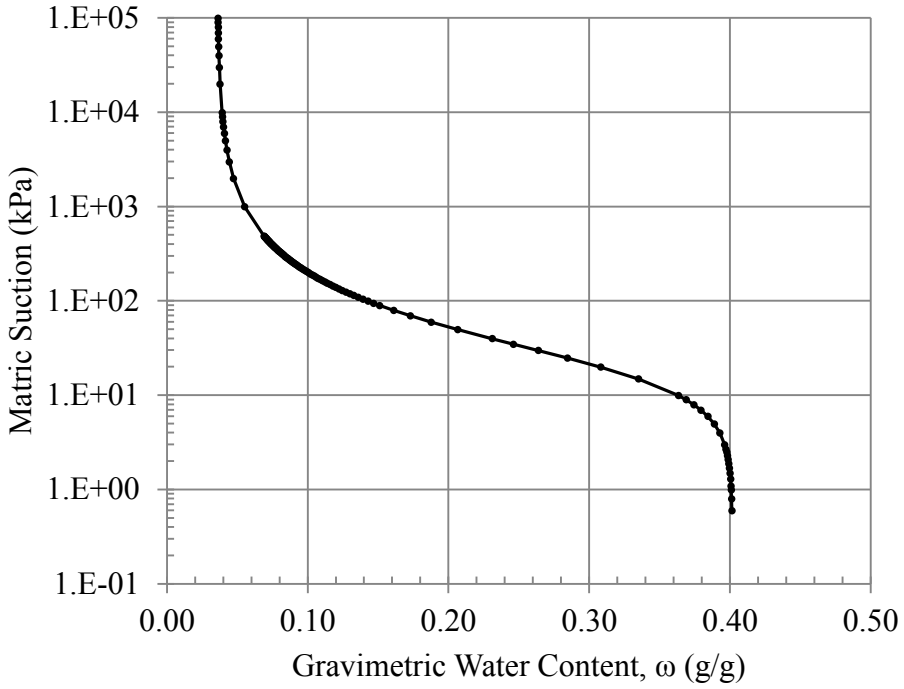

Figure 29: SWCC used for pore size distribution (CFA)

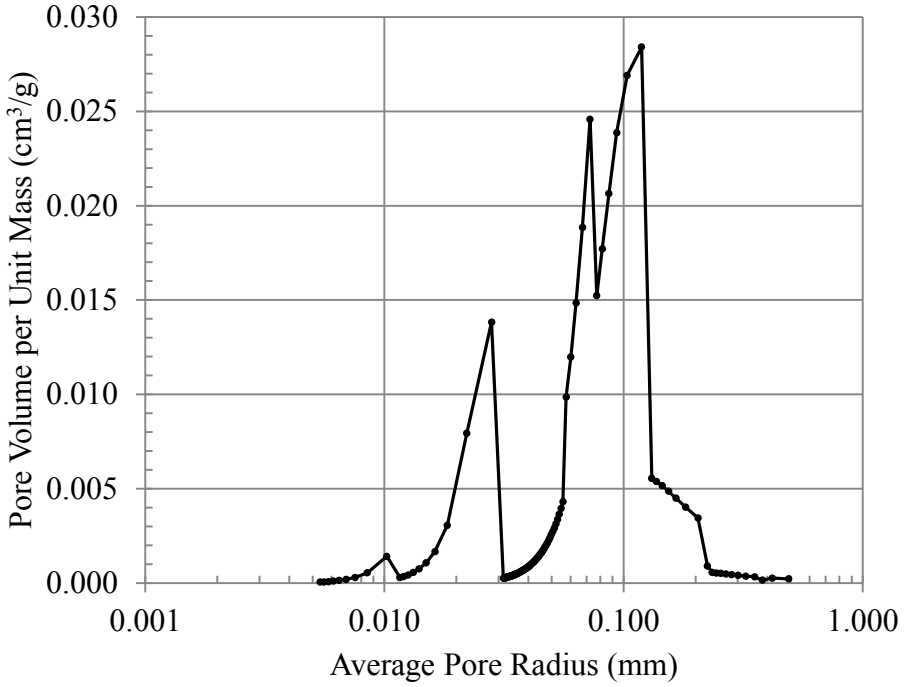

Figure 30: Pore volume per unit mass vs. average pore radius (CFA)

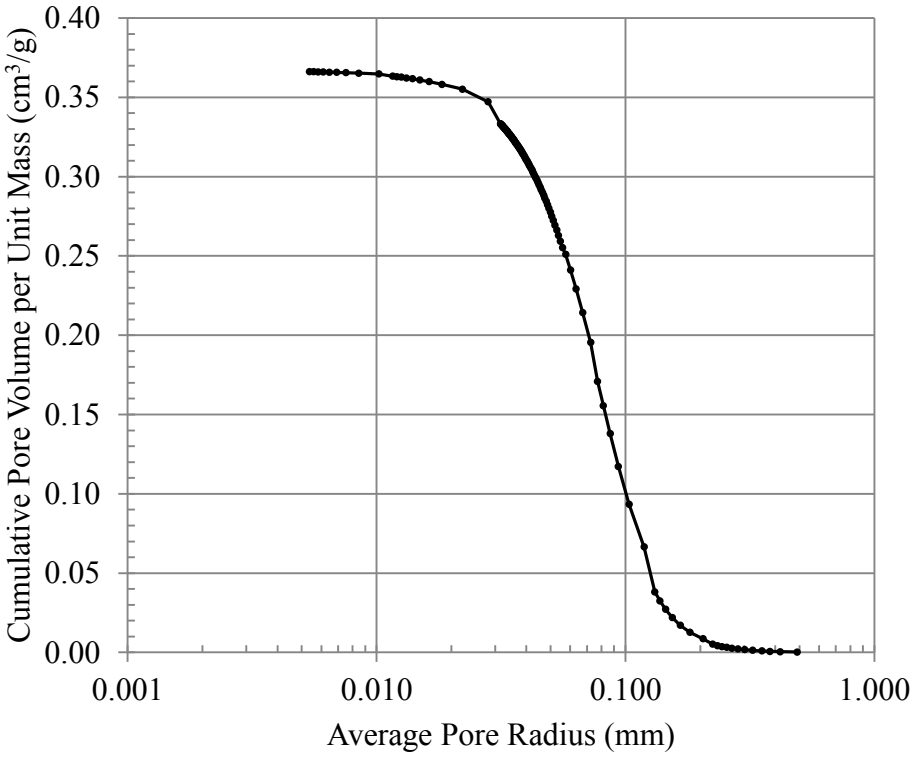

Figure 31: Cummulative pore volume per unit mass vs. average pore radius (CFA)

4.12 Experimental vs. Predicted WEP

The predicted water entry pressure values were determined based upon the Washburn equation (Eq. 4) and the pore diameters from the SWCC translation technique. Each curve in the following figures represents a different pore diameter determined either from the SWCC or empirical relationships to the effective pore diameter (D_{10}). The pore diameters used to predict the water entry pressure of hydrophobic sands and CFA for a range of contact angles are given in Table 13. Water entry pressures for the sand treated with OS_2 and the CFA treated with OS_2, as predicted by the Washburn equation (Eq. 4) and the selected pore diameters are shown in Figure 32 and Figure 33 respectively.

Table 13: Particle and pore diameters used for modeling water entry pressures

			CFA	Sand
Effective Grain Size	D_{10}	(mm)	0.0025	0.440
Pore Diameter for Simple Cubic Packing (loose)	D_{sc}	(mm)	0.0010	0.180
Pore Diameter for Tetrahedral Packing (dense)	D_{th}	(mm)	0.0004	0.066
Pore Diameter from SWCC (smallest)	D1	(mm)	0.001	0.048
Pore Diameter from SWCC (average)	D2	(mm)	0.236	0.214
Pore Diameter from SWCC (largest)	D3	(mm)	0.470	0.380

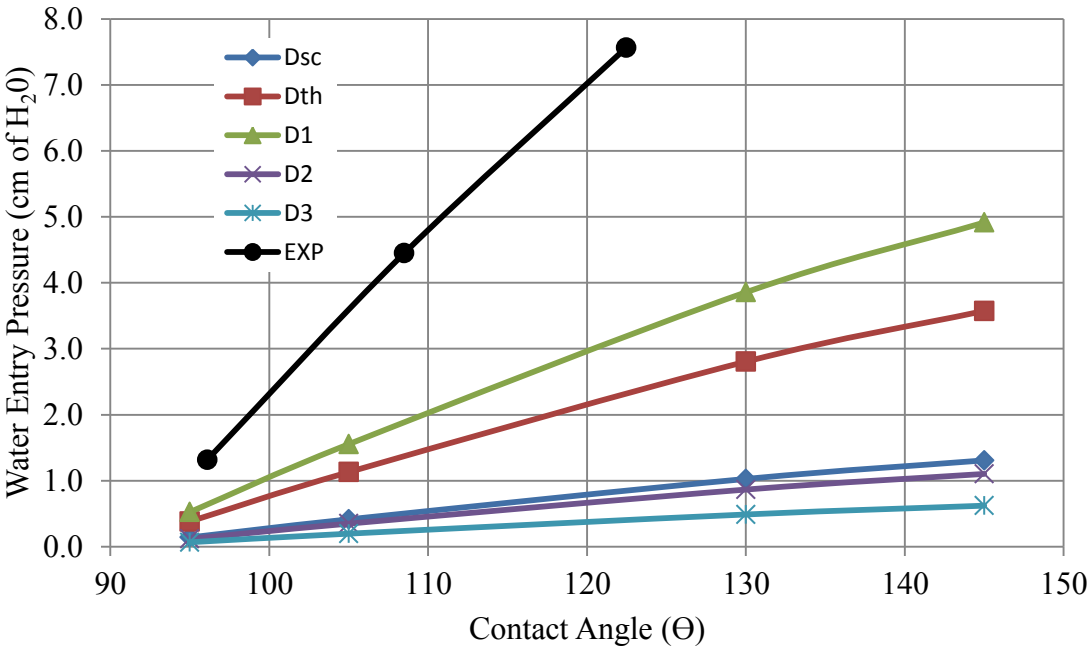

Figure 32: Predicted vs. experimental water entry pressures

(Sand and OS_1; $\rho = 1.12$ g/cm^3)

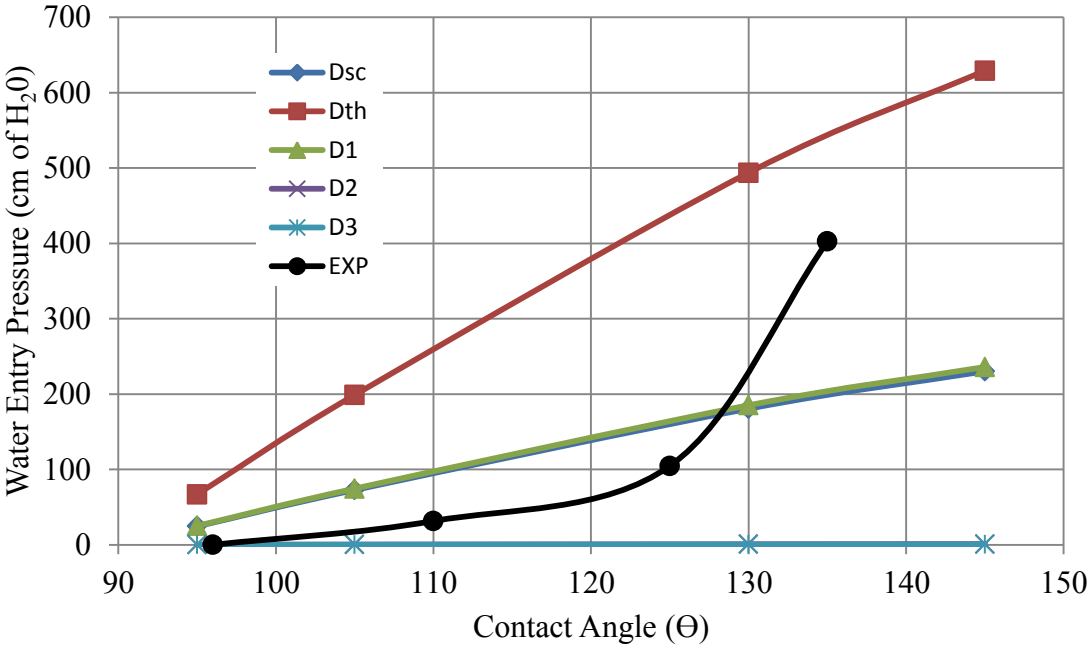

Figure 33: Predicted vs. experimental water entry pressures

(CFA and OS_2; $\rho = 1.61$ g/cm^3)

CHAPTER 5: DISCUSSION

5.1 Geotechnical Engineering Properties of OS Modified Soils

The geotechnical index properties including moisture content, specific gravity, particle size distribution, and compaction characteristics were successfully determined for untreated sand and CFA. Attempts were made at determining the same properties of the treated materials for purposes of comparison, but were unsuccessful due to the hydrophobic nature of the soil particles and the use of water as the wetting agent in all of the previously mentioned testing methods.

Fully treated sand and CFA is extremely water repellent with contact angles approaching 125° and 150° respectively. In the case where the entire soil sample is rendered hydrophobic to the highest level possible and small fractions of water are attempted to be mixed with the soil, such as for the compaction characteristic testing, water does not wet the surface of the soil particles. Instead pockets of moisture are incased within the soil particles leading to heterogeneous moisture distribution throughout the material.

In the case of testing procedures that use a larger volume of water than soil, such as the hydrometer analysis for particle size determination of fine grain soils or specific gravity by water pycnometer, the larger size and mass of the sand particles tested here allowed for the sand to become submerged in the water. A fraction of the CFA material would float on top of the water rendering the results invalid.

To address these issues new testing techniques may need to be developed to be able to accurately determine the geotechnical index properties of hydrophobic soils. The use of a wetting fluid that will fully wet hydrophobic surfaces, such as ethanol, is a potential solution.

It should also be mentioned that there is some debate regarding the applicability of specific gravity results for CFA utilizing the specific gravity by water pycnometer method. CFA has an amorphous particle morphology that includes hollow sphere-like particles (cenospheres). These hollow, lightweight, and possible waterproof spherical particles affect the results of the specific gravity testing. The CFA material tested for this research was in an as-delivered state. This condition is representative of materials that would be placed in a CFA impoundment, and presumably includes cenosphere CFA particles. An accurate measurement of the specific gravity of pure CFA material would require processing of the CFA material to break up the cenospheres.

5.2 Natural vs. Artificial Hydrophobic Soils

This document presents the results of testing performed on OS modified Ottawa sand and CFA, which can be classified as surface modification of the aforementioned materials by an artificial chemical. The research builds upon principles and methods that were primarily developed in response to naturally hydrophobic soils. It is important to recognize differences between artificially rendered hydrophobic soils and their natural counterparts.

As previously mentioned (Section 2.5) naturally hydrophobic soils can attain their water repellent properties through a variety of mechanisms including heat, organic matter, organic film coatings, fungi, or a combination such as fire resulting in organic

film coatings. Natural hydrophobic soils often occur in specific soil stratum or horizons, typically near the soil surface. The soil water repellency from natural sources can be temporary, variable, and/or time dependent. The work of Greiffenhagen et al. (2006) and Buczko et al. (2006) demonstrated that soil water repellency of hydrophobic soils in German pine forest varied with both moisture content and the time of year. Additionally, the work of Bauters (2000) addressing unstable wetting fronts of naturally hydrophobic soils, the work of Anurudda (2010) measuring the SWCC of naturally hydrophobic soil, the work of Bryant et al (2007) determining that increased compaction of naturally hydrophobic soils reduces water repellency, and the work of Moody et al. (2009) into the relationship between hydraulic conductivity and sorptivity to soil water repellency should not be considered representative of how artificially rendered hydrophobic soils will behave.

Also, artificially rendered hydrophobic soils are often mixed with water wettable soils (Bauters et al. 2000 and Nieber et al. 2000) to model naturally hydrophobic soils. Results determined from this type of sample preparation should not be used to predict behavior of fully hydrophobic materials.

Artificially rendered hydrophobic soils often demonstrate more stable hydrophobic properties, and more extreme hydrophobicity. Testing of these materials can be more difficult, and at times impossible, when water is necessary for the testing method. Artificial hydrophobic soils, when successfully treated, are completely water proof at hydraulic pressures below the critical water entry pressure (WEP). At pressures below the WEP they are water proof as opposed to water resistant. Fully treated artificially rendered hydrophobic soils should be considered in a class of their own, and

their behaviors and characteristics should not be confused with naturally occurring hydrophobic soils.

5.3 Treatment Ratios and Methods of Treatment for Hydrophobic Soils

Hydrophobic soil samples were created by mixing solutions of two different OS chemicals and water with either sand or CFA. Varying degrees of hydrophobicity were created by altering the amount of OS and soil. Treatment ratios of OS_1 and sand ranged between 20mg and 130mg OS_1 per kg of sand for contact angles ranging between 91° and 124°. Treatment ratios of OS_2 and sand ranged between 780mg and 3400mg OS_2 per kg of sand for contact angles ranging between 91° and 120°. Treatment ratios of OS_1 and CFA ranged between 2.7g and 8.0g OS_1 per kg of CFA for contact angles ranging between 96° and 137°, and treatment ratios of OS_2 and CFA ranged between 26.0g and 49.7g OS_2 per kg CFA for contact angles ranging from 105° to 144°. It can be seen in Figure 13 through Figure 16 that there is an optimization of treatment chemical as it approaches the fully treated state.

Increasing the amount of OS used in the treatment process significantly past the optimum treatment level led to decreased hydrophobicity in some cases. Up to 15 times more OS_2 was required to achieve the same levels of hydrophobicity as OS_1 for each material. This is most likely due to different chemical formulations. Up to 100 times more OS was required to treat the CFA than the sand. This is due to the difference in specific surface area of the two materials. Ultimately, the OS_1 and CFA combination was found to not produce stable hydrophobicity.

Differences between the two OS chemicals were noted during the sample preparation process. Samples prepared with OS_1 had a lubricated feeling when being

mixed, and binding of particles when cured. As mentioned in section 3.1.3, OS_1 contains ethylene glycol in its chemical formulation. The exact function of the ethylene glycol is unknown, but it seems possible that the ethylene glycol is coating, lubricating, and binding the soil particles. This may have contributed to lower optimum moisture content and higher maximum dry unit weight for CFA treated with the same chemical as determined by Daniels et al. (2009).

CFA treated with OS_2 also demonstrated some cementing of particles which required breaking apart with a mortar and pestle and passing through a #10 sieve to remove bound particles. The high pH of OS_2 (pH = 13) is hypothesized as a potential contributor to the cementing of CFA particles although the binging mechanism is unknown.

Although partially treated samples with contact angles ranging between 90° and the maximum achieved contact angle for particular OS-material combination were created and tested, the treatment ratio to contact angle relationship varied. This made creating partially treated hydrophobic samples very difficult and time consuming. Similar to treating only a fraction of soil particles for hydrophobic soil, partially treating soil particles for infiltration resistance is not advisable. It is recommended that future research focus on fully treated materials.

5.4 Measurement of the Contact Angle

For hydrophobic soils there are many methods of quantifying the degree of hydrophobicity. In this research contact angles were measured using the sessile drop technique (Bachmann et al. 2000a). A monolayer of hydrophobic soil particles was affixed to a glass slide, a calibrated drop of water was placed on the leveled surface, and

the angle at the interface of the solid and liquid phases was measured. Contact angles of the sand were measured with a precision of approximately ±7°, and the contact angles of the CFA were measured with a precision of approximately ±3°. Contact angle measurements by the sessile drop technique were relatively quick and repeatable.

As previously mentioned contact angle measurements of the partially treated materials seemed to vary considerably for intermediate treatment levels below the optimum treatment level for maximum hydrophobicity. Why this was the case can be explained by the fact that the contact angle is a three phase system that includes the gas (air) that surrounds the liquid and solid phases. It became evident through the course of this research that temperature and humidity have an effect on contact angle measurements. Further research into the effect of temperature and humidity on contact angle measurements is recommended.

Fink (1970) states that "the surface energy of any solid coated with an organic monolayer is equal to that of the exposed functional groups of the coating material, and is completely independent of the chemical properties of the solid subphase." This indicates that the apparent contact angle measured using the goniometer apparatus differs between sand and CFA primarily due to the roughness and gradation of the soil particles. This does not mean that the chemical composition of the soil particles does not have an effect on the ability of the material to be rendered hydrophobic. Sands that are close to 100% silica may be better suited to OS treatment. CFA which is approximately 50% silica may be less efficiently treated by OS. The fraction of CFA that is alumina, oxides, salts, carbon, or other trace constituents may be less likely to be rendered hydrophobic. This may explain in part the failure of OS_1 to impart stable hydrophobicity to CFA.

5.5 Water Entry Pressure of OS Modified Soils

The water entry pressure of OS modified sand and CFA was determined using standpipe apparatus capable of applying a positive hydraulic head to compacted soil samples. Water entry pressures for sand treated with OS_1 ranged between 0.2 cm of H_20 and 9.5 cm of H_20 for contact angles ranging between 96° and 122°. Water entry pressures for sand treated with OS_2 ranged between 0 cm of H_20 and 13.4 cm of H_20 for contact angles ranging between 92° and 110°. Water entry pressures for CFA treated with OS_2 ranged between 0 cm of H_20 and 542 cm of H_20 for contact angles ranging between 110° and 145°. There was a positive correlation between water entry pressure and contact angle as predicted by the Washburn equation (Eq. 4). These water entry pressures are comparable to other results found in the literature for sandy materials. Previous examples of water entry pressures of OS modified CFA was not found in the literature.

There was also a distinct positive correlation between sample density and water entry pressure. The families of curves that are presented in figures 18 through 20 indicate that for a given level of hydrophobicity the water entry pressure increases for increasing compaction. This is supported by the Washburn equation (Eq. 4) as water entry pressure is inversely related to effective pore diameter, and therefor positively related to density as increasing density decreases the pore diameters.

The positive correlation between water entry pressure and density does not hold true as the contact angle approaches the hydrophilic range (90°). This is an inflection point about which positive water entry pressure becomes capillary rise for hydrophilic soils. It is also the point about which positive water entry pressures for hydrophobic soils

becomes negative water entry pressures for hydrophilic pressures, i.e. soil suction. At 90° water entry pressure/capillary rise would be zero regardless of the soil density. The results support this conclusion, although the relationship between WEP and density appears to be reduced at a contact angle closer to 96° for the sand and 125° for the CFA. This is probably the result of the materials being partially treated at these contact angles with a fraction of the soil particle surface being hydrophilic and a fraction being hydrophobic.

5.6 Hydraulic Conductivity

Hydraulic conductivity measurements were attempted for the treated sand following the water entry pressure testing once the sample had been saturated. The untreated sand was 100% saturated and the saturation of the treated sand ranged from 87% to 94%. The hydraulic conductivity of the hydrophobic sand ranged from 0.022cm/s at the highest density level (1.76 g/cm^3) to 0.034 cm/s at the lowest density level (1.56 g/cm^3). The inverse correlation between density and hydraulic conductivity was as expected, and similar in behavior to hydrophilic soils. There was no discernable trend relating hydraulic conductivity and the contact angle. These results indicate that there is limited or no effect on the saturated hydraulic conductivity of hydrophobic soils once the water entry pressure has been exceeded.

Moody et al. (2009) states that, "sorptivity and hydraulic conductivity are inversely linked to the degree of water repellency." Many other sources present both positive and negative correlations between soil water repellency and hydraulic conductivity. It is important to highlight differences between natural and artificial hydrophobic soils and between the saturated and unsaturated hydraulic conductivity.

Moody worked with natural fire induced water repellent soils and ash, and determined hydraulic conductivity using a mini-disk infiltrometer. The hydraulic conductivity reported by Moody represents is an unsaturated hydraulic conductivity of natural soil that possesses variable hydrophobicity. Unsaturated hydraulic conductivities may be altered by partially hydrophobic soils due to unstable wetting fronts and preferential flow paths (Wang et al. 1998, Bauters 2000). The hydraulic conductivity values reported in this study represents saturated hydraulic conductivity of OS modified sand.

The saturated hydraulic conductivity of untreated CFA was determined to be $4x10^{-5}$ cm/s. Determination of the saturated hydraulic conductivity of the treated CFA was attempted, but unsuccessful due to the extreme hydrophobicity and high infiltration pressures needed to saturate the sample. Sidewall leakage or sample failure would occur before the treated samples could be fully saturated.

5.7 The SWCC and Hydrophobic Soils

The SWCC was determined for treated and untreated sand (density = 1.66 g/cm^3) using the TRIM method (Wayllace and Lu 2012) at the CSM/USGS geotechnical laboratory. Variation in the Van Genuchten fitting parameters was noted for the two samples.

The SWCC was determined for the untreated CFA (density = 1.12 g/cm$^{3)}$ at both the CSM/USGS geotechnical laboratory (TRIM method) as well as at the UNC-C geo-environmental laboratory (by dewpoint hygrometer). Variation in the Van Genuchten fitting parameters was noted for the two samples. Attempts at measuring the SWCC for treated CFA were unsuccessful for both testing methods due to the extreme hydrophobicity of the sample.

Validity of the results of the SWCC testing for treated sand is questionable. Attempts at measuring the SWCC for treated CFA at the UNCC facility were unsuccessful as water added to the samples simply ponded on top of the sample. Although the TRIM method is not designed to intentionally apply a positive hydraulic head it must be capable of applying hydraulic head of at least 10 cm of H_2O to overcome the infiltration resistance of the sample based on WEP testing results previously presented. Was the TRIM method actually measuring changes in suction for changes in volumetric moisture content of the sample, or was the test measuring changes in moisture content and suction values as the infiltration front moved across the sample? Additional research into the SWCC of hydrophobic soils is recommended especially considering the difficulties encountered performing testing on hydrophobic materials with methods that require water as the wetting fluid.

A hypothetical SWCC for hydrophobic sand is presented in the following figure.

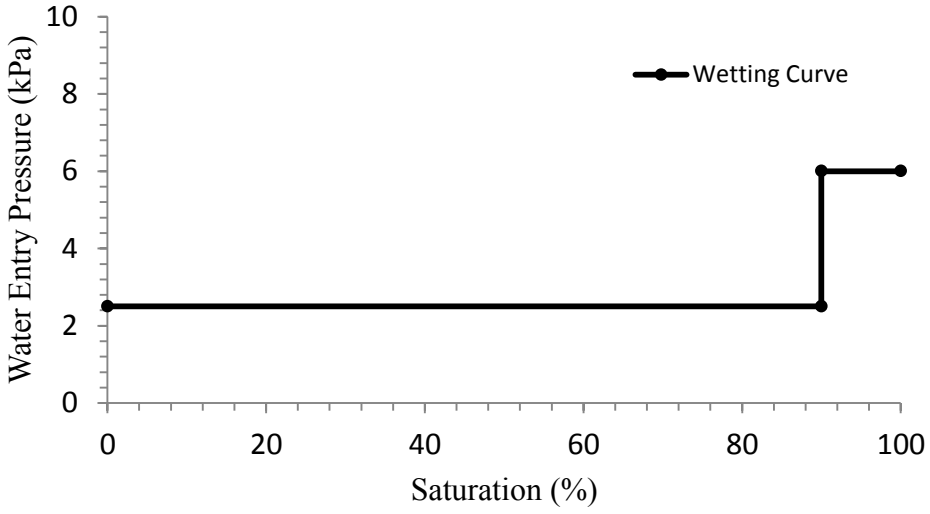

Figure 34: Hypothetical SWCC for hydrophobic sand

Figure 34 demonstrates that positive water entry pressure (negative suction) is required to initiate infiltration in hydrophobic soil to alter the moisture content. Once the water entry pressure is exceeded the sample will saturate to a point that approaches 100% saturation but will not be 100% due to air pockets entrapped in some smaller pores. This is caused by the wetting behavior of hydrophobic soils in which the large pores fill first followed by the small pores (Bauters et al. 2000). The entrapped air will not be able to exit the soil matrix unless hydraulic pore pressure reaches the point at which the gas goes into solution. This theory is supported by the presence of trapped air in the saturated treated samples during water entry pressure testing of the hydrophobic materials.

5.8 Experimental vs. Predicted Water Entry Pressures

Experimental water entry pressures were compared to water entry pressures predicted by the Washburn equation for a range of pore diameters. The effective pore diameters selected for predicting water entry pressures included the smallest, largest and average pore diameters resulting from a pore size distribution developed from the SWCC. Effective pore diameters were also developed based on empirical relationships for simple cubic (loose) packing and tetrahedral (dense) packing of spheres that were equal to the effective particle size (D_{10}).

The results shown in Figure 32 indicate that the Washburn equation under predicted the water entry pressure of the hydrophobic sand for pore diameters from the pore size distribution as well as the pore sizes from the empirical relationships. The results shown in Figure 33 indicate that the Washburn equation does a reasonable job of predicting the water entry pressure of the hydrophobic CFA using the pore diameter predicted by simple cubic packing of spheres with the effective particle size and for the

smallest pore diameter from the pore size distribution of CFA. In general, it appears from the results of this analysis that the pore size distribution from SWCC translation technique over predicted the sizes of the pore diameters.

5.9 OS Modified Soils as an Infiltration Barrier

The results of the water entry pressure testing indicate that OS modified sand can withstand infiltration pressures up to 14 cm of H_2O, and OS modified CFA can withstand infiltration pressures up to 542 cm H_2O. These results as well as others developed during the course of this research indicate OS modification of soils is a viable option for creating an infiltration barrier. Partially treating soil particles or mixing of hydrophobic and hydrophilic soil particles would not be advisable. These preparation methods may result in soils that demonstrate water repellency, but promote unstable hydrophobicity and potentially infiltration. Fully treated compaction lifts are recommended as opposed to surface treatment.

For field application, erosion of treated material at the ground surface may become an issue based on the floating of hydrophobic CFA during testing. Fink (1970) reported erosion as a durability issue for test plots of hydrophobic sand in the desert of Arizona. A cementing or binding agent would be required to prevent erosion of treated layers near the surface. Recent formulations of OS chemicals reportedly have OS combined with polymer binding agents specifically to address this issue.

Adequate compaction will be required to develop the infiltration resistance in hydrophobic soils. Compaction energies equivalent to both the standard Proctor and the modified Proctor methods resulted in acceptable water entry pressures for the sand and

CFA studied here. A sacrificial barrier layer is an option that could protect the density of the treated lifts of compacted hydrophobic soils and prevent erosion.

Application of OS chemicals in the field may present some challenges. OS solution can be used to surface treat soils or mixed in compaction lifts to fully treat a layer of soil. For soils that are dry of optimum moisture content OS solution can be mixed into the soil before compaction. For soils wet of the optimum moisture content the soil will first have to be dried to a moisture content dry of optimum, then OS solution will need to be added to bring the soil back to optimum moisture content before compaction. This could add significant costs to the application process.

Field confirmation of hydrophobicity will also be an important factor in application of OS modified soils as infiltration barriers. To address this issue Wang et al. (2000) presents a tension-pressure infiltrometer method for determining the water entry pressure of soils in the field. The water drop penetration time test and the molarity of ethanol test are two other options that could be used to quickly confirm hydrophobicity in field applications.

Additional durability issues must be addressed for hydrophobic soils to be used as infiltration barrier. Resistance to abrasion, UV radiation, freeze-thaw cycles, and wet-dry cycles are potential concerns. Fink (1970) reports some findings addressing durability issues for a range of organic coatings.

CHAPTER 6: CONCLUSIONS AND RECOMMENDATIONS

6.1 Conclusions

1. Treatment ratios can be optimized to achieve water repellency with the least amount of OS necessary to achieve maximum hydrophobicity.
2. Optimum treatment ratios are material dependent and are related to the surface area and chemical composition of the soil.
3. Infiltration of water into OS treated silica sand and one of the OS-CFA combinations was prevented at infiltration pressures less than the critical breakthrough pressure (WEP) for fully treated materials.
4. If the WEP is exceeded and the hydrophobic soil becomes saturated, then the hydraulic conductivity is similar to untreated (hydrophilic) soil.
5. Hydrophobic sand can withstand greater than 12cm of water pressure before infiltration is initiated.
6. Hydrophobic CFA can withstand greater than 500cm of water pressure before infiltration is initiated.
7. Both the degree of hydrophobicity (contact angle) and the level of compaction (density) have a positive correlation with increasing WEP.
8. The Washburn equation for capillary rise in soils predicts WEP of hydrophobic soil for the maximum treatment level using a pore diameter equal to $0.41*D_{10}$ for simple cubic packing.

6.2 Recommendations for Future Work

This line of research has specified a method of quantifying the degree of hydrophobicity of a porous material based on treatment level, and established a method for determining the relationship between soil density, hydrophobicity, and infiltration pressure resistance for hydrophobic soils. Although the results are promising additional research needs exist to allow for field implementation of OS technology for geotechnical engineering field applications. Future study of the following topics is recommended based on the experience gained during this research project.

1. Hydrophobic soils do not lend themselves to many geotechnical testing methods that require water (i.e. hydrometer analysis, specific gravity, compaction, permeability, consolidation, triaxial, etc…). Modification of these processes to use a fluid which will wet hydrophobic soil, such as ethanol, is possible.
2. Durability testing of OS treated hydrophobic soils exposed to biological degradation, UV radiation, abrasion, repeated wet/dry cycles, and repeated freeze/thaw cycles.
3. Effect of OS treatment on soil strength parameters.
4. Temperature effects on both level of hydrophobicity and WEP.
5. Time effects on contact angle and WEP.
6. Effect of high pH of treatment chemical on CFA.
7. Effect of continued drying of hydrophobic soils. Possibility of shrinkage cracking for some soils.
8. Efficacy of OS modification on natural soils that are combinations of gravel, sands, silts, and clays.

REFERENCES

Adamson, A. W. and Gast, A. P. (1997). *Physical Chemistry of Surfaces*. 6th Ed. John Wiley & Sons, Inc. New York, NY. 784 pg.

Anurudda, K. K., Chhoden, T., Kawamoto, K., Komatsu, T., Moldrup, P., de Jonge, L.W. (2010). "Estimating hysteretic soil-water retention curves in hydrophobic soil by a mini tensionmeter-TDR coil probe." 19th World Congress of Soil Sceince, Solutions for a Changing World. Brisbane, Australia, pp. 58-61.

ASTM D422-63 (2002). "Standard Test Method for Particle Size Analysis of Soils." ASTM International. West Conshohocken, PA.

ASTM D698-07 (2007). Standard Test Methods for Laboratory Compaction Characteristics of Soil Using Standard Effort (12,000 ft-lbf/ft^3 (600kN-m/m^3)). ASTM International. West Conshohocken, Pennsylvania.

ASTM D854-10 (2010). Standard Test Methods for Specific Gravity of Soil Solids by Water Pycnometer. ASTM International. West Conshohocken, Pennsylvania.

ASTM D1557-09 (2009). Standard Test Methods for Laboratory Compaction Characteristics of Soil Using Modified Effort (56,000 ft-lbf/ft^3 (2,700 kN-3/m^3)). ASTM International. West Conshohocken, Pennsylvania.

ASTM D2216-10 (2010). Standard Test Method for Laboratory Determination of Water (Moisture) Content of Soil and Rock by Mass. ASTM International. West Conshohocken, Pennsylvania.

ASTM D2434-68 (2006). Standard Test Method for Permeability of Granular Soils (Constant Head). ASTM International. West Conshohocken, Pennsylvania.

ASTM D4253-00 (2006). Standard Test Methods for Maximum Index Density and Unit Weight of Soils Using a Vibratory Table. ASTM International. West Conshohocken, Pennsylvania.

ASTM D4254-00 (2006). Standard Test Methods for Minimum Index Density and Unit Weight of Soils and Calculation of Relative Density. ASTM International. West Conshohocken, Pennsylvania.

ASTM D6836-02 (2008). Standard Test Methods for Determination of the Soil Water Characteristic Curve for Desorption Using Hanging Column, Pressure Extractor, Chilled Mirror Hygrometer, or Centrifuge. ASTM International. West Conshohocken, Pennsylvania.

Bachmann, J., Ellies, A., and Hartge, K. H. (2000a). "Development and application of a new sessile drop contact angle method to assess soil water repellency." *Journal of Hydrology*, 231-232, 66-75.

Bachmann, J., Horton, R., Van Der Ploef, R. R., and Woche, S. (2000b). "Modified sessile drop method for assessing initial soil-water contact angle of sandy soil." *Soil Science Society of America Journal*. 64. 564-567.

Bachmann, J., Woche, S. K., and Goebel, M. -O. (2003). "Extended methodology for determining wetting properties of porous media." *Water Resources Research*. 39 (12). 1-14.

Bauters, T. W. J., DiCarlo, D. A., Steenhuis, T. S., and Parlange, J.-Y. (1998). "Preferntial Flow in Water Repellent Sands." *Soil Science Society of America Journal*. 62. 1185-1190.

Bauters, T. W. J., Steenhuis, T. S., DiCarlo, D. A., Nieber, J. L., Dekker, L. W., Ritsema, C. J., Parlange, J. -Y., and Haverkamp, R. (2000). "Physics of water repellent soils." *Journal of Hydrology*. 231-232. 233-243.

Brooks, R. H. and Corey, T. A. (1964). "Hydraulic Properties of Porous Media." Hydrology Paper No. 3. Civil Engineering Dept., Colorado State Univ., Fort Collins, CO. 27pg.

Bryant, R., Doerr, S. H., Hunt, G. and Conan, S. (2007). "Effects of compaction on soil surface water repellency." *Soil Use and Management*, 23, 238-244.

Buczko, U., Bens, O., and Huttl, R. F. (2006). "Water infiltration and hydrophobicity in forest soils of a pine-beech transformation chronosequence." *Journal of Hydrology*. 331. 383-395.

Carrillo, M. L. K., Letey, J., and Yates, S. R. (1999). "Measurement of Initial Soil-Water Contact Angle of Water Repellent Soils." *Soil Science Society of America Journal*. 63 (3). 433-436.

Daniel, D. E. and Benson, C. H. (1990). "Water Content-Density Criteria for Compacted Soil Liners." *Journal of Geotechnical Engineering*. 116 (12), 1811-1830.

Daniels, J. L., Mehta, P., Vaden, M., Sweem, D., Mason, M. D., Zavareh, M. and Ogunro, V. (2009). "Nano-scale organo-silane applications in geotechnical and geoenvironmental engineering." *International Journal of Terraspace Science and Engineering*. 1 (1). 19-27.

Darcy, H. (1856). *Les Fontaines Publiques de la Ville de Dijon*. Dalmont, Paris. 647 p. & atlas.

Das, D. K. and Das, B. (1976). "Water Repellency in Soils." *Proc. Indian National Academy of Science*, 42, 480-490.

DeBano, L. F. (1981). *Water Repellent Soils: a state-of-the-art*. United States Department of Agriculture, Forest Service, General Technical Report, PSW-46, Berkeley, California, 21 pp.

DeBano, L. F. (2000). "Water repellency in soils: a historical overview." *Journal of Hydrology*, 231-232, 4-32.

Decagon Devices, Inc. (2010). "Generating a Soil Moisture Characteristic Using the WP4C." *Application Note*, www.decagon.com, 1-2.

Dekker, L. W. and Ritsema, C. J. (2000). "Wetting patterns and moisture variability in water repellent Dutch soils." *Journal of Hydrology*. 231-232. 148-164.

Doerr, S. H., Shakesby, R. A., and Walsh, R. P. D. (2000). "Soil Water repellency: its causes, characteristics and hydro-geomorphological significance." *Earth-Science Reviews*. 51. 33-65.

Emerson, W. W. and Bond, R. D. (1963). "The rate of water entry into dry sand and calculation of the advancing contact angle." *Austrail. J. Soil Res.*, 1, 9-16.

Fink, D. H. and Myers, L. E. (1969) "Synthetic Hydrophobic Sols for Harvestig Precipitation." *Proc. Symposium on Soil Wettablility*, Riverside, CA, 221-240.

Fink, D. H. (1970). "Water Repellency and Infiltration Resistance of Organic-Film-Coated Soils." *Proc. Soil Science Society of America*, Madison, WI, 34 (2), 189-194.

Fredlund, D. G. and Xing, A. (1994). "Equations for the soil water characteristic curve." *Canadian Geotechnical Journal*. 31. 521-532.

Gray, H. (1970). "Suggested Method of Test for Permeability of Porous Granular Materials by the Falling-Head Permeameter." In *Special Procedures for Testing Soil and Rock for Engineering Purposes (STP 479)*. 5th Ed., ASTM International,West Conshohocken, Pennsylvania, 157-159.

Greiffenhagen, A., Wessolek, G., Facklam, M., Renger, M., and Stoffregen, H. (2006). "Hydraulic Functions and water repellency of forest floor horizons on sandy soil." *Geoderma*. 132. 182-195.

King, P. M. (1981). "Comparison of methods for measuring severity of water repellence of sandy soils and assessment of some factors that affect its measurement." *Australian Journal of Soil Research*, 19, 275-285.

Letey, J. (1969). "Measurement of Contact Angle, Water Drop Penetration Time, and Critical Surface Tension." Proceedings of the Symposium on Water Repellent Soils. University of California, Riverside. May 6-10, 1968. 43-47.

Letey, J., Osborn, J., and Pelishek, R. E. (1962). "Measurement of Liquid-Solid Contact Angles in Soil and Sand." *Soil Science*, 93 (3), 149-153.

Lu, N. and Likos, W. J. (2004). *Unsaturated Soil Mechanics*. John-Wiley, Hoboken, N.J. 556 pp.

Miller, C. J., Yesiller, N., Yaldo, K. and Merayyan, S. (2002). "Impact of soil type and compaction conditions on soil water characteristic." *Journal of Geotechnical and Geoenvironmental Engineering*. 128 (9). 733-742.

Moody, J. A., Kinner, D. A. and Ubeda, X. (2009). "Linking Hydraulic properties of fire-affected soils to infiltration and water repellency." *Journal of Hydrology*. 379. 291-303.

Nam, S., Gutierrez, M., Diplas, P., Petrie, J., Waullace, A., Lu, N., and Muñoz, J. J. (2009). "Comparison of testing techniques and models for establishing the SWCC of riverbank soils." *Engineering Geology*. 110. 1-10.

Nguyen, H. V., Nieber, J. L., Oduro, P., Ritsema, C. J., Dekker, L. W., and Steenhuis, T. S. (1999). "Modeling solute transport in a water repellent soil." *Journal of Hydrology*. 215. 188-201.

Nieber, J. L., Bauters, T. W. J., Steenhuis, T. S., and Parlange, J.-Y. (2000). "Numerical simulation of experimental gravity-driven unstable flow in water repellent sand." *Journal of Hydrology*. 231-232. 295-307.

Ramirez-Flores, J. C., Bachmann, J. and Marmur, A. (2010). "Direct determination of contact angles of model soils in comparison with wettability characterization by capillary rise." *Journal of Hydrology*. 382. 10-19.

Richards, L. A. (1931). "Capillary Conduction of Liquids Through Porous Mediums." *Physics*, Vol. I, 318-333.

Schreiner, O. and Shory, E. C. (1910). "Chemical nature of soil organic matter." *USDA Bureau of Soils Bulletin*, 74, 2-48.

Van Genuchten, M. T. (1980). "A closed-form equation for predicting the hydraulic conductivity of unsaturated soils." *Soil Science Society of America Journal*. 44 (5). 892-898.

Van't Woudt, B. D. (1959). "Particle Coatings Affecting the Wettability of Soils." *Journal of Geophysical Research*. 64. 263-267.

Wallis, M. G. and Horne, D. J. (1992). “Soil Water Repellency.” In: Stewart, B.A. (Ed.), *Advances in Soil Science* Vol. 20, Springer, New York, 91-146.

Wang, Z., Wu, L., and Wu, Q. J. (2000).“Water-entry value as an alternative indicator of soil water-repellency and wettability.”*Journal of Hydrology*, 231-232, 76-83.

Washburn, E. W. (1921). “The Dynamics of Capillary Flow.” *The Physical Review*, 17(3), 273-283.

Watson, C. L., Letey, J. (197). “Indices for characterizingsoil-water repellency based upon contact angle-surface tension relationships.” Soil Science Society of America Proceedings, 34, 841-844.

Wayllace, A. and Lu, N. (2012).“A Transient Water Release and Imbibitions Method for Rapidly Measuring Wetting and Drying Soil Water Retention and Hydraulic Conductivity Functions.” *Geotechnical Testing Journal*, 35, 1, 1-15.

Young, T. (1805). “An Essay on the Cohesion of Fluids.” *Pilosophical Transactions of the Royal Society of London*, 95, 65-87.

Zisman, W. A. (1964). “Relation of the equilibrium contact angle to liquid solid constitution.” In Contact Angle, Wettability, and Adhesion. pp1-51. In Advances in Chemistry Series 43. Amer. Chem. Soc., Washington D.C.

APPENDIX A: CALCULATIONS

Matt Keatts

MOISTURE CONTENT

ASTM D 2216-10

CLIENT: Dr. Daniels
PROJECT: Coal Fly Ash - Moisture Conditioned

DATE: 8/3/2011
LOCATION: CHARLOTTE, NC

SAMPLE	DESCRIPTION	$Ws_{MOIST}+W_{CAN}$	$Ws_{DRY}+W_{CAN}$	W_{CAN}	MOISTURE CONTENT (%)
131	COAL ASH	34.93	30.39	16.29	32.20
151	COAL ASH	30.16	26.85	16.40	31.67
146	COAL ASH	29.71	26.45	16.17	31.71
			Bucket 1	AVG =	31.86
20	COAL ASH	32.971	28.591	13.903	29.82
5	COAL ASH	33.691	29.138	13.705	29.50
205	COAL ASH	35.944	30.901	13.667	29.26
			Bucket 1	AVG =	29.53
Z3	COAL ASH	48.74	45.22	32.59	27.87
66	COAL ASH	52.12	47.91	32.18	26.76
51	COAL ASH	59.48	53.38	31.92	28.42
			Bucket 2	AVG =	27.69
9	COAL ASH - DRY	42.620	42.408	13.686	0.74
42	COAL ASH - DRY	40.170	39.980	13.883	0.73
34	COAL ASH - DRY	40.867	40.674	13.629	0.71
			Hygroscopic	AVG =	0.73
		Overall Average Moisture Content of Ash =			29.69

OBSERVACIONES GENERALES:

Average Moisture Content of moisture conditioned ash in buckets is approvimately = 30%

Figure 35: Sample moisture content calculations

SPECIFIC GRAVITY OF SOIL SOLIDS BY WATER PYCNOMETER

Description of soil: Coal Fly Ash **Sample No.:** 1 **Standard:** ASTM D 854 - 06

Test 1:		**Test 2 (after 3 hours):**	
$W_{pycn\ 4\ +\ water}$ (g):	360.29	$W_{pycn\ 4\ +\ water}$ (g):	360.28
$Temperature_{pycn\ 4}$ (°C):	18.5	$Temperature_{pycn\ 4}$ (°C):	18.5
$W_{pycn\ 5\ +\ water}$ (g):	360.29	$W_{pycn\ 5\ +\ water}$ (g):	360.87
$Temperature_{pycn\ 5}$ (°C):	18.5	$Temperature_{pycn\ 5}$ (°C):	18.4
W_{soil} (g):	49.61	W_{soil} (g):	49.52
$W_{pycn\ 3\ +\ water\ +\ soil}$ (g):	387.57	$W_{pycn\ 3\ +\ water\ +\ soil}$ (g):	388.22
$Temperature_{mean}$ (°C):	17.0	$Temperature_{mean}$ (°C):	17.0

Calibrated pycnometer volume, Vp:

$M_{pw,c}$ (g):	360.29	Mass of pycnometer + water at calibration temperature.
M_p (g):	111.16	Mass of pycnometer at calibration temperature.
$\rho_{w,t}$(g/ml):	0.99852	Water density at calibration temperature (see Table 1 in the standard)

$$Vol_{pic} = \frac{M_{pwc} - M_p}{\rho_{w,c}}$$ Vp (ml) = 249.50

Mass of picnometer + water at test temperature, $M_{pw,t}$:

M_p (g):	111.16	Mass of pycnometer + water at test temperature (Tt)
V_p (g):	249.50	Mean mass of pycnometer
$\rho_{w,t}$(g/ml):	0.99852	Water density at test temperature (Tt) (see Table 1 in the standard)

$$M_{pw,t} = Mp + (V_p \times \rho_{w,t})$$ $M_{pw,t}$ (g) = 360.29

Specific Gravity of soil at test temperature, Gt:

M_s (g):	49.61	Mass of oven dry soil	ρ_s = soil density
$M_{pws,t}$ (g):	387.57	Mass of pycnometer + water + solids at test temperature	

$$G_t = \frac{\rho_s}{\rho_{w,t}} = \frac{Ms}{(M_{pw,t} - (M_{pws,t} - Ms)}$$ Gt= 2.22

Specific gravity of the soil at 20°C, G_s:

k: 1.00057 Temperature coefficient (See Table 1 for T=17.0)

$$G_{20°C} = KxG_t$$ G_s = 2.22

Remarks:

Figure 36: Specific gravity of CFA

Standard Proctor																
Target MC	%	24			27			30			33			36		
W_{mold}	g	2283			2283			2283			2283			2283		
$W_{mold}+W_{soil}$	g	3501			3547			3645			3697			3684		
W_{soil}	g	1218			1264			1362			1414			1401		
Moist Unit Weight, γ_m	g/cm^3	1.291			1.339			1.443			1.498			1.484		
Moist Unit Weight, γ_m	lb/ft^3	80.56			83.60			90.08			93.52			92.66		
Dry Unit Weight, γ_d	lb/ft^3	66.02			66.69			68.70			69.50			66.36		
Can ID	#	4-S	33	35	41	450	13	10%	57	45	16	32	\	51	66	Z3
W_{can}	g	13.97	13.83	13.66	14.13	13.77	13.73	13.82	13.80	13.77	14.02	13.56	13.77	31.93	32.18	32.60
$W_{can} + W_{soil,wet}$	g	41.15	42.12	40.24	30.18	32.55	30.98	31.41	35.34	36.38	40.52	37.21	33.34	68.49	79.24	74.56
$W_{can} + W_{soil,dry}$	g	36.22	37.04	35.44	26.93	28.76	27.49	27.22	30.23	31.03	33.69	31.10	28.36	58.24	65.85	62.53
W_s	g	22.25	23.21	21.78	12.80	14.99	13.76	13.40	16.43	17.26	19.67	17.54	14.59	26.31	33.67	29.93
W_w	g	4.93	5.08	4.80	3.25	3.79	3.49	4.19	5.11	5.35	6.83	6.11	4.98	10.25	13.39	12.03
Moisture Content, MC	%	22.2	21.9	22.0	25.4	25.3	25.4	31.3	31.1	31.0	34.7	34.8	34.1	39.0	39.8	40.2
Avgerage MC	%	22.0			25.3			31.1			34.6			39.6		
γ_d (ZAV, S = %100)	lb/ft^3	93.03			88.65			81.92			78.38			73.68		

Volume Mold	ft^3	0.03333
Volume Mold	cm^3	943.75671
Volume Mold	m^3	0.00094376
Specific Gravity Soil, G_s		2.22
Unit Weight Water, γ_w	lb/ft^3	62.4

Figure 37: Compaction characteristics of CFA using standard energy

Modified Effort Compaction Characteristics																
Target MC	%	25			27			29			31			33		
W_{mold}	g	2083			2083			2083			2083			2083		
$W_{mold}+W_{soil}$	g	3438			3487			3538			3523			3499		
W_{soil}	g	1355			1404			1455			1440			1416		
Unit Weight, γ_m	g/cm^3	1.436			1.488			1.542			1.526			1.500		
Unit Weight, γ_m	lb/ft^3	89.62			92.86			96.23			95.24			93.65		
Unit Weight, γ_d	lb/ft^3	73.24			74.18			76.07			71.98			68.63		
Can ID	#	107	187	131	184	134	121	300	20	420	189	151	42	44	205	20
W_{can}	g	16.01	16.44	16.25	16.56	16.17	16.40	16.67	13.41	13.77	16.34	16.38	13.82	13.83	13.70	13.94
$W_{can} + W_{soil,wet}$	g	35.71	35.02	33.56	37.63	35.33	34.48	33.61	36.57	42.62	36.59	42.00	40.61	37.75	44.48	31.46
$W_{can} + W_{soil,dry}$	g	32.11	31.62	30.40	33.38	31.48	30.85	30.03	31.76	36.58	31.67	35.71	34.07	31.44	36.19	26.76
W_s	g	16.10	15.18	14.15	16.82	15.31	14.45	13.36	18.35	22.81	15.33	19.33	20.25	17.61	22.49	12.82
W_w	g	3.60	3.40	3.16	4.25	3.85	3.63	3.58	4.81	6.04	4.92	6.29	6.54	6.31	8.29	4.70
Moisture Content, MC	%	22.4	22.4	22.3	25.3	25.1	25.1	26.8	26.2	26.5	32.1	32.5	32.3	35.8	36.9	36.7
Avgerage MC	%	22.4			25.2			26.5			32.3			36.5		
γ_d (ZAV, S = %100)	lb/ft^3	92.57			88.86			87.22			80.67			76.57		

Volume Mold	ft^3	0.03333
Volume Mold	cm^3	943.75671
Volume Mold	m^3	0.00094376
Specific Gravity Soil, G_s		2.22
Unit Weight Water, γ_w	lb/ft^3	62.4

Figure 38: Compaction characteristics of CFA using modified effort

- Material Properties

Specific Gravity of Soil	G_s	2.65

- Mold Volume Calibration

		1	2	3	Average	
Diameter	D	15.2	15.175	15.2	15.19167	(cm)
Height	h	15.5	15.5	15.5	15.5	(cm)

Mold Volume	V_m	2809.522	(cm^3)
Mold Volume	V_m	0.099215	(ft^3)

- Minimum Index Density

		1	2	3	
Mass of Mold	M_m	4964	4964	4964	(g)
Mass of Mold + Soil	M_{m+s}	9362	9363	9372	(g)
Mass of Soil	M_s	4398	4399	4408	(g)
Minimum (dry) Index Density	$\rho_{dmin,n}$	1.565391	1.565747	1.56895	(g/cm^3)
Minimum-index Unit Weight	γ_{dmin}	15.35179	15.35528	15.38669	(kN/m^3)
Minimum-index Unit Weight	γ_{dmin}	97.72422	97.74644	97.94642	(lbf/ft^3)
Maximum-index Void Ratio	e_{max}	0.692868	0.692483	0.689027	

- Maximum Index Density

Plate Thickness	t	0.5	(in)	12.70003	(mm)

Height Change Base Plate (mm)	1	2	3	4	5	6
Trial 1	1.75	1.55	0.40	-0.55	-0.40	1.20
Trial 2	4.80	5.40	4.80	3.65	3.00	3.40
Trial 3	10.10	11.05	10.70	9.80	9.45	9.90

		1	2	3	
Volume of Tested Soil	V	2567.389	2503.646	2395.041	(cm^3)
Mass of Mold	M_m	4964	4964	4964	(g)
Mass of Mold + Soil	M_{m+s}	9494	9091	9164	(g)
Mass of Soil	M_s	4530	4127	4200	(g)
Maximum (dry) Index Density	$\rho_{dmax,n}$	1.764439	1.648396	1.753623	(g/cm^3)
Maximum-index Unit Weight	γ_{dmax}	17.30385	16.16582	17.19778	(kN/m^3)
Maximum-index Unit Weight	γ_{dmax}	110.1504	102.9061	109.4752	(lbf/ft^3)
Minimum-index Void Ratio	e_{min}	0.501894	0.607623	0.511157	

Figure 39: Calculations for index density testing of sand

UNC CHARLOTTE	Pressure vs Infiltration

Sample Prep Date	7/13/12	Performed By	Matt Keatts
Trial	120-D-2	Advisor	Dr. John Daniels
Material	Sand	Contact Angle (deg)	120.0 ± 7.0
Chemical	WSD	Treatment Ratio (gSand:gBS)	299.9 : 1.0

- Sample Preparation

Target Compaction	Dense	(-)
Target Dry Density, ρ_{tgt}	1.76	(g/cm^3)
Target Length	13.5	(cm)
Target Mass Sand	750.0	(g)

Actual Sample Length	1	2	3	AVG
	13.64	13.58	13.57	13.60

Permeameter Used	I	(-)
Mass of Cell, Dry	2061.37	(g)
Mass of Cell, H_20 only	2575.82	(g)
Mass of Cell, Test	2077.82	(g)
Mass of Cell + Sand	2827.58	(g)
Mass of Sand	749.8	(g)
Sample Length	13.60	(cm)
Sample Diameter	6.345	(cm)
Sample Area	31.619	(cm^2)
Sample Volume	429.918	(cm^3)
Sample Dry Unit Weight	1.744	(g/cm^3)
	108.87	(pcf)

NOTES:

Figure 40: Water entry pressure testing sample preparation data sheet

UNC CHARLOTTE	Pressure vs Infiltration

Sample Prep Date	7/13/12	Performed By	Matt Keatts
Trial	120-D-2	Advisor	Dr. John Daniels
Material	Sand	Contact Angle (deg)	120 ± 7.0
Chemical	WSD	Treatment Ratio (gSand:gBS)	299.9

- Pressure vs. Infiltration Test

Test Room Temperature (°C):	22.5	(deg)		(°F)
Test H_2O Temperature (°C):	22.5	(deg)		
Test Humidity:		(%)		

Height to bottom of Sample	37.6	(cm)

	H_{H20} (cm H20)						H_{sample}	ΔH
Time / Trial	0	1	2	3	4	5	(cm H_20)	(cm H20)
1	(*** Breakthrough Pressure ***)					47.0	37.6	9.4
2	59.0	50.7	50.3	50.1	50.0	49.9	41.2	8.7
3	62.1	53.0	52.5	52.3	52.2	52.1	43.2	8.9
4	64.8	55.7	55.0	54.7	54.6	54.5	45.5	9.0
5	66.2	57.7	56.8	56.5	56.4	56.3	48.2	8.1
6	68.0	59.6	58.7	58.5	58.4	58.3	49.9	8.4
7								
8								
9								
10								

Breakthrough Pressure	9.40	(cm H_20)
Max Pressure Head Supported	9.00	(cm H_20)
Average Equilibrium Pressure Head Supported	8.60	(cm H_20)
Standard Deviation	0.42	
Estimated pore diameter		(mm)

NOTES: Time in Minutes, Pressure Head in cm of H_20

Δh = 23mL D.I. H_20 ~ 12 cm Head

Figure 41: Water entry pressure testing data sheet

UNC CHARLOTTE	Permeability
	ASTM D2434-68

Sample Prep Date	7/13/12	Performed By	Matt Keatts
Trial	120-D-2	Advisor	Dr. John Daniels
Material	Sand	Contact Angle (deg)	120 ± 7.0
Chemical	WSD	Treatment Ratio (gSand:gBS)	299.9

Test Room Temperature (°C):	22.5	(deg)
Test H_2O Temperature (°C):	22.5	(deg)
Test Humidity:	0.0	(%)

Length of Sample, L	13.60	(cm)
Sample Diameter, D	6.345	(cm)
Sample Area, A	31.619	(cm^2)
Height to permeameter	22.2	(cm)
Height to water reservoir	98.2	(cm)
Hydraulic Head, ΔH	76.0	(cm H_2O)

Constant Time			
Trial	Time, t	Vol., Q	Perm., k
	(sec)	(ml)	(cm/sec)
1	30	161.0	0.030365
2	30	160.0	0.030176
3	30	160.0	0.030176

Constant Volume			
Trial	Time, t	Vol., Q	Perm., k
	(sec)	(ml)	(cm/sec)
1	29.00	160.0	0.031217
2	28.84	160.0	0.03139
3	28.56	160.0	0.031698

Average Hydraulic Conductivity, k	0.0308	(cm/sec)
Correction Factor	0.942	
Hydraulic Conductivity at 20°C, $k_{20°C}$	0.0290	(cm/sec)

$$k = \frac{QL}{At\,\Delta H}$$

Mass of Saturated Cell	3026.36	(g)
% Saturation	0.889164	(%)

NOTES:

Figure 42: Hydraulic conductivity testing data sheet

u_a-u_w	w	RH	V_p	r_k	t	r_p	ΔV_p	$(r_k)_{avg}$	$(r_p)_{avg}$	ΔS	$\sum(V_p)$
(kPa)	(g/g)	(%)	(cm^3/g)	(Å)	(Å)	(Å)	(cm^3/g)	(mm)	(mm)	(m^2/g)	(cm^3/g)
7.6	0.357143	99.99	0.358	189473.7	124.3	189598.0					
37.6	0.339286	99.97	0.340	38297.9	73.0	38370.8	0.018	113885.8	113984.4	0.009	0.018
67.6	0.294643	99.95	0.296	21301.8	60.0	21361.8	0.045	29799.8	29866.3	0.042	0.063
47.6	0.276786	99.97	0.278	30252.1	67.5	30319.6	0.018	25776.9	25840.7	0.012	0.081
157.6	0.25	99.89	0.251	9137.1	45.3	9182.3	0.027	19694.6	19750.9	0.059	0.107
167.6	0.232143	99.88	0.233	8591.9	44.3	8636.2	0.018	8864.5	8909.3	0.041	0.125
207.6	0.214286	99.85	0.215	6936.4	41.3	6977.7	0.018	7764.2	7807.0	0.051	0.143
277.6	0.196429	99.80	0.197	5187.3	37.5	5224.8	0.018	6061.9	6101.3	0.069	0.161
367.6	0.178571	99.73	0.179	3917.3	34.1	3951.4	0.018	4552.3	4588.1	0.091	0.179
437.6	0.160714	99.68	0.161	3290.7	32.2	3322.9	0.018	3604.0	3637.2	0.108	0.197
517.6	0.133929	99.62	0.134	2782.1	30.4	2812.5	0.027	3036.4	3067.7	0.191	0.224
677.6	0.116071	99.51	0.116	2125.1	27.8	2153.0	0.018	2453.6	2482.8	0.166	0.242
1087.6	0.089286	99.21	0.090	1324.0	23.8	1347.8	0.027	1724.6	1750.4	0.399	0.269
1037.6	0.080357	99.25	0.081	1387.8	24.1	1412.0	0.009	1355.9	1379.9	0.127	0.278
1607.6	0.053571	98.84	0.054	895.7	20.9	916.6	0.027	1141.8	1164.3	0.586	0.304
2247.6	0.035714	98.38	0.036	640.7	18.7	659.3	0.018	768.2	788.0	0.543	0.322
		100.00	0.000	#DIV/0!	#DIV/0!	#DIV/0!	0.036	#DIV/0!	#DIV/0!	#DIV/0!	0.358
							0.000			#DIV/0!	0.358

Figure 43: Pore size distribution worksheet

APPENDIX B: FIGURES

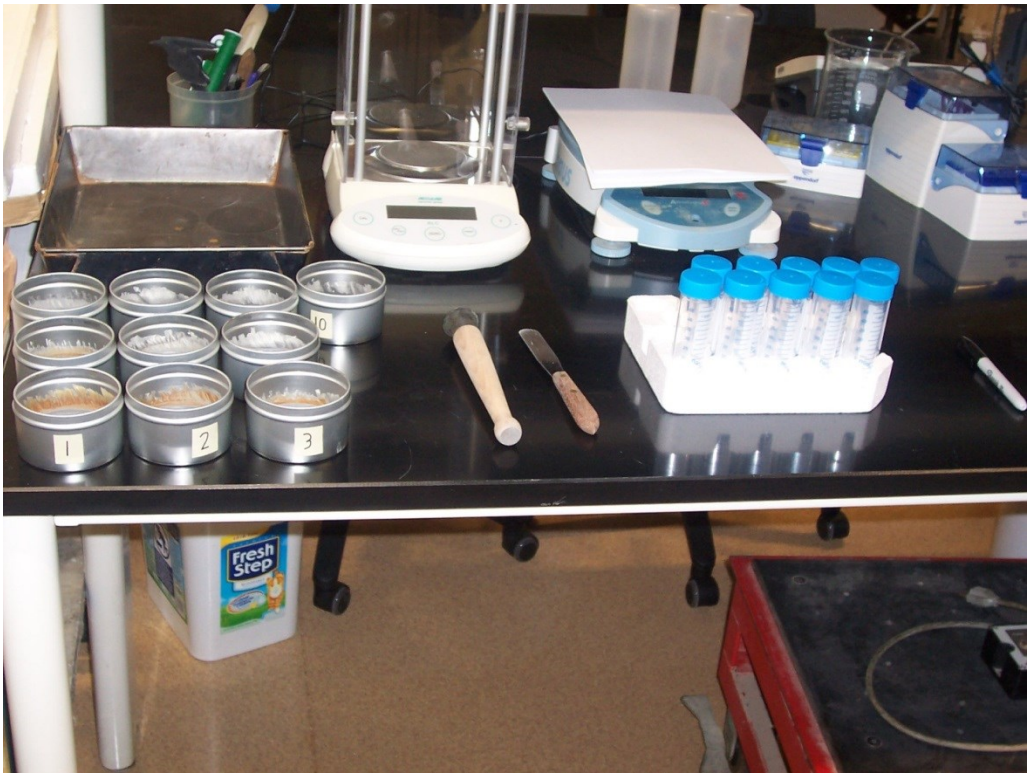

Figure 44: Equipment setup for treatment ratio vs. contact angle determination

Figure 45: Processing of small samples (CFA)

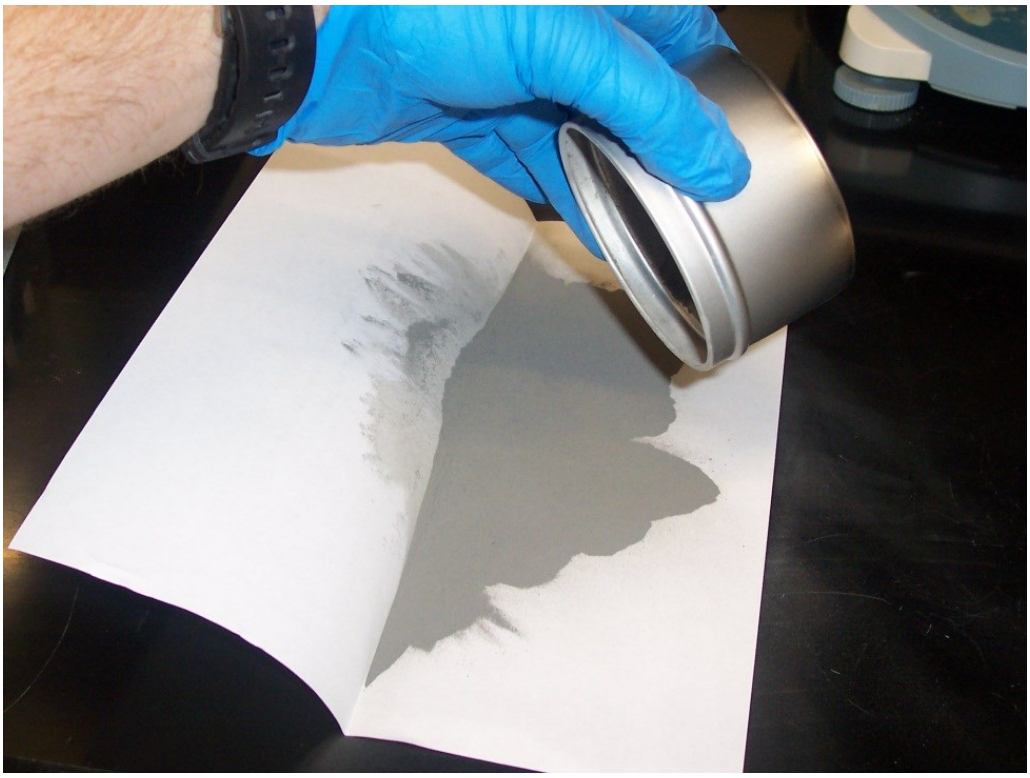

Figure 46: Transfering samples to storage

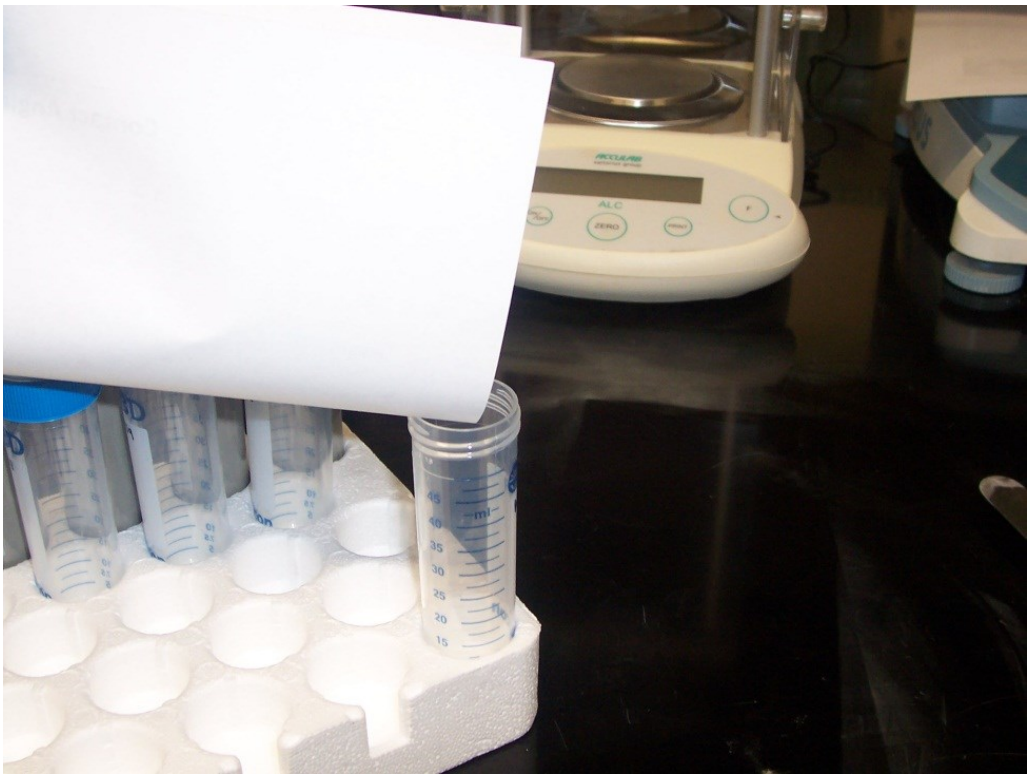

Figure 47: Storing samples in centerfuge tubes

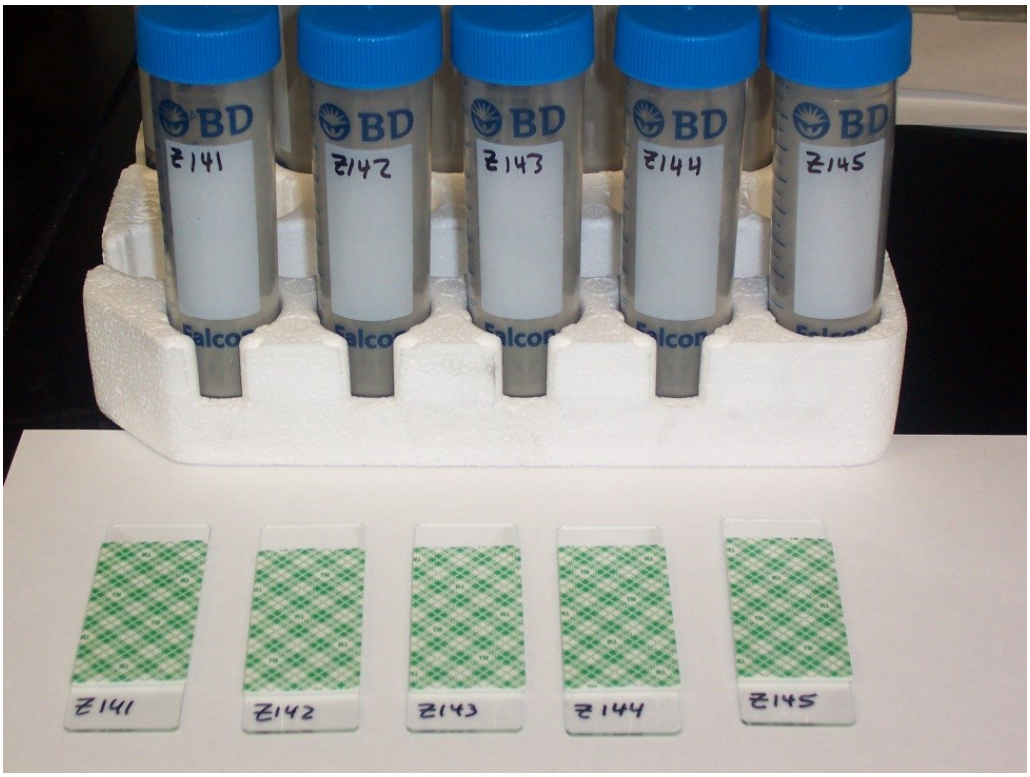

Figure 48: Preparing slides for contact angle measurements

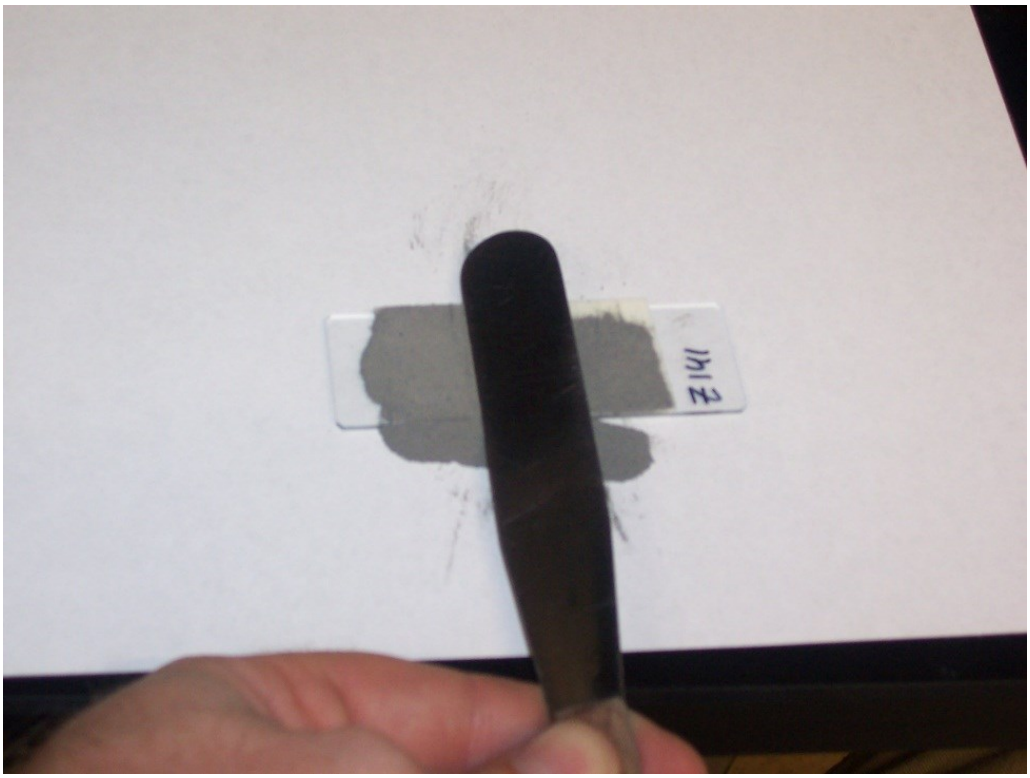

Figure 49: Applying monolayer of soil particles to slides

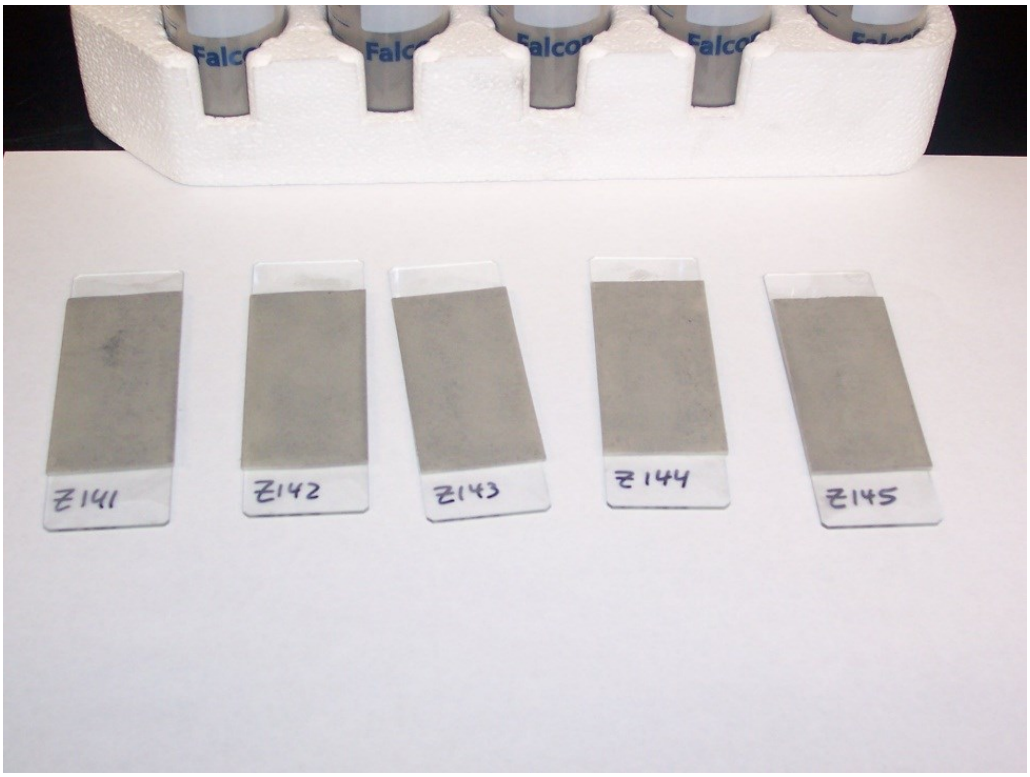

Figure 50: Slides prepared for sessile drop method

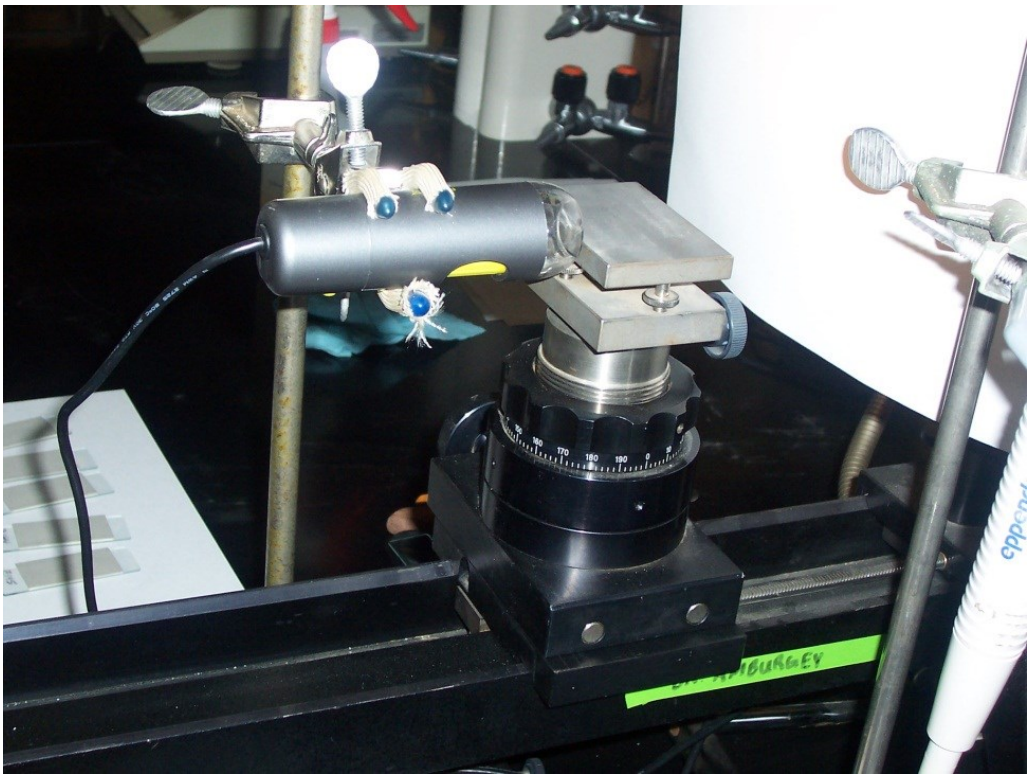

Figure 51: Goniometer setup for contact angle measurements

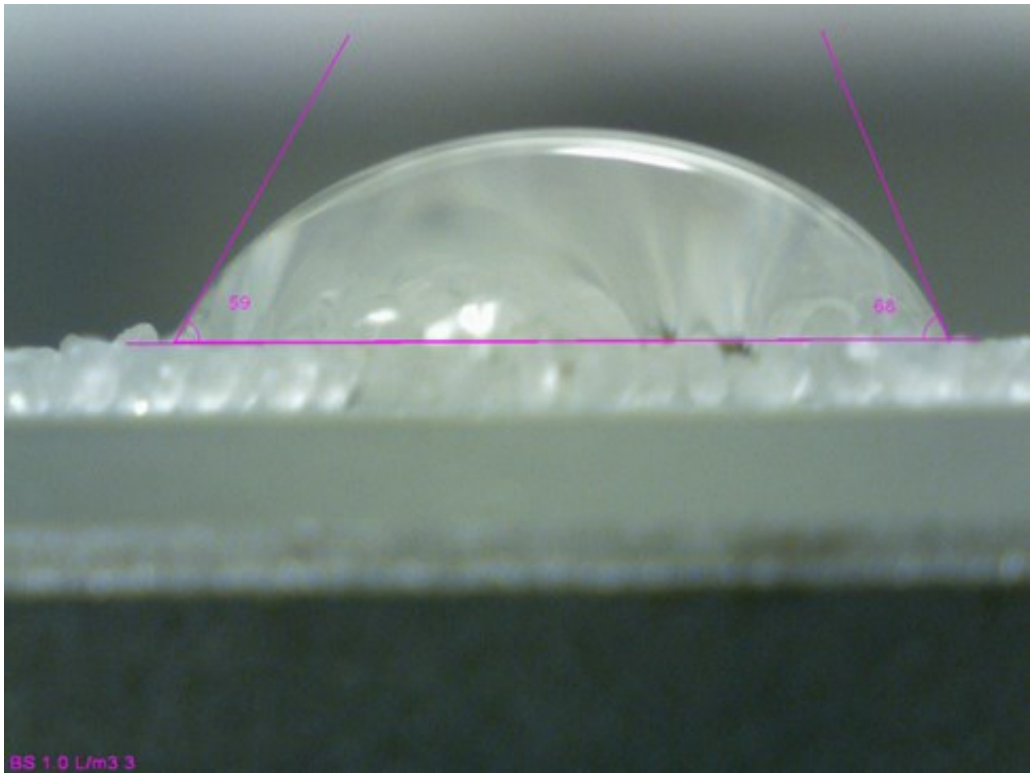

Figure 52: Contact angle measurement hydrophilic sand

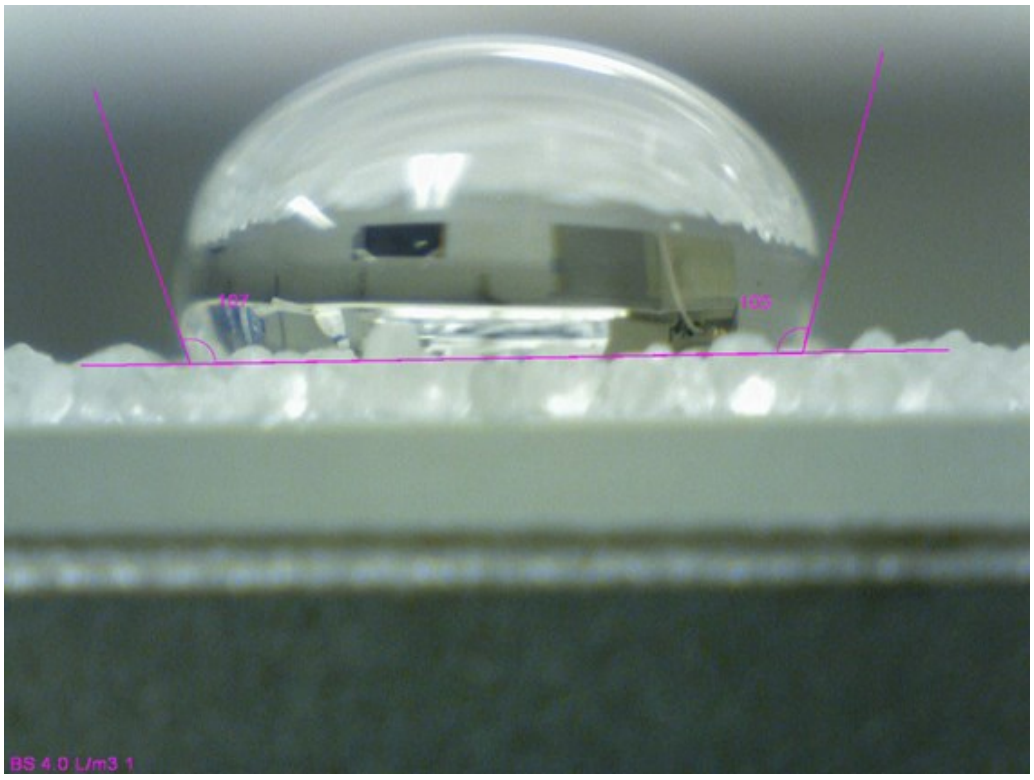

Figure 53: Contact angle measurement hydrophobic sand

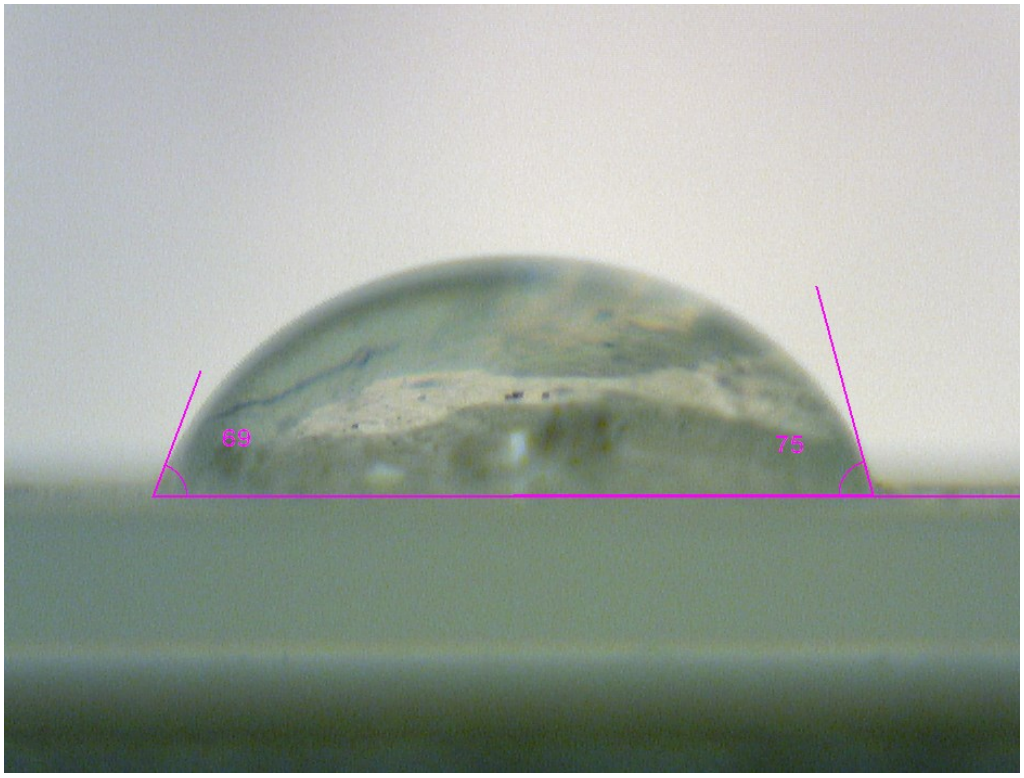

Figure 54:Contact angle measurement hydrophilic CFA

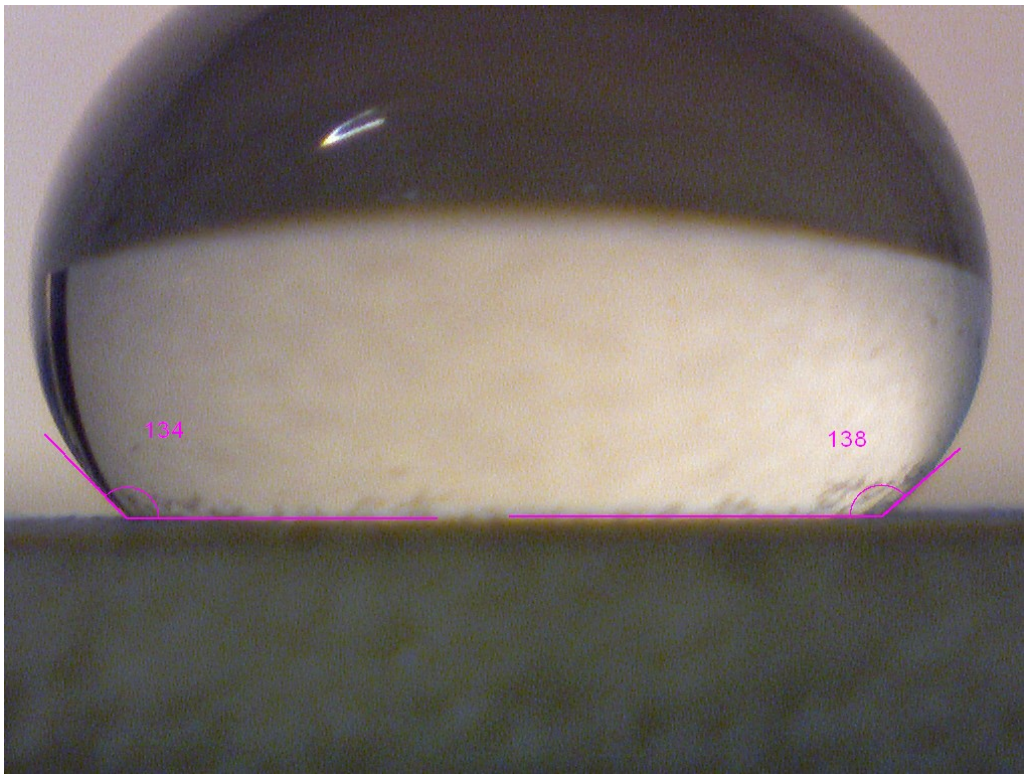

Figure 55: Contact angle measurement hydrophobic CFA

Figure 56: Large sample mixing with treatment solution

Figure 57: Large samples after oven drying

Figure 58: Equipment setup for processing treated soils

Figure 59: Processing of treated CFA

Figure 60: Passing treated CFA through #10 sieve

Figure 61: Storage of treated CFA

Figure 62: Permeameter for hydrophobic sand

Figure 63: Hydrophilic sand in standpipe apparatus

Figure 64: Hydrophobic sand in standpipe apparatus

Figure 65: Permeameter for hydrophobic CFA

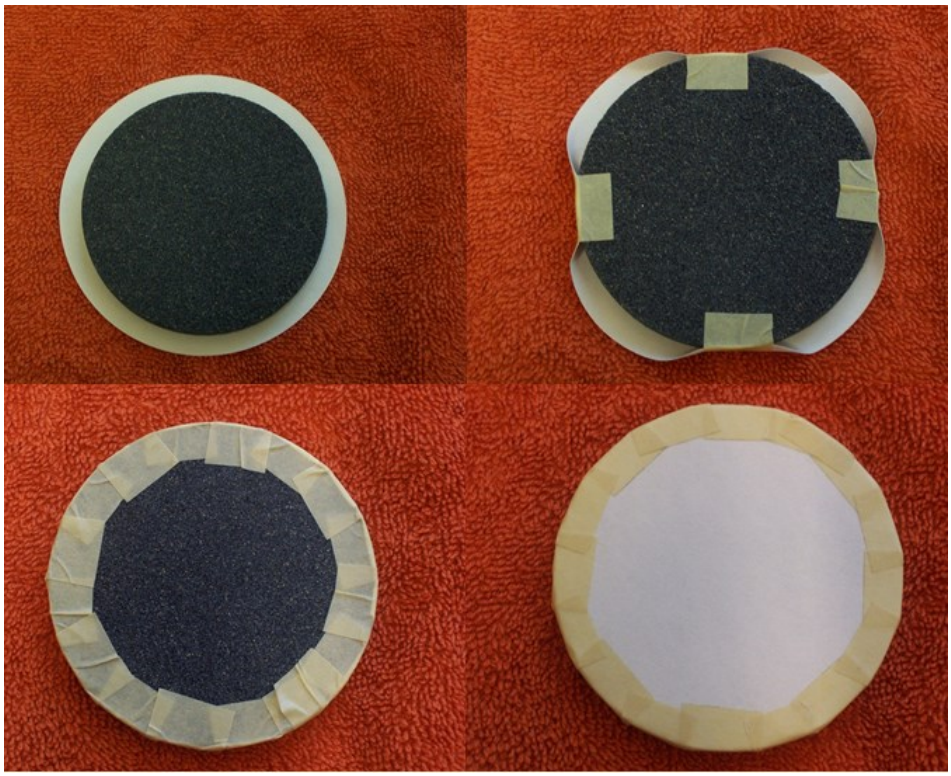

Figure 66: Overwrapping of porous stone for WEP method

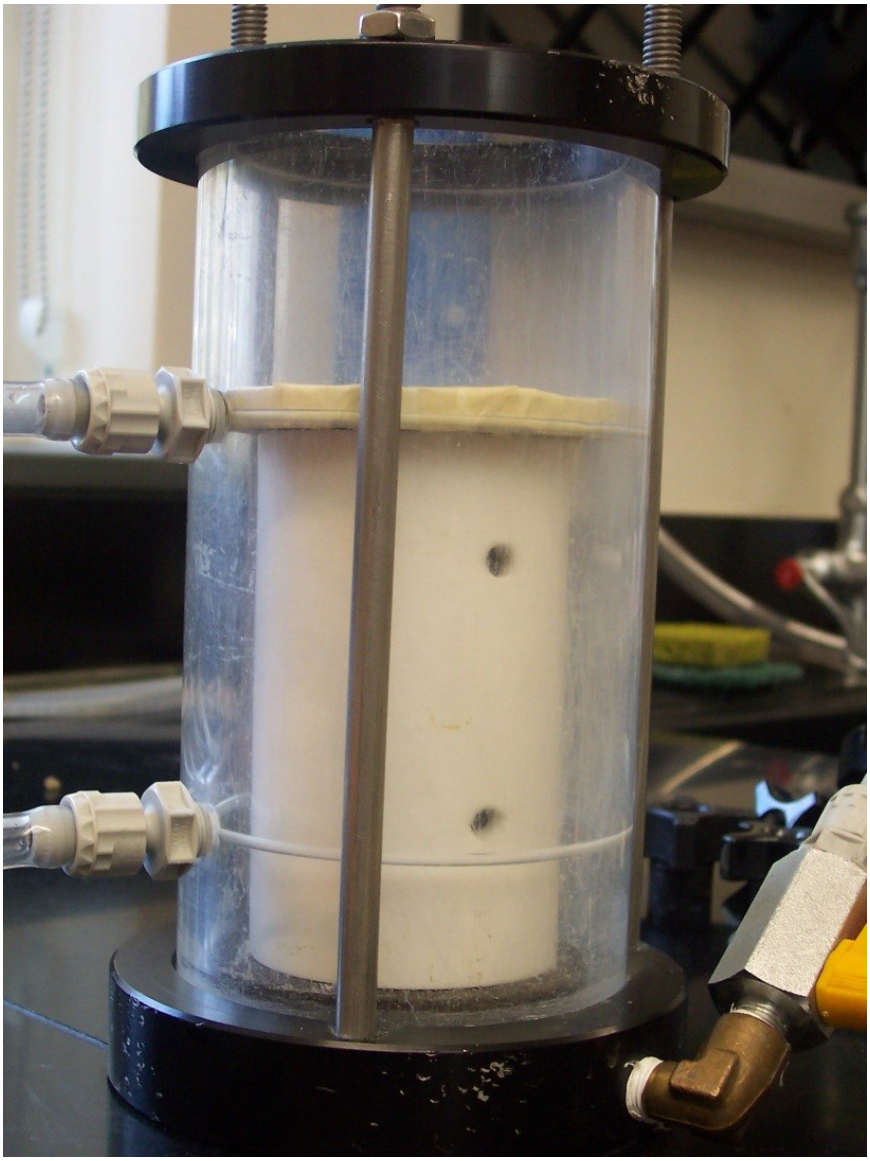

Figure 67: Cell setup for CFA testing using solid spacers

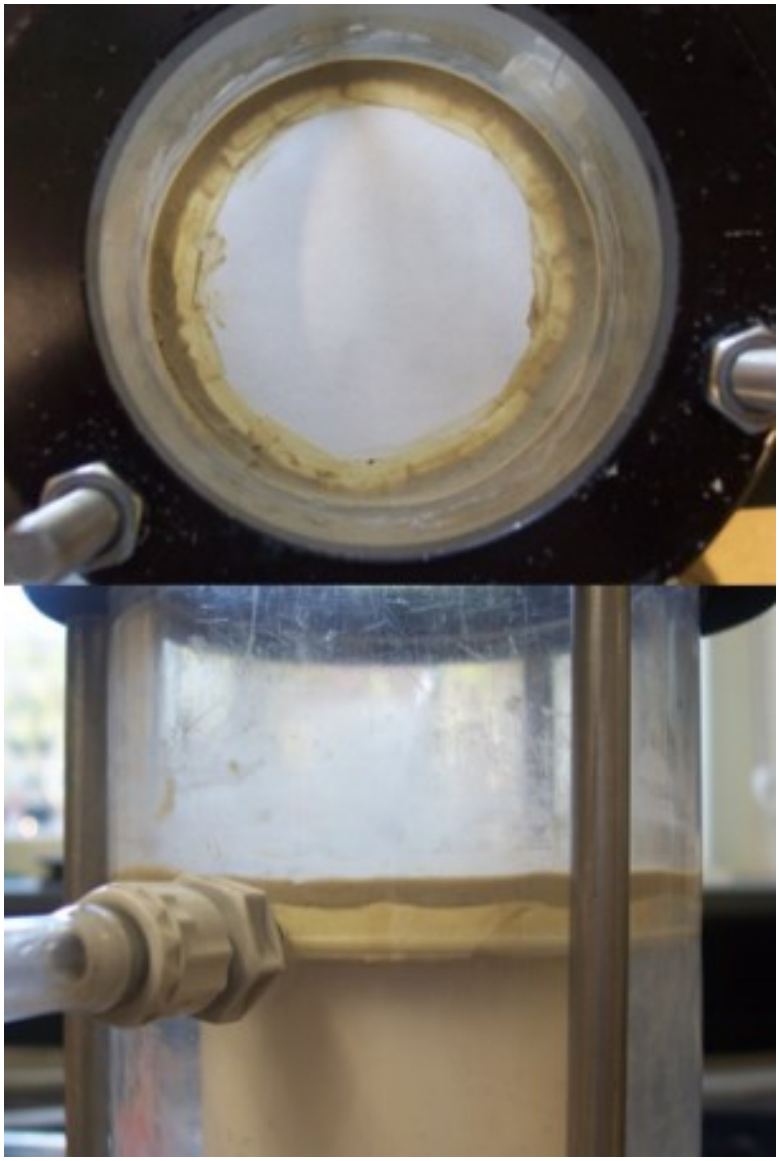

Figure 68: Bentonite seal to prevent sidewall leakage

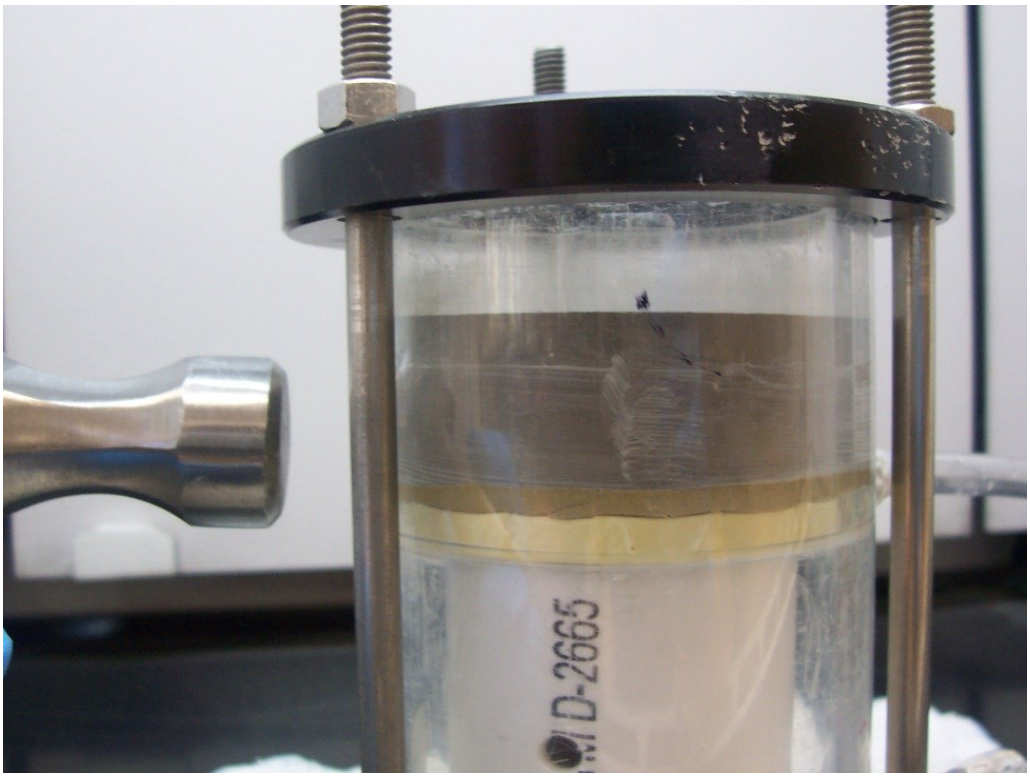

Figure 69: Tapping/vibrating cell to compact sample to desired density

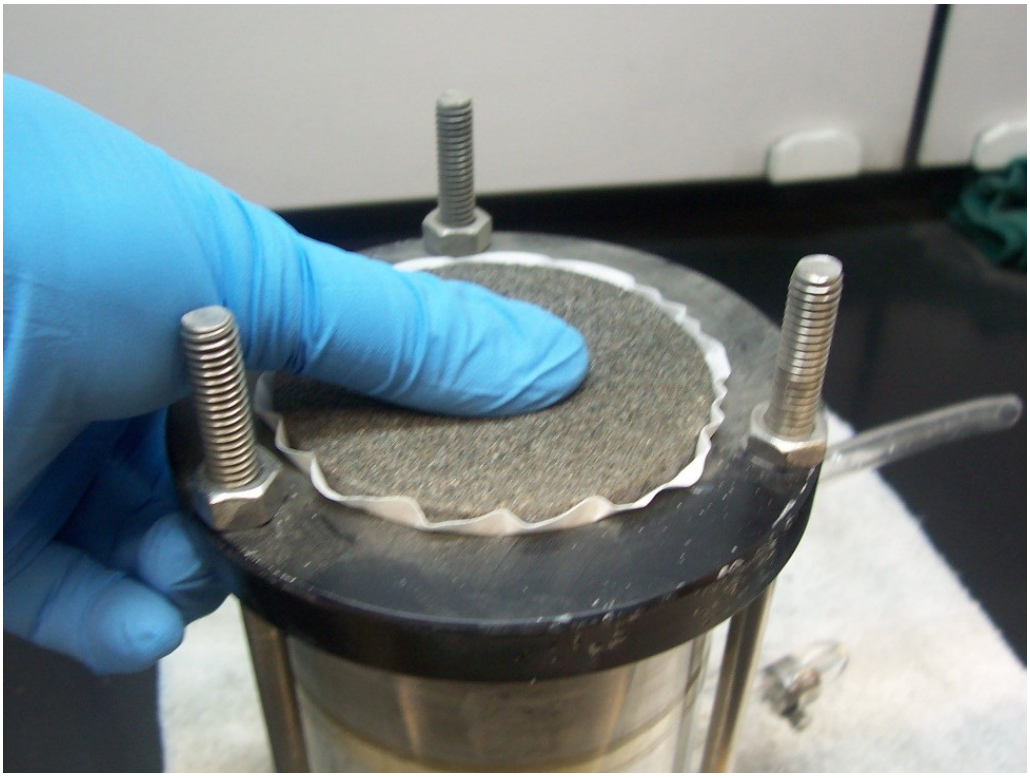

Figure 70: Installing clean/dry top porous stone

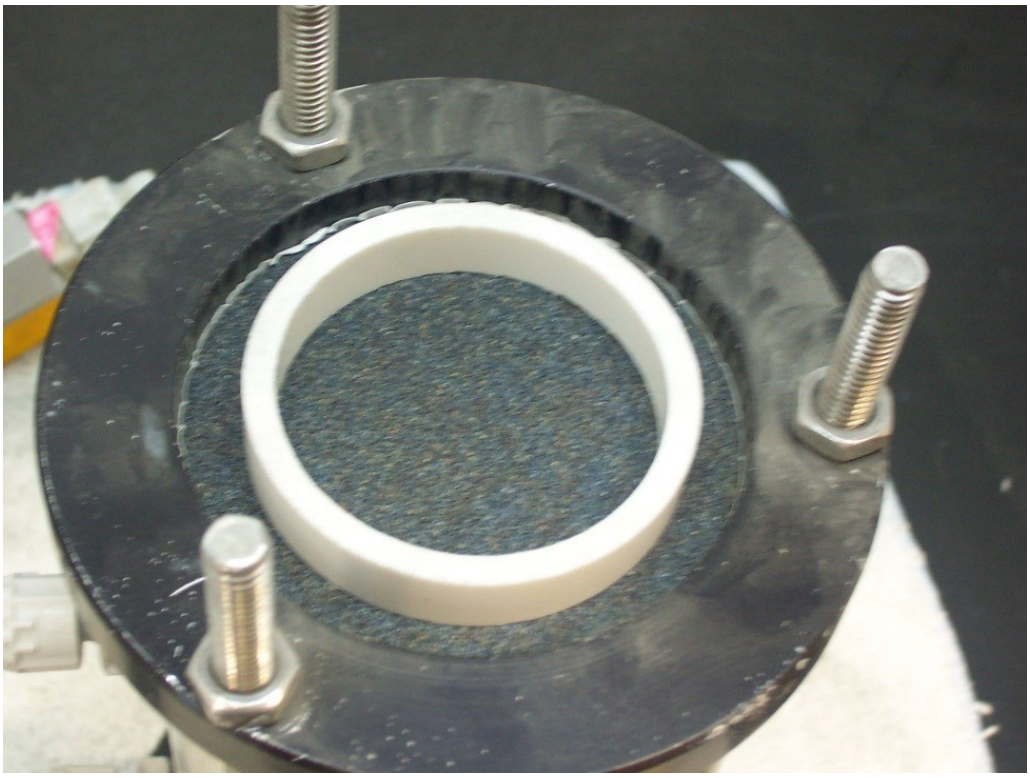

Figure 71: Top rigid spacer

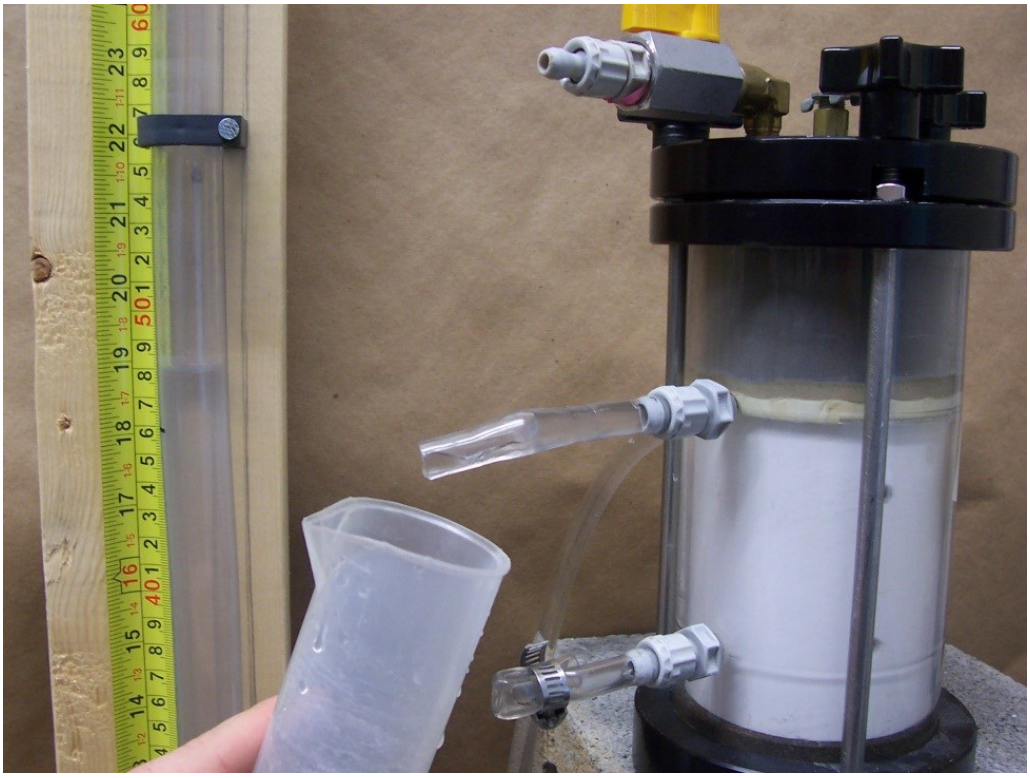

Figure 72: Dewatering of cell through manometer ports

Figure 73: Hydrophilic CFA in standpipe apparatus

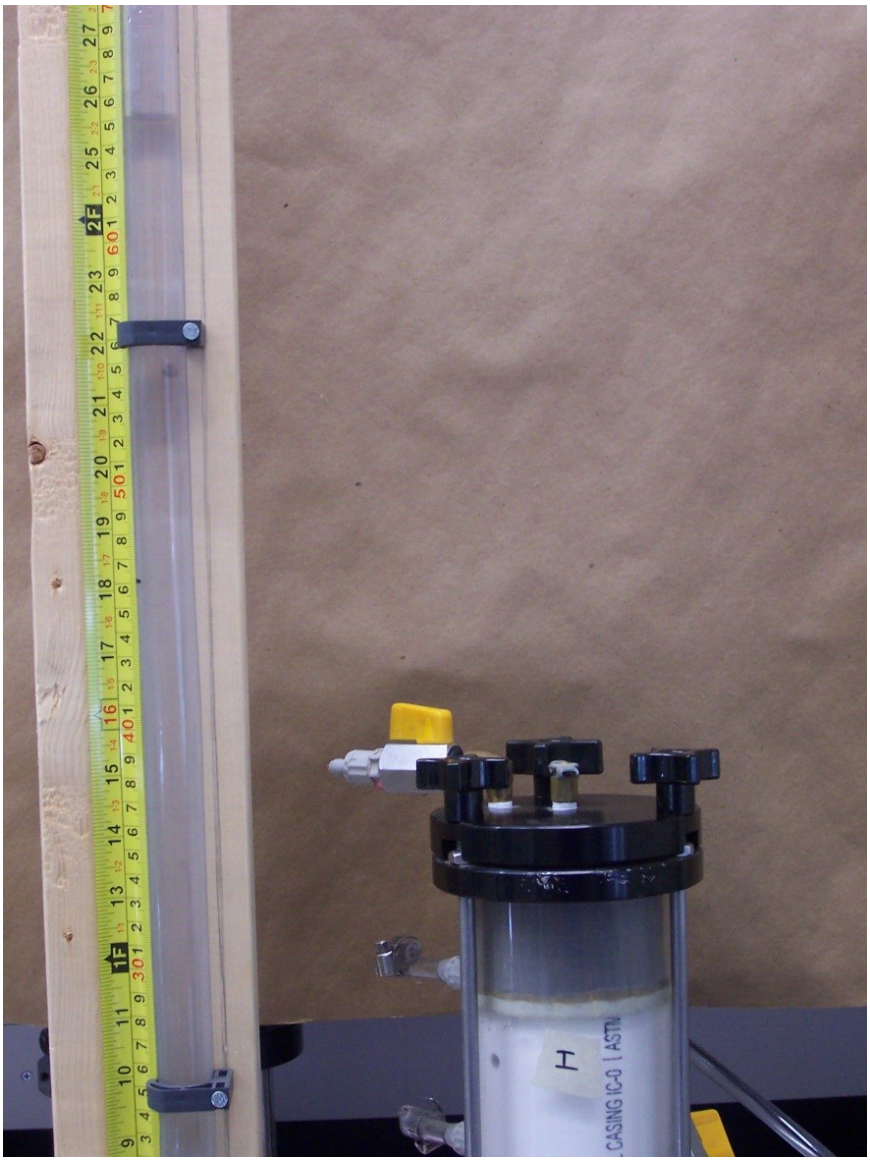

Figure 74: Hydrophobic CFA in standpipe apparatus

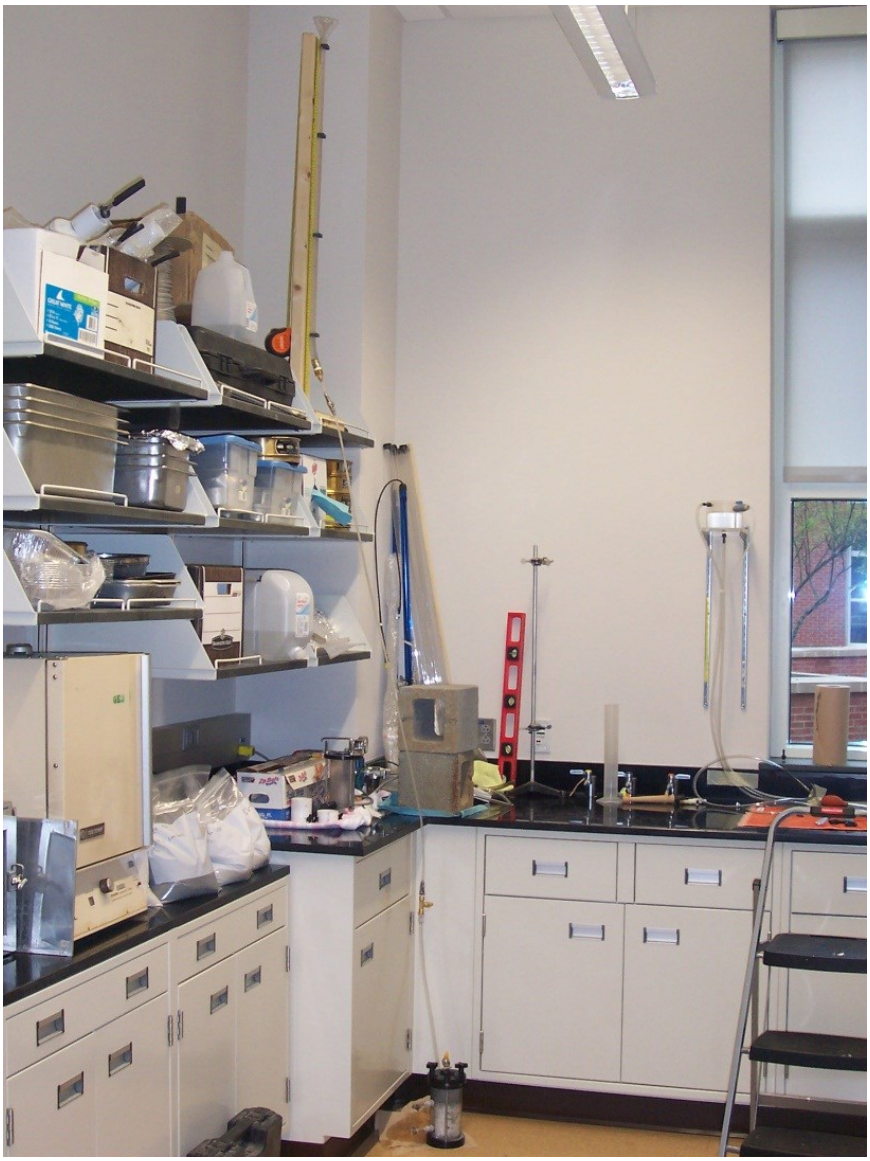

Figure 75: Standpipe apparatus with up to 3 meters of head

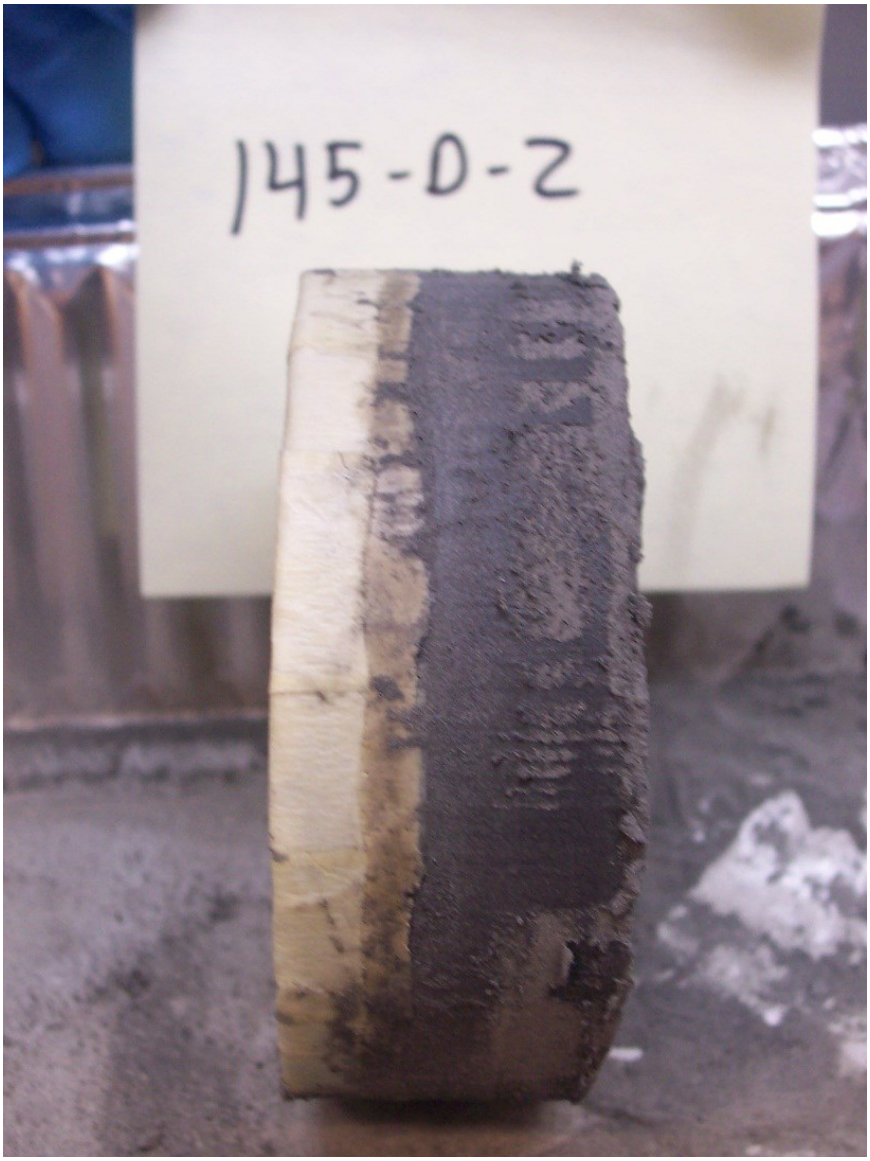

Figure 76: Confirming sample infiltration (1)

Figure 77: Confirming sample infiltration (2)

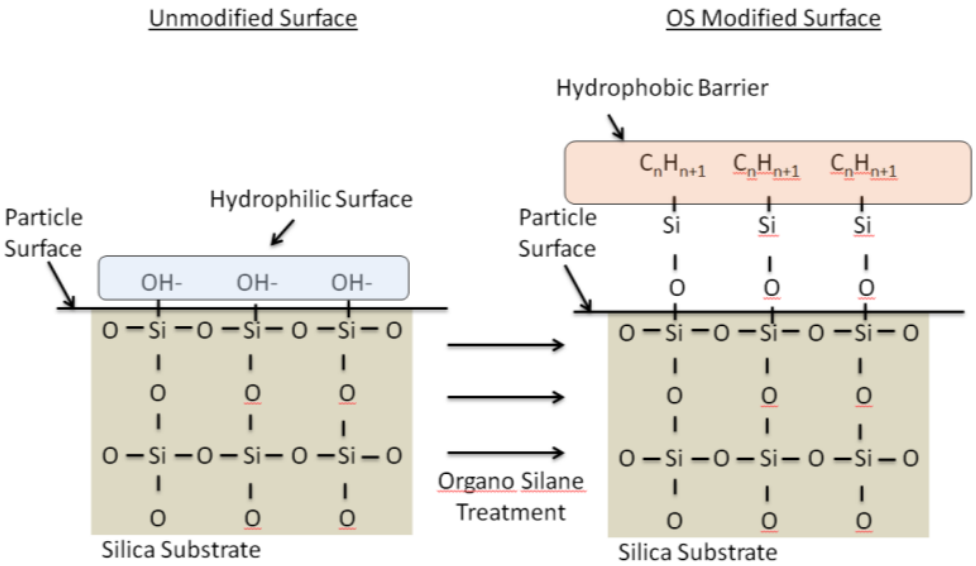

Figure 78: OS modification of silica substrate

APPENDIX C: DATA TABLES

Table 14: Water entry pressure of sand treated with OS_1 (cm of H_2O) (1)

Contact Angle	Density	Trial							
(deg.)	(g/cm^3)	1	2	3	4	5	6	7	8
96.1	1.56	1.9	9.4	6.1	6.1	5.8	5.6	5.5	5.5
96.1	1.66	10.4	5.5	5.5	5.3	5.3	5.1	5.0	-
96.1	1.76	1.9	0.9	1.0	1.1	1.3	1.0	1.1	-
108.5	1.56	5.2	15.1	4.4	4.5	4.3	4.6	-	-
108.5	1.66	7.9	12.1	4.7	4.8	4.8	5.7	5.5	-
108.5	1.76	6.7	5.9	6.0	6.1	6.2	5.8	5.9	-
122.5	1.56	8.9	7.1	7.0	7.3	7.1	8.0	-	-
122.5	1.66	8.2	7.7	7.9	8.3	7.9	8.3	8.5	-
122.5	1.76	9.8	9.2	9.7	9.5	9.4	9.4	-	-

Table 15: Water entry pressure of sand treated with OS_1 (cm of H_2O) (2)

Contact Angle	Density	Trial							
(deg.)	(g/cm^3)	1	2	3	4	5	6	7	8
96.1	1.56	1.6	1.4	1.2	1.4	1.2	1.1	-	-
96.1	1.66	0.8	-0.1	0.0	0.0	0.0	0.2	-	-
96.1	1.76	1.9	0.9	1.0	1.1	1.3	1.0	1.1	-
108.5	1.56	5.2	15.1	4.4	4.5	4.3	4.6	-	-
108.5	1.66	7.9	12.1	4.7	4.8	4.8	5.7	5.5	-
108.5	1.76	6.7	5.9	6.0	6.1	6.2	5.8	5.9	-
122.5	1.56	8.9	7.1	7.0	7.3	7.1	8.0	-	-
122.5	1.66	8.2	7.7	7.9	8.3	7.9	8.3	8.5	-
122.5	1.76	9.8	9.2	9.7	9.5	9.4	9.4	-	-

Table 16: Water entry pressure of sand treated with OS_2 (cm of H_2O) (1)

Contact Angle	Density	Trial							
(deg.)	(g/cm^3)	1	2	3	4	5	6	7	8
91.5	1.56	2.0	1.3	1.4	1.7	1.4	1.8	-	-
91.5	1.66	5.5	5.8	9.1	8.5	8.1	6.9	6.9	-
91.5	1.76	7.9	6.2	6.1	6.6	5.3	1.8	1.0	-
95.2	1.56	4.0	3.2	3.5	3.4	3.4	3.9	-	-
95.2	1.66	6.5	6.4	6.3	6.5	6.2	7.2	13.7	13.0
95.2	1.76	4.5	4.7	4.7	4.2	4.0	3.4	-	-
111.5	1.56	5.0	5.0	5.1	4.9	5.1	5.3	-	-
111.5	1.66	7.5	7.1	7.1	7.3	7.4	7.2	-	-
111.5	1.76	9.0	7.4	7.0	7.1	6.8	7.3	-	-
117.5	1.56	8.7	7.2	5.9	5.8	5.6	5.9	-	-
117.5	1.66	6.0	6.6	6.7	8.1	9.0	9.2	9.9	10.0
117.5	1.76	12.6	14.7	9.3	12.9	12.8	11.5	-	-

Table 17: Water entry pressure of sand treated with OS_2 (cm of H_2O) (2)

Contact Angle	Density	Trial							
(deg.)	(g/cm^3)	1	2	3	4	5	6	7	8
91.5	1.56	0.6	0.1	0.3	0.5	0.0	-0.1	-	-
91.5	1.66	0.4	0.6	0.9	1.2	1.0	1.1	-	-
91.5	1.76	0.0	-0.8	-1.0	-1.0	-1.1	-	-	-
95.2	1.56	1.2	3.4	2.5	2.6	2.6	2.3	-	-
95.2	1.66	4.0	4.4	4.0	4.2	4.0	4.2	-	-
95.2	1.76	13.5	4.6	4.9	3.9	3.8	-	-	-
111.5	1.56	3.9	5.3	5.0	4.4	4.2	3.7	3.2	3.3
111.5	1.66	9.5	9.6	10.1	10.2	9.6	9.4	-	-
111.5	1.76	22.4	32.3	15.3	13.2	12.7	12.3	-	-
117.5	1.56	8.3	5.9	6.1	6.3	6.1	6.3	-	-
117.5	1.66	8.4	6.9	6.8	6.8	7.3	8.8	-	-
117.5	1.76	9.4	8.7	8.9	9.0	8.1	8.4	-	-

Table 18: Water entry pressure of CFA treated with OS_2 (cm of H_2O)

Contact Angle	Density	Trial		
(deg.)	(g/cm^3)	1	2	3
96	1.02	0.0	0.0	0.0
96	1.12	0.0	0.0	0.0
96	1.22	0.0	0.0	0.0
110	1.02	8.1	21.1	26.1
110	1.12	0.0	0.0	0.0
110	1.22	0.0	0.0	0.0
125	1.02	31.8	51.0	54.4
125	1.12	28.9	31.6	27.8
125	1.22	40.9	30.6	31.7
135	1.02	136.3	153.3	154.0
135	1.12	208.4	205.7	204.7
135	1.22	261.6	268.5	250.3
145	1.02	262.8	257.2	258.0
145	1.12	402.4	397.1	416.1
145	1.22	562.6	527.5	536.8